Order Number 9238242

Dynamics of a galloping quadruped

Nanua, Prabjot, Ph.D.

The Ohio State University, 1992

U·M·I
300 N. Zeeb Rd.
Ann Arbor, MI 48106

DYNAMICS OF A GALLOPING QUADRUPED

DISSERTATION

Presented in Partial Fulfillment of the Requirements for
the degree Doctor of Philosophy in the Graduate
School of the Ohio State University

by

Prabjot Nanua, B.Tech., M.S.

* * * * *

The Ohio State University

1992

Dissertation Committee:

Prof. K. J. Waldron

Prof. G. L. Kinzel

Prof. K. Ishii

Approved by

Prof. K. J. Waldron - Advisor

Department of Mechanical Engineering

ACKNOWLEDGEMENTS

I would like to express my gratitude to Prof. K. J. Waldron for his guidance and support during the course of this work. I would also like to thank Prof. G. L. Kinzel and Prof. K. Ishii for their suggestions and comments. Lastly, this thesis would not have been possible without the support of my family.

VITA

September 8, 1965	Born - New Delhi, India.
1987..	Bachelor of Technology, Mechanical Engineering, Indian Institute of Technology, Kanpur, India.
1988..	Master of Science, Mechanical Engineering, The Ohio State University, Columbus, Ohio.
1988 to present.......................................	Graduate Research Assistant / Graduate Teaching Assistant, Department of Mechanical Engineering, The Ohio State University, Columbus, Ohio.

FIELDS OF STUDY

Major Field: Mechanical Engineering

Robotics

TABLE OF CONTENTS

LIST OF TABLES

TABLES PAGE

LIST OF FIGURES

CHAPTER I

INTRODUCTION

1. Introduction

Quadruped locomotion has been of interest to researchers for many centuries now. The abundance of quadrupeds in nature and the ease with which they are able to negotiate unstructured terrain has fascinated many researchers. Thus, it is natural for quadrupeds to be strong contenders for man-made machines. Quadruped locomotion and in general legged locomotion has many advantages over wheeled/tracked locomotion. In legged locomotion, we can choose the appropriate locations to place the feet and thus traverse difficult terrain with limited number of secure footholds. These legs also act as suspensions and are able to provide a smooth ride. Further, due to the limited contact between the machine and environment, legged locomotion is less damaging to the environment than wheeled locomotion. These advantages have motivated many researchers in the past to study and construct quadruped machines. Others have performed simulation studies with models of varying complexity to understand the basics of quadruped locomotion.

Another approach to study this problem has been to observe the locomotions of animals. Most of the animals around us are quadrupeds. The study of their locomotion should enhance our understanding of the quadruped locomotion. The success of this approach strongly depends upon our ability to gather data from the animals. Unfortunately, this is not always feasible due to the lack of appropriate sensors. Still the limited data that has been obtained from the four legged animals have been vital to our study of quadruped locomotion.

2. Overview

In this dissertation the limited quantitative data available from the observations of quadrupeds is used in conjunction with simulation studies and explains many of the facts known about them. A simple model of the quadruped has been developed for the simulation studies. Using the results from the simulation studies and principles of symmetry, a controller has been designed for quadruped gallop. This controller enables the quadruped to gallop at a constant speed, change speed and further turn with a small curvature. Although many simulations and control schemes are available for quadruped trot, none have been conducted for quadruped gallop.

Chapter II starts with a simple mass spring model and continues with the development of a technique to obtain stable solutions for various quadruped gaits (trot, gallop and bound). There are no dissipative elements in the model. This chapter includes a qualitative discussion of the various gaits. The energy trade-offs are discussed and an attempt is made to generate the optimal gait (lowest energy gait). The energy expenditure in the various gaits is compared at different speeds and it is shown that the trot consumes the lowest energy at low speeds and the gallop uses the minimum energy at higher speeds.

Chapter III uses the results and insights developed in Chapter II to develop control strategies for a gallop at constant speed. A viscous damper combined with a force actuator has been added to each leg. Symmetry principles have been used to design a non-linear controller for the quadruped gallop. It is shown that an explicit controller is not required to control the pitch motion of the body. The stability of the system is studied using Poincare maps. It has been shown that a chaotic behavior of the system leads to instability. The stable system shows either periodic or quasiperiodic behavior. The effect of different initial conditions on the system is studied. Further, parameter variation studies have been performed for the system. From these studies, it is shown that the system is stable for a range of leg stiffness. For a leg stiffness outside this range, the system shows chaotic motion.

The controller described above is enhanced in Chapter IV to include changes in speed. This controller permits the quadruped to change speed without affecting the stability of the system. The stability is again examined using Poincare maps. The controller developed in this chapter changes the speed linearly.

In Chapter V, the controller is extended to control a three dimensional quadruped machine. Additional controllers are developed to control the sideways speed, roll and yaw. A simple proportional-differential controller is used to control the sideways speed. To control yaw and roll without affecting the pitch motion, proportional-differential controllers with feedforward terms are used. These additional controllers do not apply any moment in the pitch direction. This enables us to use the controller developed in the two dimensional case for the three dimensional machine. Further, a control strategy is developed to enable the quadruped to turn. This strategy turns the quadruped with a relatively small curvature.

3. Description of the problem

The dynamic equations of quadruped locomotion are highly non-linear. Therefore, the problem of controlling quadruped gait is not very amenable to linear control techniques. Researchers, have in the past come up with novel approaches to this problem (Raibert 1984, Wong 1992). They have devised non-linear controllers for quadruped locomotion. These non-linear controllers are either based on symmetry principles, or assume super-real time simulations.

The other difficulty with this problem is the definition of the desired output. In general terms, the quadruped should retain its balance with the control scheme. However, there is no mathematically precise definition of balance. Does it imply that the the system should be periodic ? The obvious answer is: not necessarily. Either a periodic or a quasiperiodic system should be able to retain balance. Is it possible that a chaotic system will also be able to retain its balance ? Are chaotic systems inherently unbalanced ?

Let us take the case of quadruped trot. In this case, the diagonally opposite legs act together and, thus, the body does not undergo any angular displacement. Therefore, we could develop a controller for trot that will ensure that the main body does not undergo any angular displacement. Now let us consider the case of quadruped gallop. For gallop to be feasible, the body has to undergo a pitching motion. Roll and yaw are not essential and could be set to zero (assuming the quadruped is travelling in a straight line). The problem definition for this case becomes more complicated. We can design a controller to set the roll and yaw to zero but what should be the pitch angle ?

An added constraint to the problem could be that the energy losses of the gait should be minimized. That is, for a given speed, in addition ensuring that the system to retains its balance, the controller should ensure that the system is following the minimum energy path for that gait. This further complicates the problem. Now what path will give us this optimal solution ? Does the system now have to be periodic, quasiperiodic or chaotic ? This dissertation will try to answer these and related questions about the quadruped gallop.

4. Literature Survey

Locomotion of terrestrial quadrupeds has a long history of study. As early as 1779, Goiffon and Vincent conducted an aural study of gaits in horses. They attached bells, each with a specific ring, to each of the legs and developed the concepts of gaits at different speeds. Marei (1875) devised a more perfect way of recording movements. He invented a recording apparatus which enabled him to estimate the duration of support and aerial phase. At about the same time Muybridge (1887) analyzed animal movements by means of sequential still photographs. He stretched out threads across a track and attached these threads to the shutters of a series of cameras. As the animal moved along the track, it tripped these threads and photographs were taken by the cameras. This technique enabled him to study quadruped locomotion in greater detail.

More recently, with the advent of better technology, more sophisticated techniques have been used to analyze quadruped motion. Pennycuick (1975) used a simple optical method to measure the stride frequencies of various animals in the Serengeti National Park. The stride frequency in walk, trot and canter were analyzed for 14 mammal species. The stride frequency was found to vary with about the -0.5 power of the linear dimensions (shoulder height) in all three gaits.

Other researchers (Cavagna, Heglund and Taylor, 1977) have used force plates to measure the force exerted on the ground by quadrupeds during walking and running. They have found that the total energy stays almost constant during walking. There is an energy exchange between the potential energy and forward kinetic energy leading to an almost constant total energy. During running, the changes in potential energy and the forward kinetic energy are in phase with each other. Thus there are large variations in the total energy during each stride.

McMahon (1975) used the treadmill and high speed cameras to study the locomotion of various quadrupeds. He found that many parameters of gait including stride frequency, stride length, maximum speed, and the rate of O_2 uptake are power law functions of body weight of the quadruped. He has further shown that the theoretical model based on elastic similarity makes the most successful prediction of stride frequency, stride length, limb excursion angles, and the metabolic power required for running at the trot-gallop transition in quadrupeds ranging in size from mice to horses.

In another study McMahon et. al. (1989) have shown that the legs of bipeds could be modelled as constant stiffness springs. They have shown that a constant non-dimensional stiffness spring could be used to model bipedal gaits at various running speeds.

Alexander et. al. (1985) have done significant work in the area of quadruped locomotion. They have compared trotting and galloping in quadrupeds from an energy expenditure perspective. Hoyt and Taylor (1981) trained small ponies to run on a treadmill using different gaits on command. They measured the ponies rate of oxygen consumption and found that trotting consumed less oxygen than galloping at speeds below 4.5 m/s. However, at speeds above 4.5 m/s, galloping used less oxygen than trotting. When the ponies were allowed to move at will in a paddock, they trotted at 2.8-3.8 m/s but galloped at speeds over 5 m/s. They chose whichever gait was more energy efficient for the speed at which they were moving. Alexander et. al. (1985) have hypothesized that during galloping additional internal energy stored, due to the flexion of the back, is returned at an appropriate time during the stride. This additional energy storage mechanism is economical only above a certain range of speed and thus gallop is preferred only above certain speeds.

Pandy et. al. (1988) have used nubian goats to study the dynamics of quadruped locomotion. One of the important conclusions from their work has been that the inertial effects of the legs are negligible compared to the inertial effects of the body.

In the late 1960's and 1970's, many researchers started building computer controlled quadrupeds. The first legged vehicle to walk by itself under computer control was the "Phoney Pony", built by A. A. Frank and R. B. McGhee at the University of California in 1966 (McGhee, 1966). This machine had four legs powered by electric motors. The hip joints and the knee joints each had a single degree of freedom. Two twelve-volt batteries supplied power through a trailing cable. The whole machine weighed about a hundred pounds and had a top speed of 0.5 mph. It was about the size of a small pony.

A larger vehicle was built by R. A. Liston and R. S. Mosher at General Electric Corporation in 1968. A 100 hp engine supplied the hydraulic power through trailing hydraulic lines. The driver was strapped into a seat and controlled each of the twelve joints by a system of levers. The legs of the operator controlled the hind limbs of the machine and the hands controlled the forelimbs of the machine. Force feedback from the legs altered the feel of the levers, aiding the driver in knowing what the legs were doing. A major problem with the machine was the strain on the operator; most operators could not operate the machine for more than one or two minutes.

Since the early 1980's, Raibert et al. have built one-legged, two legged and four legged machines. Raibert started with the one legged machines since he was more concerned with studying the issues related to the dynamic balance of the machine. He later extended his work to two legged and four legged machines. These machines have a rigid body with springy telescoping legs connected to the body. He has shown that symmetry can simplify the control of dynamic legged systems (Raibert, 1986). Using principles of symmetry, controllers were developed to separately control the hopping height, body attitude and forward running speed. The hopping height was controlled by determining the losses in the system during each cycle and adding the required amount of energy by applying thrust through the leg actuator during the stance phase. The body attitude was controlled by applying torques to the body during the stance phase using a simple proportional-differential controller. The forward speed was controlled by properly choosing an appropriate forward position for the foot that accelerated the body properly during the next support phase. This control scheme was extended to bipedal running and quadruped trot, pace and bound using the concept of a virtual leg developed by Sutherland and Ullner (1984).

Brandolino (1990) has assumed that the impact or the support phase during a quadruped trot can be modelled as controlled impulses delivered to the body. An impulse formulation of the dynamic equations has been used to model these impacts. These dynamic equations have been linearized and appropriate variables were chosen to control the quadruped while trotting.

Wong (1992) has shown that symmetry principles and super real time simulation can be used to control quadrupeds during standing and running jumps. During the aerial phase, open loop leg forces and leg touchdown angles are planned so that they will completely remove the linear and angular momentum of the body during landing. Using the principles of symmetry, it has been shown that the forces applied during landing can also be applied for a takeoff. The leg forces and leg touchdown angles are computed using super real time simulation.

CHAPTER II

STABLE SOLUTIONS FOR TROT, GALLOP AND BOUND

1. Introduction

In this chapter, the dynamics of a simple spring and mass system will be examined. It will be shown that symmetry plays an important part in the locomotion of this simple system (Raibert, 1986). A technique will be developed to obtain a stable solution for the locomotion of this simple system. This method will be extended to quadrupeds and stable solutions will be computed for the quadruped trot, bound and gallop. The energy levels for these gaits will be computed at various speeds. These results will be compared with the experimental results obtained by observing quadruped gaits in nature. An attempt will be made to further extend the above technique to a model that includes body flexibility of the quadruped.

2. Modelling of a simple mass-spring system

Before the details of the model of the quadruped gait are presented, it is essential to start from a simple mass and spring system. This system is shown in the Figure 2.1. It consists of a simple point mass which represents the body mass and a single leg modelled as a linear spring.

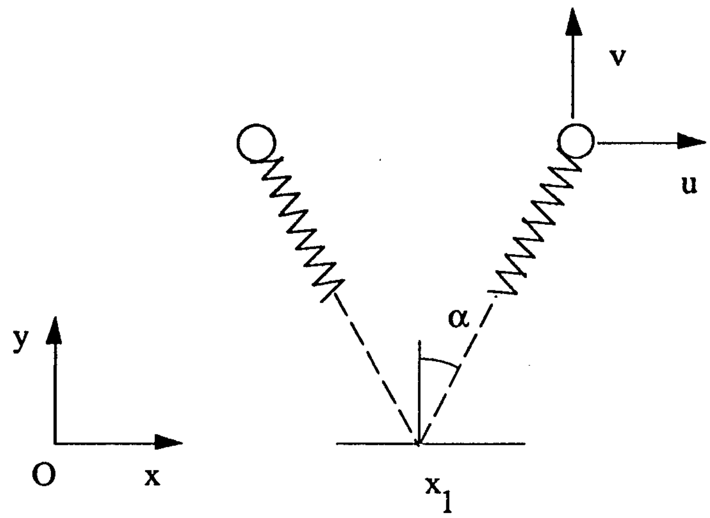

Figure 2.1. Simple mass-spring system.

A typical gait of this system would consist of alternating stance phases and aerial phases. The stance phase refers to the period of the gait when the leg is in contact with the ground. When none of the feet are in contact with the ground, the phase will be referred to as the aerial phase. A combination of a stance phase followed by an aerial phase would be considered as a step. Two steps would constitute a stride.

Let v and u denote the vertical and horizontal velocities and F denote the force applied by the spring. For a stable gait the trajectory generated over a stride (or many strides) should be repeatable over time. If it is assumed that the trajectory of a single stride is repeated, then the states of the mass-spring system at the end of a stride should be the same as the ones at the beginning of a stride. To satisfy this condition, it helps to place a further restriction on the trajectory: to assume that the trajectory is symmetric. In mathematical terms this leads to:

During the stance phase:

$$y(x_1-\delta) = y(x_1+\delta)$$
$$u(x_1-\delta) = u(x_1+\delta)$$
$$\gamma(x_1-\delta) = \gamma(x_1+\delta)$$
$$v(x_1-\delta) = -\, v(x_1+\delta)$$

where x_1 is the position of the mass at the middle of the stance phase. The last condition reflects the effect of gravity.

Similarly during the aerial phase:

$$y(x_2-\delta) = y(x_2+\delta)$$
$$u(x_2-\delta) = u(x_2+\delta)$$
$$v(x_2-\delta) = -\, v(x_2+\delta)$$

where x_2 is the position of the mass at the middle of the aerial phase. These conditions are trivially satisfied if the direction of $v(x_2-\delta)$ is opposite to that of gravity.

To satisfy the symmetry condition during the stance phase the condition on the force applied by the spring is:

$$F(x_1-\delta) = F(x_1+\delta)$$

This condition can be satisfied if the trajectory is symmetric about the y-axis (Figure 2.1) and the end of the spring is placed at x_1 as shown in the Figure 2.1.

The above conditions can be satisfied by choosing appropriate initial conditions. One possible set of initial conditions that will satisfy the conditions for a stable gait are given below. At the middle of the stance phase:

$y(x_1) = y_i$

$v(x_1) = 0$

$u(x_1) = u_i$

u_i and y_i can have any value within certain bounds. These values should be such that, at the end of the stance phase, the vertical velocity of the mass is zero, or is upwards (opposite to the direction of gravity). This condition is discussed in more detail later in this section. If the values of y, u, and v satisfy this condition then a stable gait is possible.

The equations for the simple mass-spring system are derived below.

Initial horizontal velocity = u_i, and

Initial vertical position of the mass = y_i.

The free body diagram is shown in Figure 2.2 for any angle θ. The equations of motion are:

$$F\,\mathrm{Sin}\theta = m\,\ddot{x}$$
$$F\,\mathrm{Cos}\theta - m\,g = m\,\ddot{y}$$

where

$$F = k\left[L - \left(x^2 + y^2\right)^{\frac{1}{2}}\right] = \text{spring force}$$

k = spring constant.

L = free length of the spring.

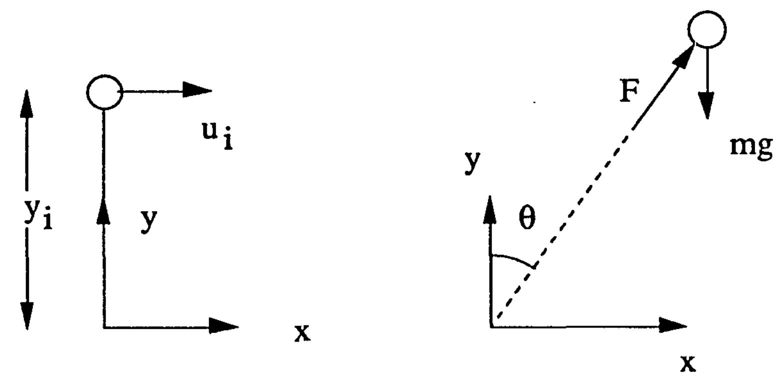

Figure 2.2. Initial Conditions for stable solution.

Using non-dimensional variables

$$X = \frac{x}{L} \quad ,Y = \frac{y}{L} \quad ,T = t\sqrt{\frac{g}{L}}$$

the above equations are:

$$\ddot{X} = \frac{kL}{mg}\left(\frac{X}{\sqrt{X^2+Y^2}} - X\right)$$
$$\ddot{Y} = \frac{kL}{mg}\left(\frac{Y}{\sqrt{X^2+Y^2}} - Y\right) - 1 \qquad (2.1)$$

Substitute $K_{leg} = \frac{kL}{mg}$ which gives the ratio of the spring force to the weight of the leg.

The above equations suggest constraints on the initial conditions. The first condition is:

$$K_{leg}\left(1-\frac{y_i}{L}\right)>1$$

If this condition is not satisfied then the initial acceleration in the y-direction is negative and the mass will never leave the ground. In fact, if this expression becomes less than one at any time during the contact phase, then the mass has negative acceleration in the y-direction. If the leg does not leave the ground before the velocity in the y-direction becomes zero, once again stable gait is not possible. Also since the maximum value of $\left(1-\frac{y_i}{L}\right)$ is one, we get the condition $K_{leg} > 1$. This condition is reasonable since it suggests that the ratio of the spring force to the weight of the mass should be greater than one. Thus the initial conditions are not completely arbitrary.

From the above equations note that the time is scaled as $\sqrt{L}$. Thus the stride frequency will be scaled as $1/\sqrt{L}$. Figure 2.3 shows the stride frequency as a function of the shoulder height for a number of animals in a variety of gaits (Pennycuick, 1975). This graph shows that the stride frequency in indeed scaled to $1/\sqrt{L}$. This is encouraging since it shows that the modelling is consistent with the observed results.

An inherent assumption in the above simulation is that the angle made by the leg with the vertical at the end of the stance phase is the mirror image of the one it made at the beginning of the stance phase. This is approximately true of animals at low speeds. As the speed increases the difference between the angles also increases. Usually the angle at the beginning of the stance phase is smaller than the angle at the end of the phase. We can deduce from the equations of motion, that this accelerates the system. Animals probably use this to compensate for the energy losses in the system. If no external energy is added to the system, it gradually loses

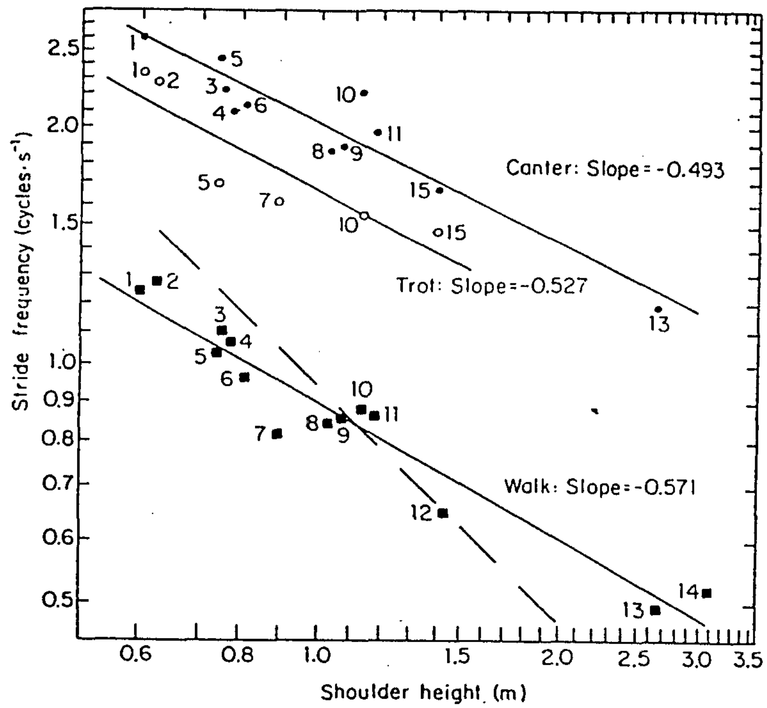

Figure 2.3.Stride frequencies versus shoulder heights in 14 species of mammals. Animals include: (1) Thomson's gazelle; (2) warthog; (3) gnu (calf); (4) spotted hyaena; (5) Grant's gazelle; (6) impala; (7) lion; (8) kongoni; (9) topi; (10) zebra; (11) gnu; (12) black rhinoceros; (13) giraffe; (14) elephant; (15) buffalo (Pennycuick, 1975).

height and a stable gait is not possible. Thus in addition to above method of compensation some external energy has to be added to the system. The discrepancy in the angles is also probably used to decelerate the foot so that it reaches approximately zero speed before it touches the ground.

3. Quadruped gait: Trot

Let us assume that there are two springs attached to the point mass. During successive stance phases, alternate legs then can be used for propulsion. The other leg could utilize this and the following aerial phase to reposition itself for the next stance phase. This scheme would lead to biped running. Note that a stable solution for this system would be the same as the one developed for the single spring above.

Let use extend this concept further and consider four springs attached to a rigid beam (Figure 2.4). The above solution translates into a fast trot for this system. This is explained further below.

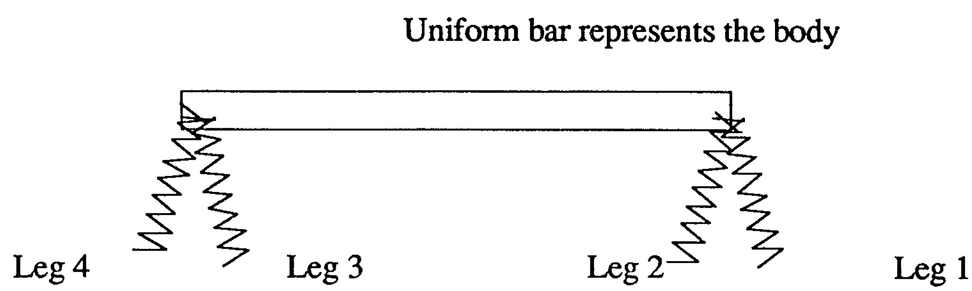

Figure 2.4. Model for a Quadruped.

In a fast trot, the diagonally opposite legs act together. After the stance phase of a pair of diagonally opposite legs is over, it is followed by an aerial phase, and then followed by the stance phase for the other pair of diagonally opposite legs. This can be represented by a support graph shown in Figure 2.5. In this figure, the circles represent the legs. Shaded circle signify that the corresponding foot is in contact with the ground and empty circle signifies that the foot is in the air.

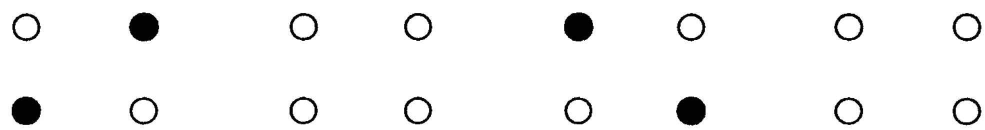

Figure 2.5. Support Graph for Quadruped Fast Trot

Since the diagonally opposite pair of legs act together, there is no net moment acting on the body about the center of mass. Thus the main body does not rotate. As a result, the above gait can be modelled by lumping the mass at the center of mass of the system and attaching the legs below the center of mass. This leads to the simple mass-spring system described earlier. The equations for kinetic energy, potential energy and internal energy are given by:

$$\text{Kinetic energy} = \frac{1}{2}M\left(\dot{x}^2 + \dot{y}^2\right) + \frac{1}{2}J\dot{\theta}^2$$

$$\text{Potential energy} = Mgy$$

$$\begin{aligned}
\text{Internal energy} = {} & \frac{1}{2}K\delta_1\left(\left(x - \frac{L}{2}\cos\theta - p_{x1}\right)^2 + \left(y - \frac{L}{2}\sin\theta\right)^2\right) \\
& + \frac{1}{2}K\delta_2\left(\left(x - \frac{L}{2}\cos\theta - p_{x2}\right)^2 + \left(y - \frac{L}{2}\sin\theta\right)^2\right) \\
& + \frac{1}{2}K\delta_3\left(\left(x + \frac{L}{2}\cos\theta - p_{x3}\right)^2 + \left(y + \frac{L}{2}\sin\theta\right)^2\right) \\
& + \frac{1}{2}K\delta_4\left(\left(x + \frac{L}{2}\cos\theta - p_{x4}\right)^2 + \left(y + \frac{L}{2}\sin\theta\right)^2\right)
\end{aligned} \quad (2.2)$$

where

(x,y) are the coordinates of the center of mass,

θ is the angular orientation of the body,

M is the mass of the body,

J is the moment of inertia of the body,

p_{xi} is the x-coordinate of the ith foot, and

$$\delta_i = \begin{cases} 1 \text{ if the ith foot is in contact with the ground} \\ 0 \text{ if the ith foot is in the air} \end{cases}$$

Consider the equations for obtaining stable solutions for the above system (equation 2.1). There are two initial conditions: the initial speed u_i and the initial position y_i. For a given speed, u_i can be fixed. But it is still possible to obtain an infinite number of stable solutions by varying the initial displacement y_i. The initial displacement y_i controls the

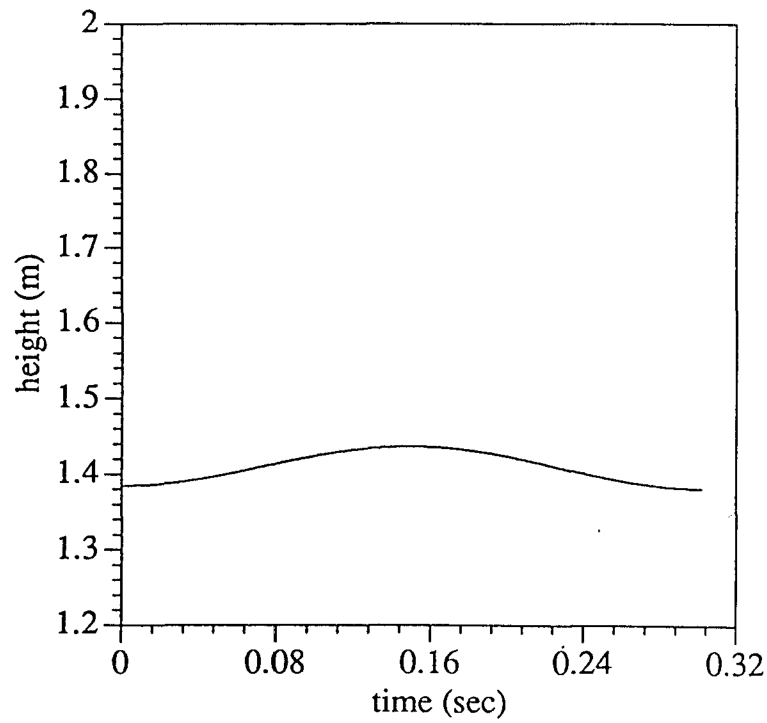

Figure 2.6. Trajectory of the center of mass in quadruped trot (equation 2.1).

initial compression of the spring and thus the energy level of the system. Thus for a given speed, a unique stable solution can be obtained by fixing an optimal energy level. The optimal energy level can be evaluated by considering the energy losses in the system.

There are two main energy dissipation processes in the mass-spring system. One of these includes the friction losses, impact losses, etc and these can be assumed to be proportional to the total energy in the system. The other energy loss is associated with repositioning the legs in the air for the next stance phase. For a simple mass-spring system being driven by a sinusoidal forcing function, this power loss is given by (assuming that the energy during the return cycle is not re-used):

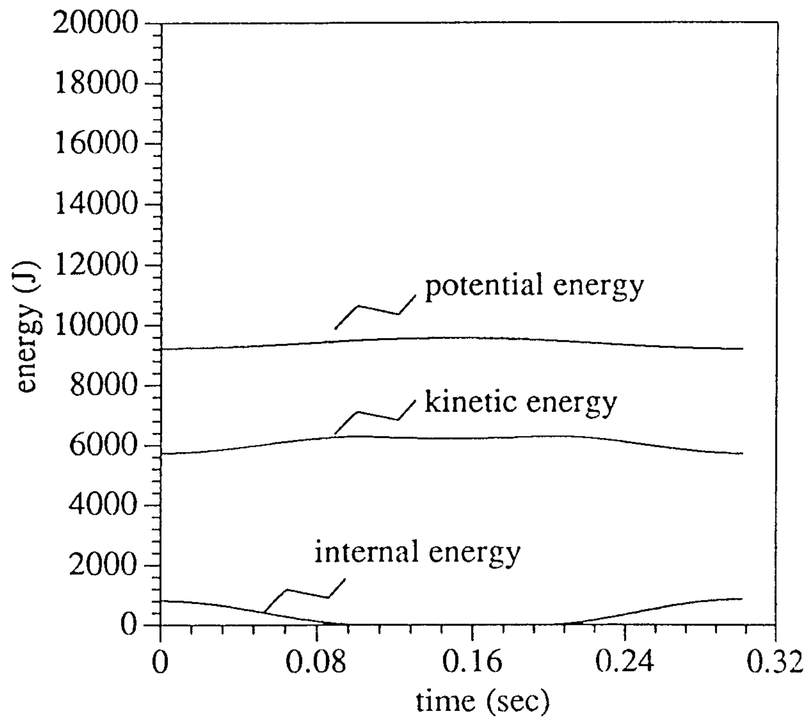

Figure 2.7. Energy variations in quadruped trot (equation 2.2).

Power required $\propto A(\Omega^2 - \omega^2)\Omega$

where A = Amplitude

Ω = Forcing frequency

ω = Natural frequency

If the energy level of the system is low, the time for the aerial phase reduces and thus the power required to reposition the legs for the next stance phase is high, and vice versa. The optimum solution can be obtained by minimizing the sum of the two energy losses. Some simulations were done with the above theory. The result did not agree too well with the actual data for horses. Thus the model for power losses in the system used above is not a good one.

Since a satisfactory model for the energy losses in the system could not be obtained, experimental data were used to fix the energy level of the system (initial condition y_i) at any given speed. The simulation results for a typical case are shown in Figures 2.6 and 2.7. The animal was assumed to be a 680 kg horse with a leg length of 1.5 m. The non-dimensional spring stiffness K_{leg} was assumed to be 14 (McMahon, 1981). From experimental results (Heglund et. al., 1974), it is known that the stride frequency for this horse is 100 min^{-1} at a speed of 15 mph. This data was used to fix the initial compression of the spring. Figure 2.6 shows the height of the center of mass for a single stride. Figure 2.7 shows the energy exchange between the kinetic energy, gravitational potential energy and the internal spring energy. From the graph, it can be seen that the variations in these energy components are approximately equal.

If y_i is reduced to a low enough value (low energy gait), then the above gait changes to the gait shown in Figure 2.8. This gait is observed in the animals at slow trot. In this case, the aerial phase disappears.

Figure 2.8. Support Graph for Quadruped Slow Trot.

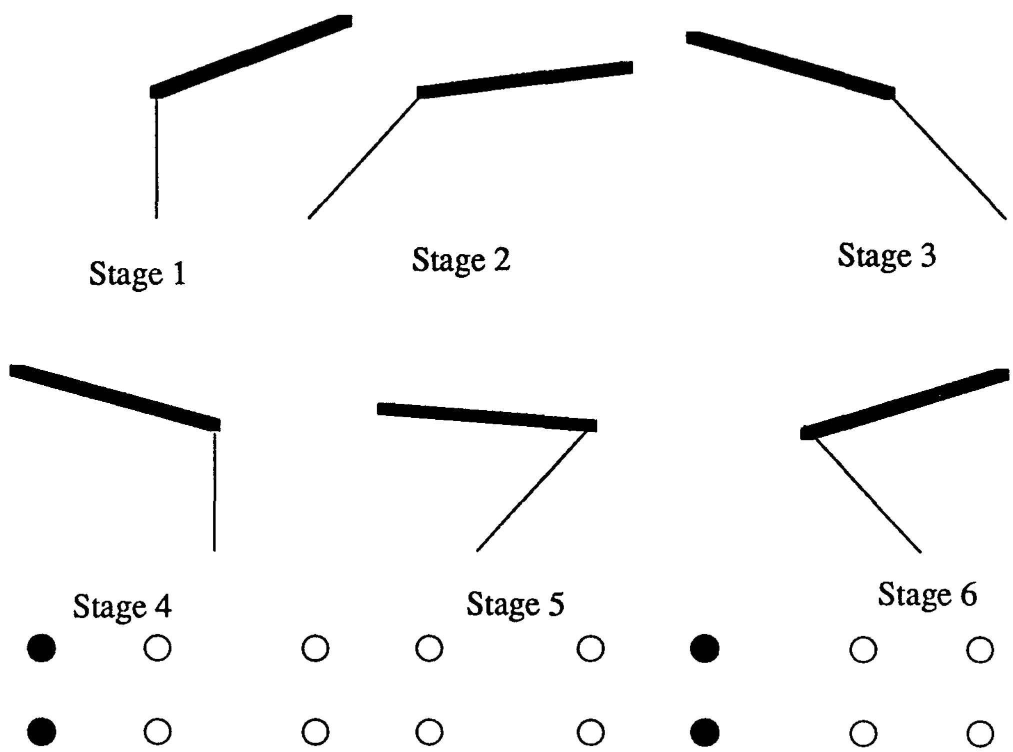

Figure 2.9. Bound for Quadruped and its Support Graph.

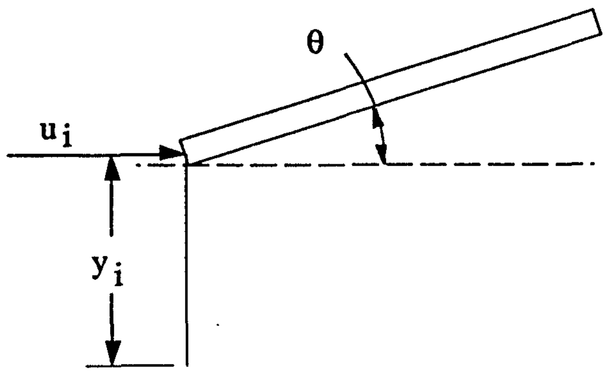

Figure 2.10. Initial Conditions for a Stable Solution for Quadruped Bound.

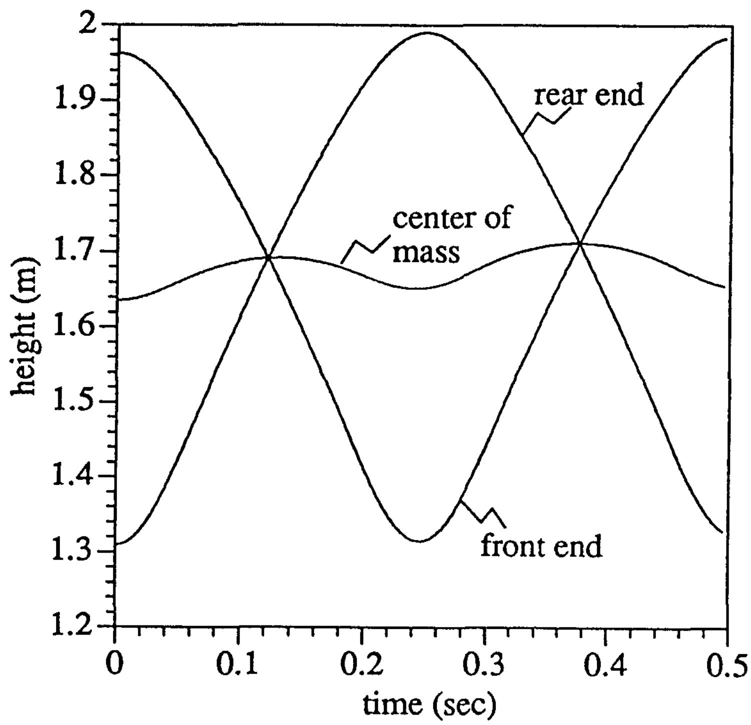

Figure 2.11. Trajectory of the quadruped in a typical bound (equation 3.1).

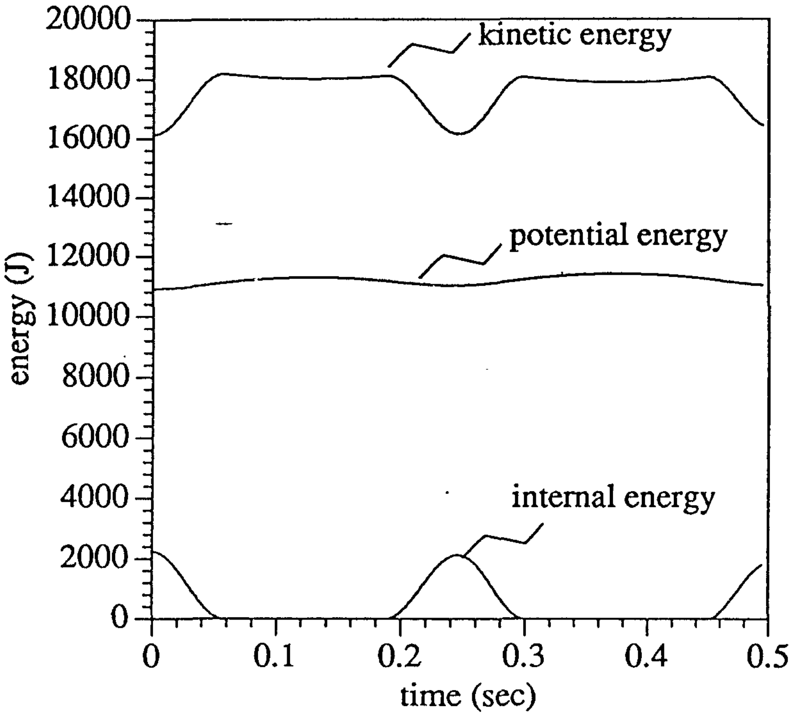

Figure 2.12. Energy variations in a typical quadruped bound (equation 2.2).

No experimental data reliable data is available at this time for comparison. The stride frequency for this gait can be used to fix the value of K_{leg}.

4. Quadruped gait: Bound

The above model can be used to generate other gaits for a quadruped. One of those is the bound. In this gait, the front two legs and the back two legs act together. This gait is shown in Figure 2.9. This leads to a rocking motion of the main body. To obtain a stable solution, the simulation is again started from the middle of the stance phase. The rear legs are compressed and the main body is given some initial horizontal velocity. The angular velocity of the main body is set to zero (using symmetry arguments) and the body is given some inclination. This is illustrated in Figure 2.10.

The only unknown in the above set of initial conditions is the initial body angle θ. This can be obtained by trial and error. There is also a systematic method of obtaining this value. The simulation is run for some body angle for a single stride. For the next run, the new guess of the body angle is taken to be the body angle obtained at the end of the stride from the previous run. This procedure is repeated till the solution converges. This method fails if the difference between the initial guess of the body angle and the actual body angle is large. In our simulations, the method failed if the difference was more than 10 to 20 degrees.

The results for a typical simulation run are shown in Figures 2.11 and 2.12. The speed for this run was set at 25 mph and the stride frequency at 120 min^{-1}(Heglund et. al., 1974). Figure 2.11 shows the trajectories for the center of mass, the front end of the horse and the rear end of the horse. Figure 2.12 shows the kinetic energy, the gravitational potential energy and the internal spring energy. Note that, from this graph, most of the energy exchange takes place between the kinetic energy and the internal energy. This can be compared with the results for a trot. In that case, the energy exchange was between all of the three types of energy. Other investigators (Alexander, 1988) have speculated about this result but they have not been able to quantitatively verify it. Also the mean internal energy is larger in this case than in that of the trot.

Another variation of this gait is shown in Figure 2.13. In this case, the potential energy is minimized by eliminating the aerial phase.

Figure 2.13. Support Graph for Quadruped Slow Bound.

5. Quadruped gait: Gallop

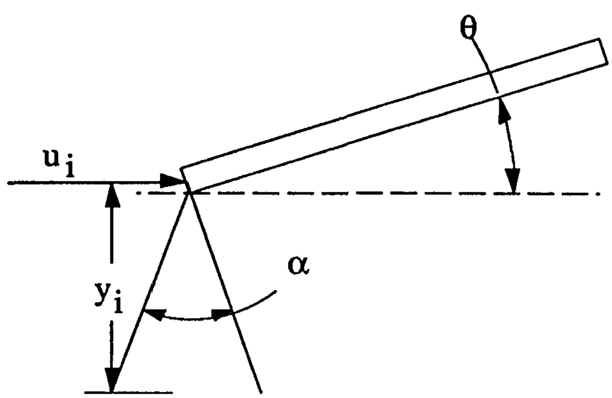

Figure 2.14. Initial Conditions for a Stable Solution for Quadruped Gallop.

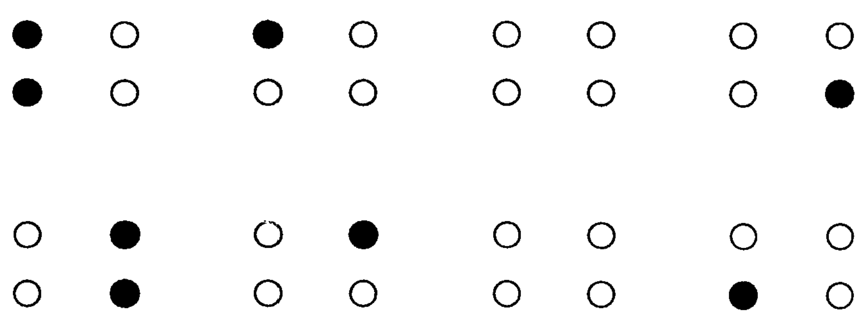

Figure 2.15. Support Graph for Quadruped Gallop.

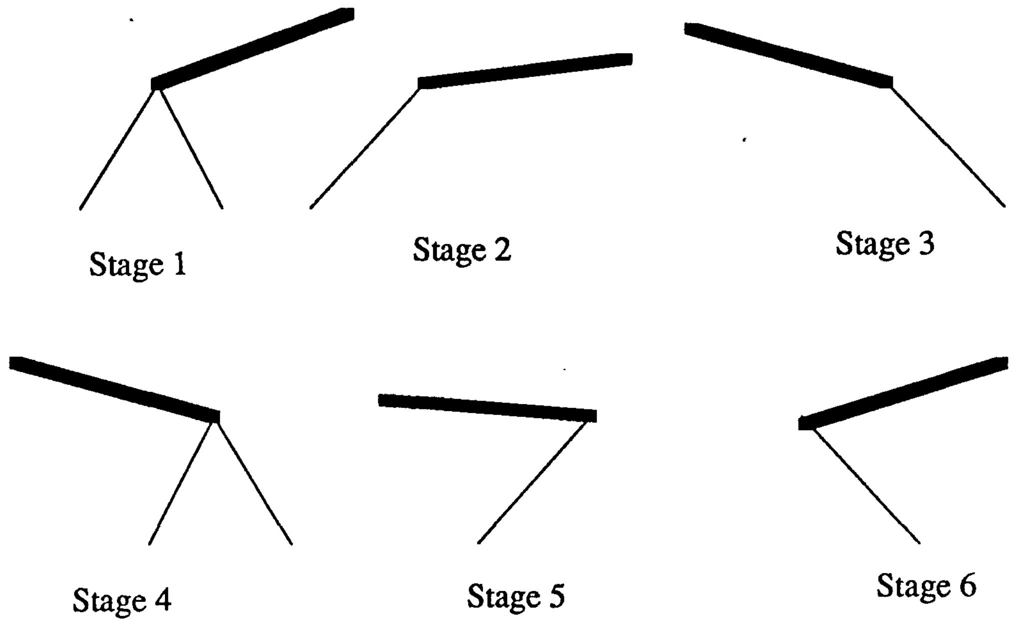

Figure 2.16. Quadruped Gallop (Legs not in contact with the ground are not shown).

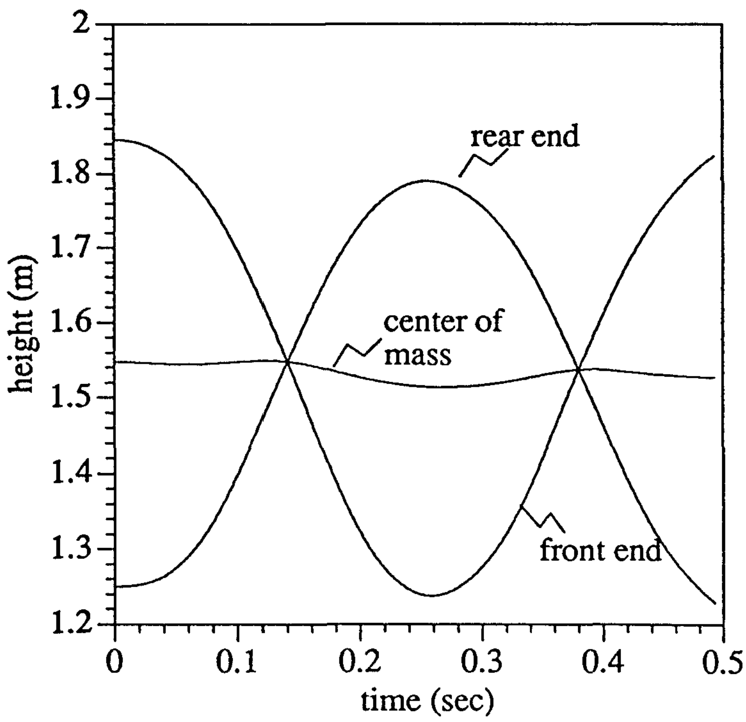

Figure 2.17. Trajectories for a typical quadruped gallop (equation 3.1).

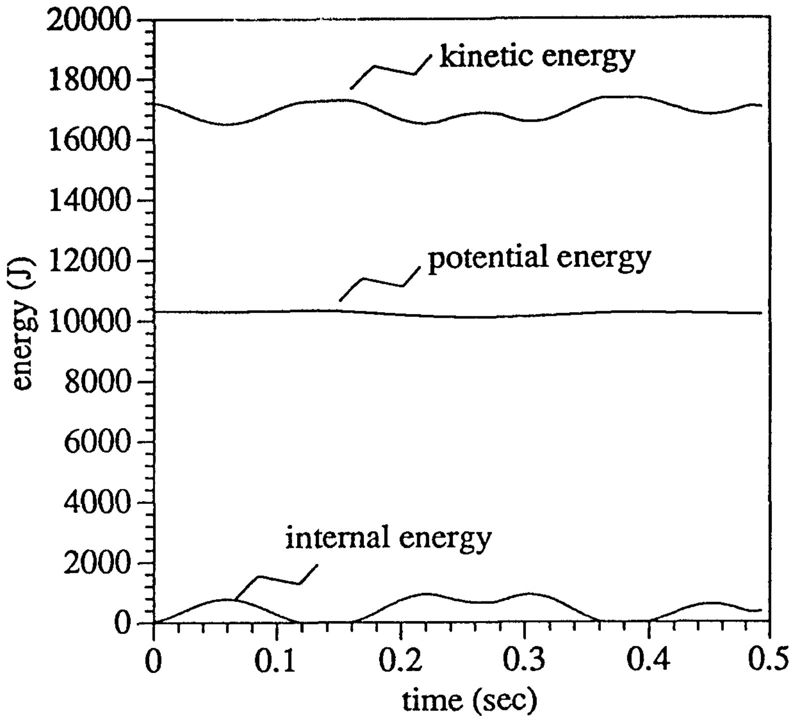

Figure 2.18. Energy variations for a typical quadruped gallop (equation 2.2).

The primary difference between gallop and bound is that the rear legs and the front legs do not act together in gallop. This adds another variable to the simulation (in the case of a two-dimensional model). Fortunately, this can be accommodated easily in the simulation by choosing appropriate initial conditions. Now the starting position is that shown in Figure 2.14.

The legs are separated by an angle α in the initial position. The feet are placed symmetrically on the ground with respect to the rear end of the body and the simulation is started by setting initial height y_i and speed u_i. As each foot leaves the ground the angle made by that leg with the vertical is stored. When the body starts descending, the legs are again placed at the same angle at which they left the ground. If the setting for the body angle is correct, then a stable solution can be obtained. In this case also only the body angle has to be tuned, which can be accomplished as was described in the previous section. This gait is shown in Figures 2.15 and 2.16.

Unlike the case of a bound, a unique solution can no longer be obtained by fixing the energy level and the speed. For a given energy level, an infinite number of solutions are possible by appropriately varying the angle α and y_i.

To observe the effect of α on the gait, simulations were conducted based on the above model. It was observed that at the same energy level, an increase in α resulted in a decrease in the stride frequency. The results are tabulated below:

For bound: speed = 25 kph, stride frequency = 120 min^{-1}
For gallop: speed = 25 kph,stride frequency = 90 min^{-1}, $\alpha = 0.429$ rad.

A lower stride frequency implies a lower energy loss to repostiion the legs. Thus, the the gallop is more energy efficient than the bound at the given speed. The energy was then reduced to obtain a stride frequency of 120 min^{-1}. The simulation results for this case are shown in Figures 2.17 and 2.18. These can be compared to the results for the bound in the previous section. It is observed that the trajectory of the center of gravity is flatter in the case of a gallop. This is also observed in the graph for the potential energy. Also the magnitudes of the variations in both the kinetic energy and the internal energy are reduced.

If the energy is minimized in the case of gallop, the aerial phase disappears and the gait shown in figure 2.19 is obtained.

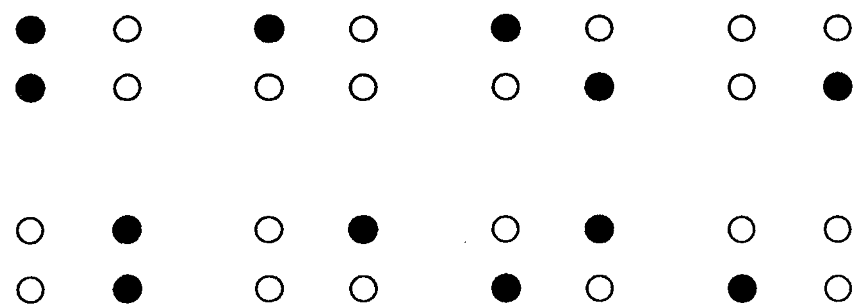

Figure 2.19. Support Graph for Quadruped Slow Gallop.

6. Energy Comparison between trot, bound and gallop

The above results were compared to the actual results shown in Figure 2.20 (Heglund et. al., 1974). From this figure, stride frequency as a function of the speed was obtained for a horse. The weight of the horse was set at 680 kg (given in the graph) and the leg length and body length were set at 1.5 m (not given in the reference, thus an approximate number was assumed).

In the first experiment, the trot and gallop simulations were run at their appropriate speed and frequency. The energy levels were obtained for these simulations at four preset speeds (10, 15, 25, 40 kph). All the three gait (trot, gallop and bound) simulations were then run at each speed with the same energy level as that obtained previously. The stride frequency was noted at each speed and plotted against speed. A polynomial curve was fitted through these data points. This is shown in Figure 2.21. Note that, at the trotting speeds, the stride

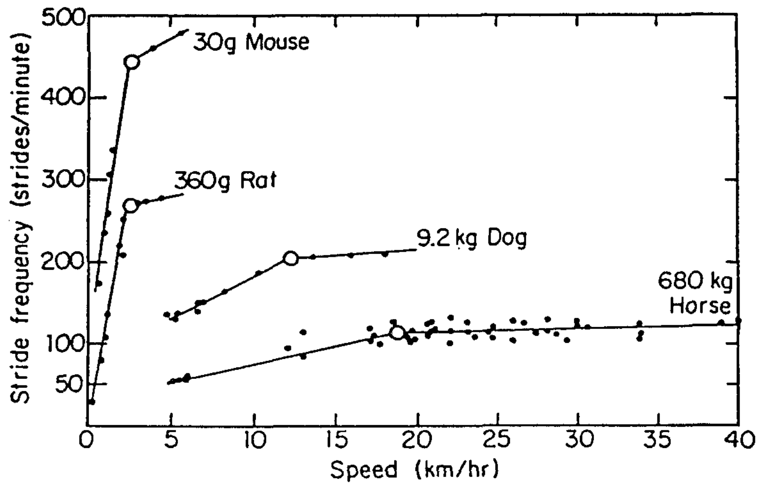

Figure 2.20. Stride frequency as a function of speed for a mouse, rat, dog and horse running on a treadmill (McMahon, 1975). The circles show the transition speed between trotting and galloping.

frequency of the trot simulation is the least, and at galloping speeds the stride frequency of the gallop is the least. This confirms the graph shown in Figure 2.20. Also this plot predicts a trot-gallop transition speed of 21 kph. The actual transition speed is about 18 kph (from Figure 2.20).

In another experiment, all the simulations (trot, gallop and bound) were forced to follow the speed-stride frequency curve shown in Figure 2.20. The energy level were obtained from these runs and plotted against speeds. Again, a polynomial curve was fitted through the data points. This is shown in Figure 2.22. From this figure, observe that the energy

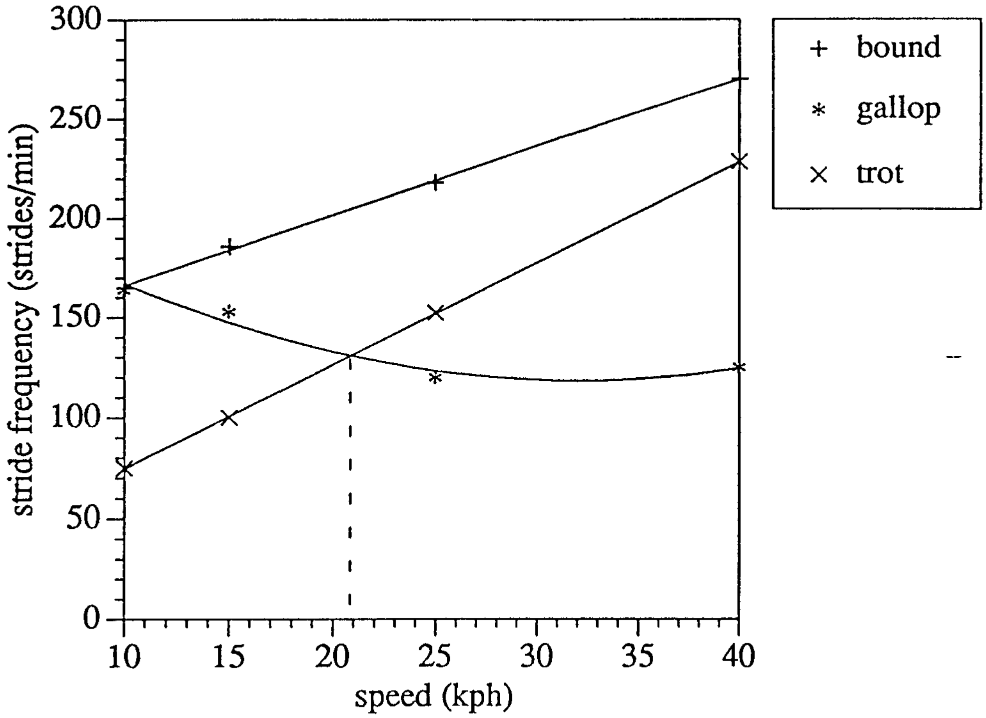

Figure 2.21. Stride frequency as a function of speed for trot, bound and gallop at the same energy level for a horse.

level of the trot is the least at trotting speeds, and the energy level of the gallop is least at the galloping speeds. From this graph the trot-gallop transition speed is 21 mph which is the same as that obtained from the previous experiment.

This simulation experiment was repeated for a dog. The weight of the dog is 9.2 kg and the length of the legs is assumed to be 0.5 m. The dog was forced to follow the stride frequency-speed curve shown in Figure 2.20. The results are shown in Figure 2.23. This figure shows that the energy level for the trot is the least at low speeds and the energy level for gallop is the least at faster speeds. The trot-gallop transition speed from this graph is 15 kph and the actual trot-gallop transition speed from Figure 2.20 is 16 kph.

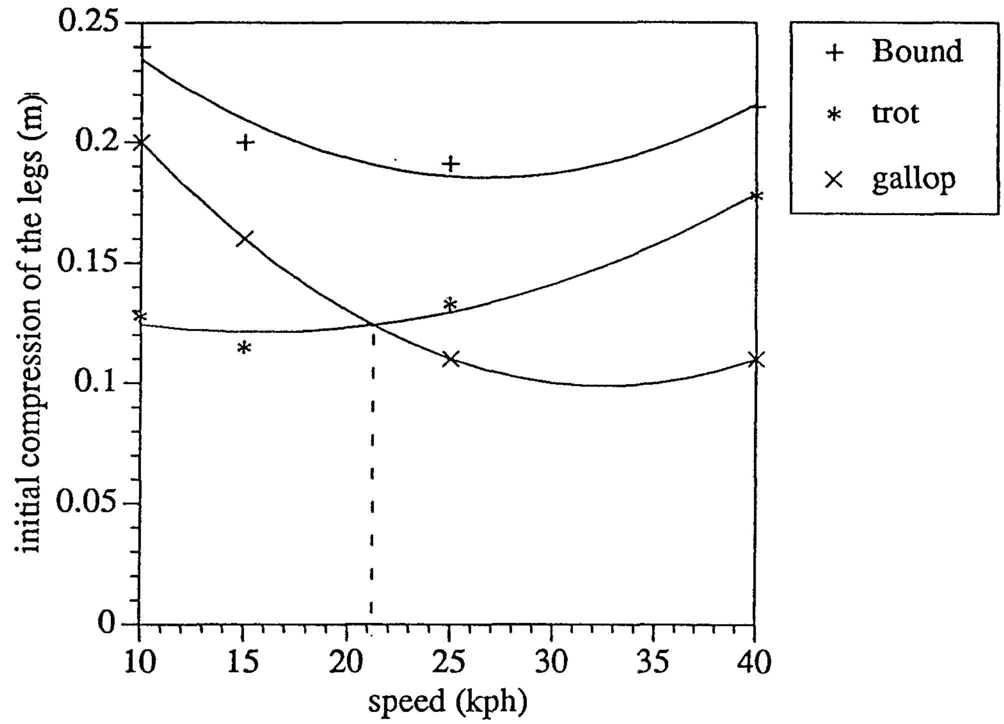

Figure 2.22. Maximum internal energy as a function of speed for trot, bound and gallop at the same stride frequency for a horse.

The above results are similar to those obtained by Hoyt and Taylor, 1981. They trained small ponies to run, using different gaits on command on a treadmill. They then measured the ponies rate of oxygen consumption and found that trotting consumed less oxygen than galloping at speeds below 4.5 m/s. However, at speeds above 4.5 m/s, galloping used less oxygen than trotting. When the ponies were allowed to move at will in a paddock, they trotted at 2.8-3.8 m/s but galloped at speeds over 5 m/s. They chose whichever gait was more energy efficient for the speed at which they were moving. Alexander et. al. (1985) had hypothesized that the flexion of the back played a significant role in the above results. The results from the above simulation suggest that even without the body flexion, there are significant energy advantages in choosing an appropriate gait at a given speeds.

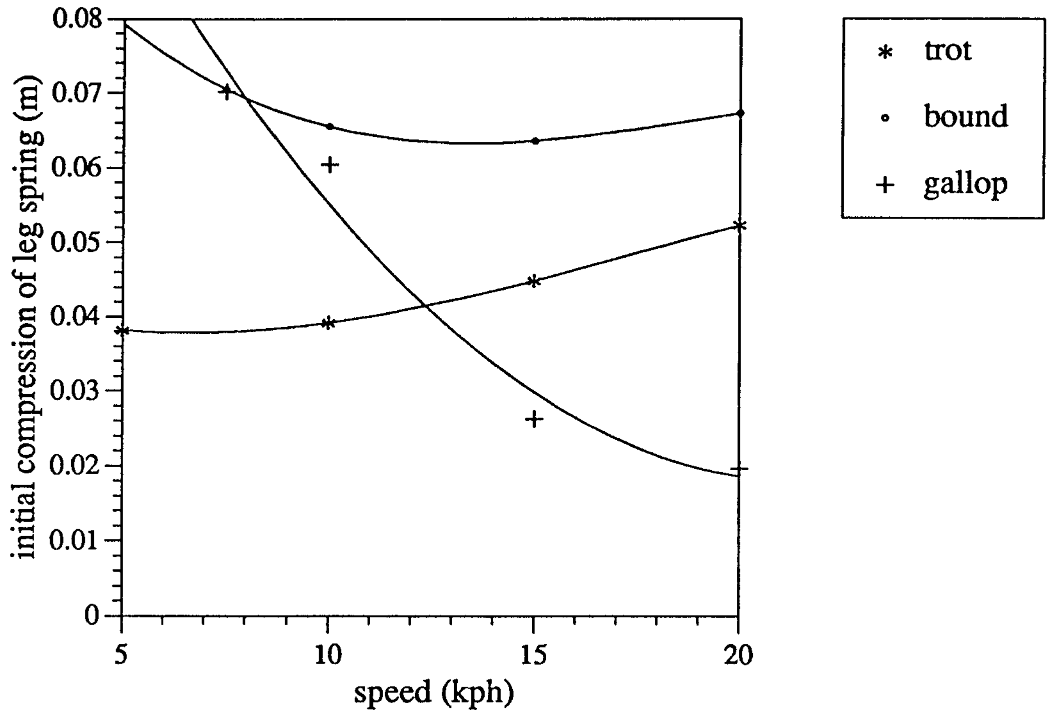

Figure 2.23. Maximum internal energy as a function of speed for trot, bound and gallop at the same stride frequency for a dog.

7. Bound/Gallop with body flexibility

To model body flexure during bounding or galloping, a torsional spring was introduced in the body (Figure 2.24). The initial conditions for this case are shown in Figure 2.24. The legs are given some initial compression (y_i and α) and an initial horizontal velocity. The initial angular velocity for both the segments is set to zero and the angular positions are set to the same value. The stiffness of the torsional spring and the initial angular positions ($\theta_1 = \theta_2$) are varied until a stable solution is obtained.

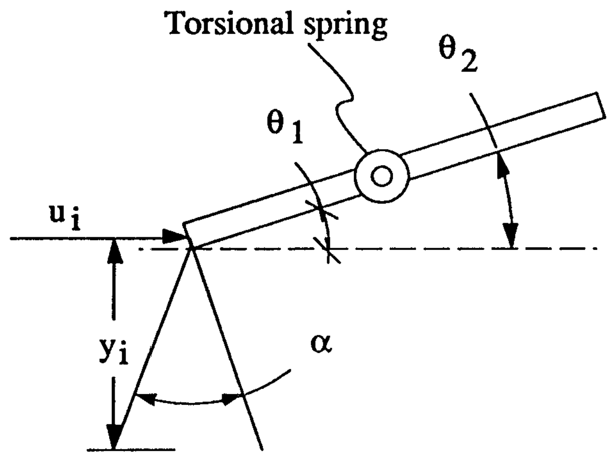

Figure 2.24. Initial Conditions for Quadruped gallop for Model with Body Flexibility.

The equations of motion for this system are given by:

$$\begin{bmatrix} m & 0 & \frac{mL}{8}\text{Sin}\theta_1 & -\frac{mL}{8}\text{Sin}\theta_2 \\ 0 & m & -\frac{mL}{8}\text{Cos}\theta_1 & \frac{mL}{8}\text{Cos}\theta_2 \\ \frac{mL}{8}\text{Sin}\theta_1 & -\frac{mL}{8}\text{Cos}\theta_1 & J+\frac{mL^2}{32} & 0 \\ \frac{mL}{8}\text{Sin}\theta_2 & -\frac{mL}{8}\text{Cos}\theta_2 & \frac{mL^2}{32}\text{Cos}(\theta_1-\theta_2) & J \end{bmatrix} \begin{bmatrix} \ddot{x} \\ \ddot{y} \\ \ddot{\theta}_1 \\ \ddot{\theta}_2 \end{bmatrix} = \begin{bmatrix} a \\ b \\ c \\ d \end{bmatrix} \tag{2.3}$$

where

(x,y) = coordinates of the center of the torsional spring

m = total mass

L = length of the legs and the body

J = mass moment of inertia each segment of the body

a, b, c and d are given by the expressions:

$$a = f_{2x} + f_{1x} + \frac{mL}{8}\left(-\dot{\theta}_1^2\,\text{Cos}\theta_1 + \dot{\theta}_2^2\,\text{Cos}\theta_2\right)$$

$$b = f_{2y} + f_{1y} + \frac{mL}{8}\left(-\dot{\theta}_1^2 \, Sin\theta_1 + \dot{\theta}_2^2 \, Sin\theta_2\right) - mg$$

$$c = k_b(\theta_2 - \theta_1) + \frac{mL}{8} g \, Cos\theta_1 - 0.5L\left(f_{1y} \, Cos\theta_1 - f_{1x} \, Sin\theta_1\right)$$

$$d = -k_b(\theta_2 - \theta_1) + \frac{mL}{8} g \, Cos\theta_2 + 0.25L\left(\left(f_{2y} - f_{1y}\right) Cos\theta_2 + \left(f_{1x} - f_{2x}\right) Sin\theta_2\right) +$$

where

k_b = stiffness of the torsional spring

f_{1x} = force applied by the legs at the rear end in the x-direction

f_{1y} = force applied by the legs at the rear end in the y-direction

f_{2x} = force applied by the legs at the front end in the x-direction

f_{2y} = force applied by the legs at the front end in the y-direction

An attempt was made to find a solution for an example case. The various stages of the gait are shown in Figure 2.25. Note that between stages 2 and 3 and stages 5 and 6, there is an aerial phase. The arrows indicate the direction of the moment applied to the body by the legs. From the directions of these moments, it is clear that the moments will try to increase the angle (θ_1 - θ_2). The initial conditions were: y_i = 1.39 m and u_i=25 kph. The following two approaches were tried in an effort to obtain the solution:

It was assumed that the stages 1 to 3 are symmetrical with stages 4 to 6 (Figure 2.25). This is a reasonable assumption because the loading is symmetrical over the two stages. In stage 1, it was assumed that the body angles θ_1 and θ_2 are equal to each other. Their angular velocities were assumed to be zero. These conditions are as the same as that for gallop without the torsional spring. The simulation was allowed to proceed till stage 4 where it was stopped and the system variables were examined.

This was done repeatedly until the following conditions were obtained at stage 4.

$$(\theta_1)_4 = (\theta_2)_4 = (\theta_1)_1 = (\theta_2)_1$$

The subscript outside the bracket denotes the stage at which the variable is measured. With these tuned initial conditions and torsional spring stiffnesses the simulation was repeated until the end of stage 6 (which should be the same as stage 1). The results are shown in Figures 2.26, 2.27, 2.28 and 2.29. These results were obtained with the following settings:

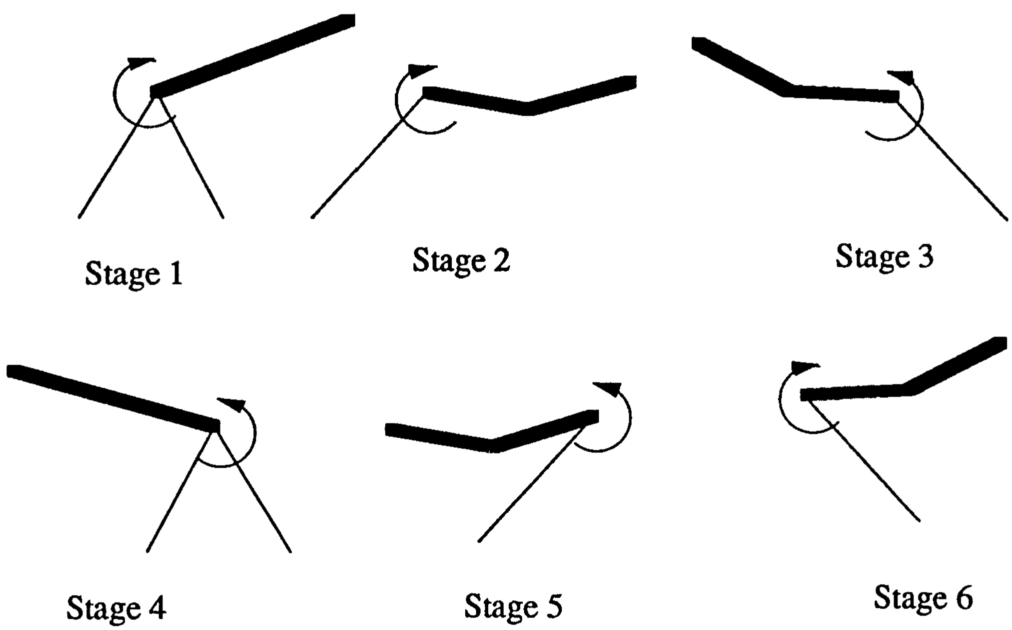

Figure 2.25. Quadruped Gallop with Body Flexibility (Legs not in contact with the ground are not shown).

$K_b = (1.225\ mg/L)\ N/m$

$(\theta_1)_i = 0.0828$ radians.

$(\theta_2)_i = 0.0828$ radians.

Stride frequency = 248.0 strides/min.

The body angles are shown in Figure 2.26. It can be seen from this figure that the body angles at successive strides do not go back to the initial body angles. We need this repeatibility for a stable gait. Initially it was suspected that the simulation was not being done with sufficient accuracy. However, a decrease in the time step did not have any significant effect on the results. Also it was observed that the errors in the system increased with any increase in the energy level of the system. Thus, this simulation could not be repeated for a lower stride frequency. Figure 2.29 shows the energy variations during the stride. The potential energy curve is flatter when compared to the potential energy curve for a gallop without the body flexibility. Most of the energy exchange is taking place between the kinetic energy and the internal energy.

Upon further investigation, it was found that the angular velocities are not zero at stage 4. Also the system seems to be highly sensitive to errors in the angular velocities. An increase in the accuracy of the simulation did not decrease these angular velocities to zero. This indicated the need for a different approach to solve the problem.

The simulation was repeated with different conditions at stage 4. The system was now tuned with the following conditions.

$(\theta_1)_4 = (\theta_2)_4$

$\dot{\theta}_1 = \dot{\theta}_2 = 0$

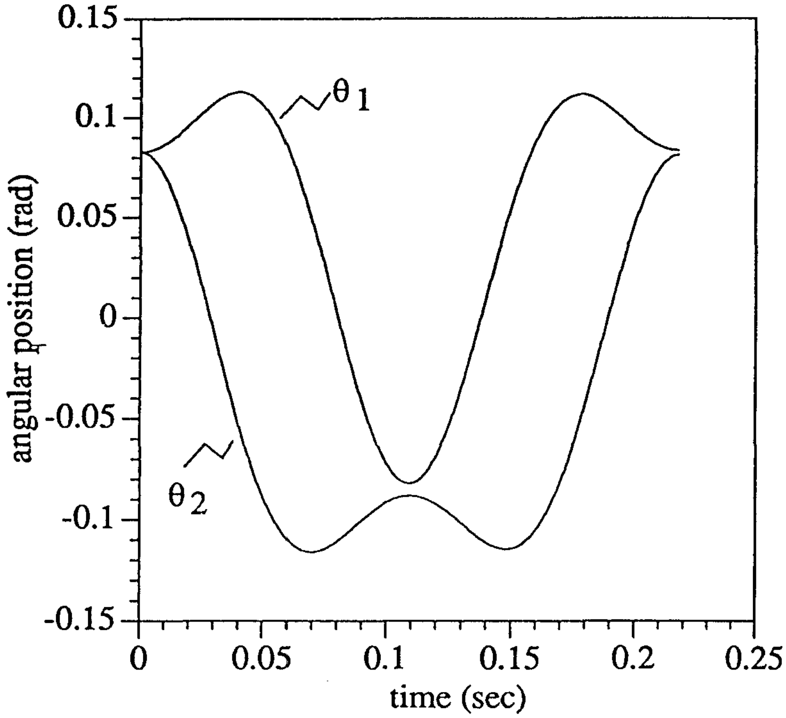

Figure 2.26. Angular orientations of the body segments during the stride (equation 2.3).

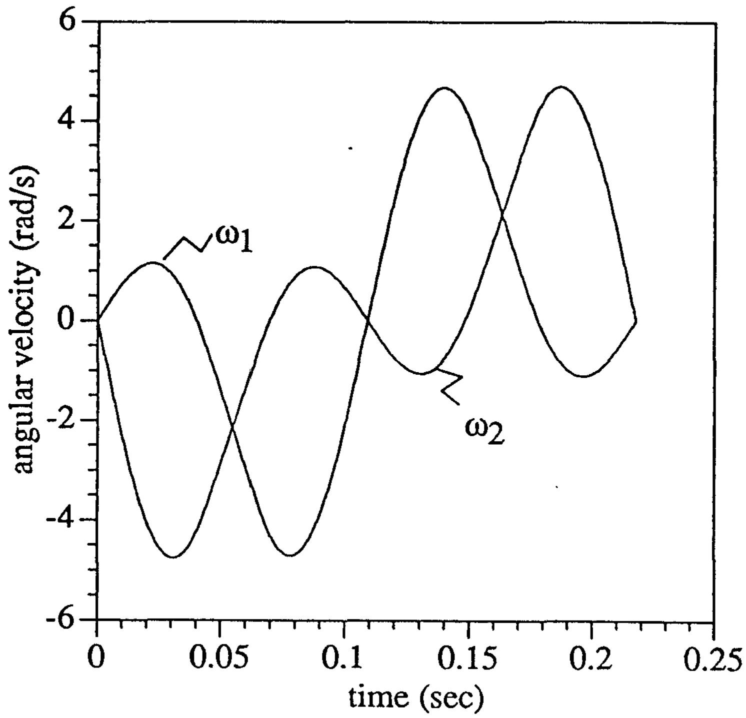

Figure 2.27. Angular velocities of the body segments during the stride (equation 2.3).

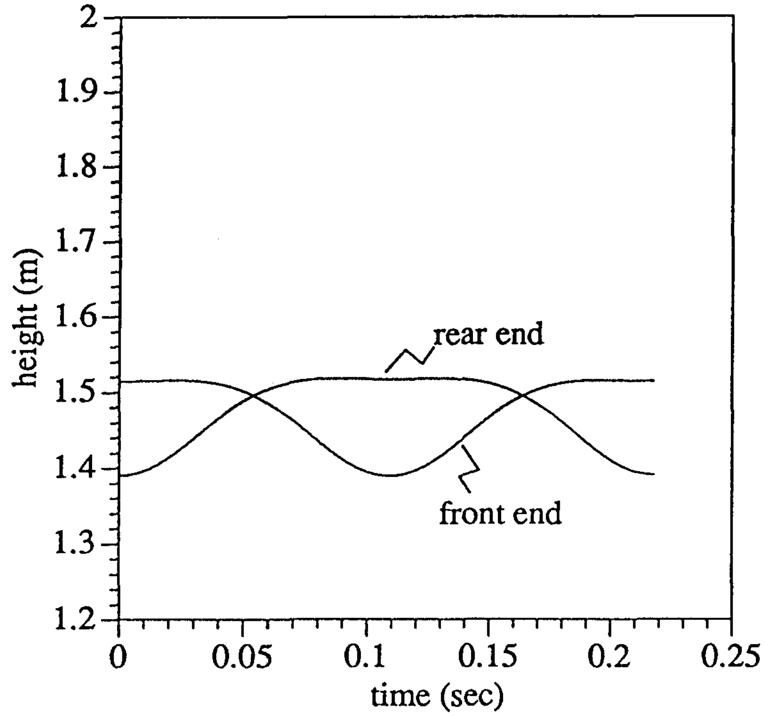

Figure 2.28. Trajectories of the front and rear end of the body for a stride (equation 2.3)

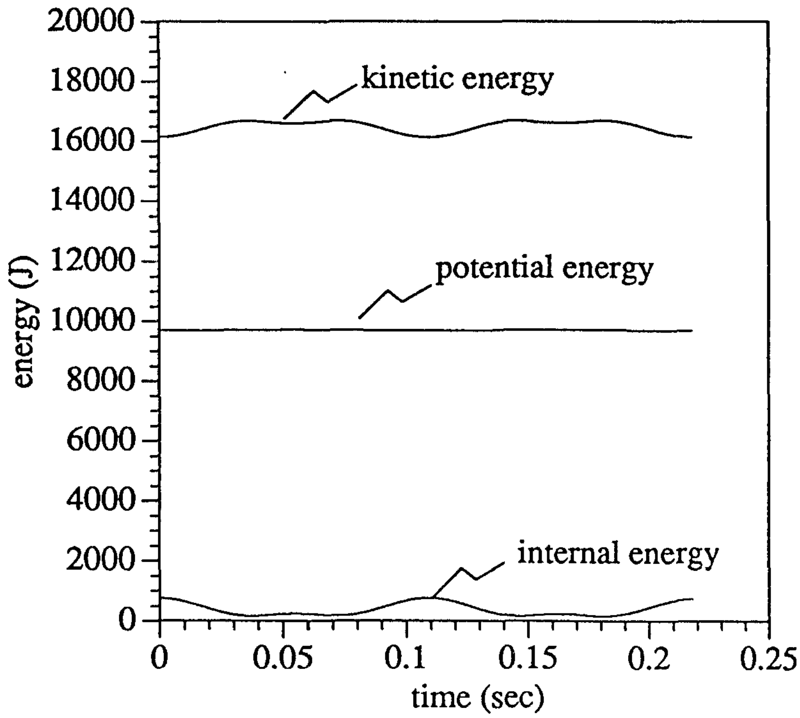

Figure 2.29. Energy variations during the stride (equation 2.2).

The condition on the body angles is easy to satisfy, but the conditions on angular velocities could not be satisfied. The angular velocities can be made to be small (0.2 to 0.3 rad/s), but they do not disappear. Some simulations were conducted with minimized angular velocities. The error increased as compared to the previous approach.

8. Discrepancies between an actual gallop and the above simulations

An actual gallop with body flexibility is shown in Figure 2.30.

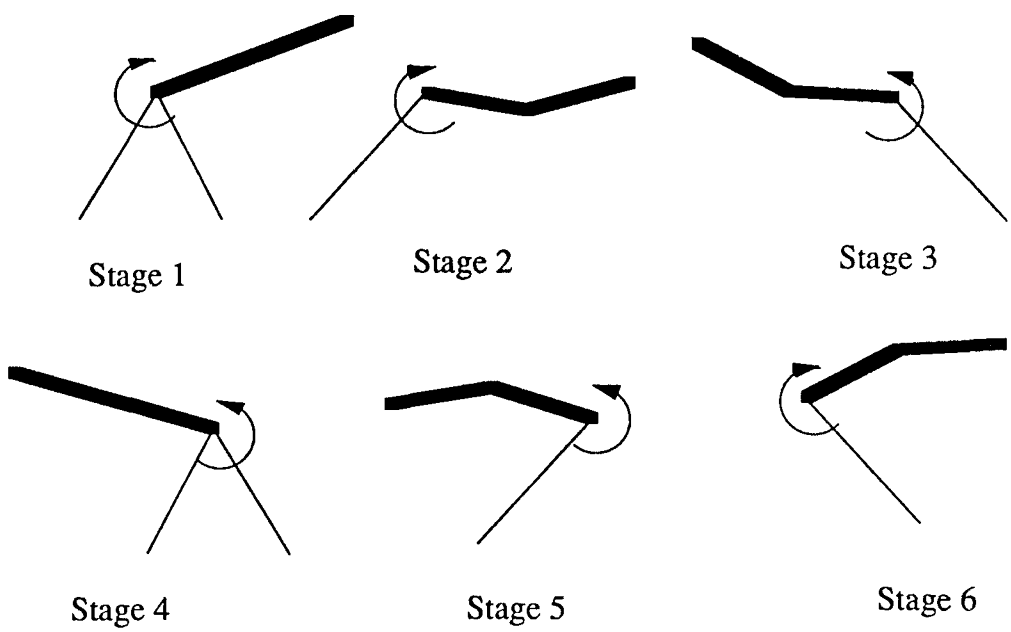

Figure 2.30. An Actual Quadruped Gallop with Body Flexibility (Legs not in contact with the ground are not shown).

The differences between an actual gallop and our simulation are in stages 5 and 6. Observe the moment applied to the main body by the legs in stages 5 and 6. The body seems to be flexing in opposition to the moments. This is possible if the angular velocities at stage 4 are not equal to zero, or if the torsional spring is not a passive actuator. An attempt was made to obtain a stable solution by removing the condition that the angular velocities at stages 1 or 4 have to be equal to zero. The results were not encouraging enough to pursue this approach any further.

9. Note on Numerical Solutions

The differential equations in this thesis were solved using a commercially available simulation package called Advanced Continuous Simulation Language (ACSL). A time step of 1 msec was found to be sufficient for an accurate simulation. Runge-Kutta fourth order was used to solve these equtaions in ACSL. For later simulations involving Poincare maps, a stand alone fortran program was also developed. This program used Runge-Kutta-Fehlberg to solve the differential equations. The time step used was 1 msec except in the viccinity of the leg touchdown phase. During these periode the time step was reduced to 10 μsec. To obtain data for each Poincare map from this program, it was not unusual to run the program for upto 10 cpu hours on a VAX-8550.

The results from the simulations were displayed using a stick figure animation on the VAX-8550. The body was represented by a wire frame model of a . Each of the legs in contact with the ground were represented by two links. The position of the knee was computed using a kinematic constraint. The legs not in contact with the ground were not shown.

10. Summary

In this chapter, a simple model for the quadruped has been used to obtain trajectories (stable trajectories) of a single stride for trot, gallop and bound. These trajectories are assumed o be symmetric over a stride. It has been shown that, for a given speed, an infinite number of stable trajectory can be obtained. The exact trajectory is obtained using the stride frequency data from field observations conducted by earlier researchers. These trajectories have been compared at various speeds. It has been shown that in the case of a trot, the energy exchange takes place between the gravitational potential energy, kinetic energy and the internal energy (stored in springs). In contrast, during a gallop, the energy exchange takes place between the internal energy and the kinetic energy only. Further, it has been shown that a trot is more energy efficient at slower speeds and a gallop is efficient at faster speeds. Two sample cases of a horse and a dog have been considered. An effort was made to consider the flexibilty of the body by including a torsional spring. It was difficult to compute the stable trajectory. It was laborious to compute the stiffness of the torsional spring and the results were dubious at best. In the later chapters, it will be shown that a stable gallop is possible without the flexion of the back. These results suggest that from a design point of view, it is not a good idea to have flexion in the back.

CHAPTER III

CONTROLLER FOR CONSTANT SPEED (TWO DIMENSIONAL MODEL)

1 Introduction

A dynamic model for the two dimensional quadruped has been developed. The main body is modelled as a rigid bar and each leg consists of a constant stiffness spring, a viscous damper and a force actuator. Using the techniques developed in the previous chapter, we will devise a controller that will enable the quadruped to gallop at constant speed. It will be shown that symmetry principles can be used to devise simple control strategies for a two-dimensional gallop. The controller consists of two parts: an energy controller which will apply the required amount of force through the legs, and the speed controller that will control the forward speed by appropriately placing the legs. It will be shown that the body pitch need not be explicitly controlled. The stability of this controller will be examined using Poincare maps. Stable systems show either periodic or quasi-periodic response. Further, a chaotic response leads to an unstable system. The stability of the system with changes in the initial conditions, as well as variations in the system parameters, will also be examined. It will be shown that the system is stable for a range of leg stiffnesses. Outside this range, the system shows chaotic behavior.

2. Problem statement

The gallop consists of two phases: aerial phase and the stance phase. During the stance phase, one or more legs are in contact with the ground. At the end of this phase, the legs push the body off the ground and the legs are no longer in contact with the ground. This is the beginning of the aerial phase. During the aerial phase, the quadruped repositions its legs for the next stance phase. This process is repeated and we obtain a stable gait. The period from the beginning of the stance phase to the end of the aerial phase will be referred to as a step.

As described earlier, there are two free variables in this system. One of them is the horizontal speed, u, and the other is the total energy, E, of the system. At any given speed, the only free variable is the total energy of the system. The energy level for a particular speed is set to minimize the energy lost in the system. At this optimum energy level, the quadruped has an optimum stride frequency. Since we have not modelled the energy required to reposition the leg for the next stance phase, we cannot calculate the optimum energy or the optimum stride frequency for a given speed. Thus the stride frequency at a particular speed will be set from the experimental data.

The control problem for this system can be stated as follows: The problem is to generate a control scheme for this system that will provide a stable gait for a given energy level and speed. The important objective here is to obtain a stable gait; the speed and energy level are of secondary importance. The speed and the energy of the system are not constant during the stance phase, but they are constant over the aerial phase. Thus we will try to approximately control the speed and energy level during the aerial phase.

3. Two dimensional dynamic model for a quadruped

The two dimensional model for the quadruped is shown in Figure 3.1. The main body is modelled as a rigid beam. Two legs are attached to the front end of the beam and the other two legs are attached to the rear end of the beam. Each leg is modelled as a massless spring and damper in parallel. Let the coordinates of the center of mass of the quadruped (the center of the main body) be (x, y) and the velocity of the center of mass denoted by the pair (u, v). The angular orientation of the body is given by the pitch angle θ. Let the coordinates of the front end of the body be (x_1, y_1) and the coordinates of the rear end of the body be (x_2, y_2). The legs are attached to these points. Then

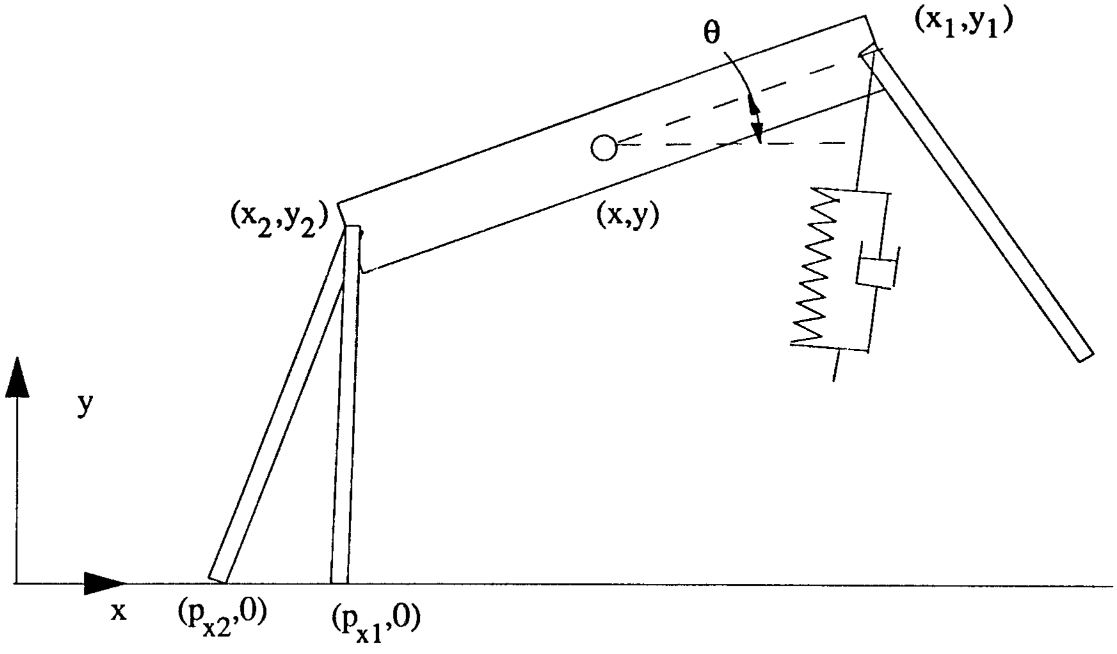

Figure 3.1. Two dimensional model of the quadruped.

$$x_2 = x - \frac{L}{2}\cos\theta$$
$$y_2 = y - \frac{L}{2}\sin\theta$$
$$x_1 = x + \frac{L}{2}\cos\theta$$
$$y_1 = y + \frac{L}{2}\sin\theta$$

Let the front two legs be placed at the coordinates (p_{x1}, 0) and (p_{x2}, 0), and the rear two legs be placed at coordinates (p_{x3}, 0) and (p_{x4}, 0). Then the force acting on the main body due to the spring in the front legs is given by

$$f_{si} = K_{sp}\sqrt{(p_{xi} - x_1)^2 + y_1^2} \qquad i = 1,2$$

Similarly the force acting on the main body due to the spring in the rear legs is given by

$$f_{si} = K_{sp}\sqrt{(p_{xi} - x_2)^2 + y_2^2} \qquad i = 3,4$$

The forces generated by the damper in the legs are proportional to the velocity component of the leg ends relative to the body directed along the legs. These velocity components are:

$$v_{li} = \frac{(u - L/2\sin\theta)(x_1 - p_{xi}) + (v + L/2\cos\theta)y_1}{\sqrt{(x_1 - p_{xi})^2 + y_1^2}} \qquad i = 1,2$$
$$v_{li} = \frac{(u + L/2\sin\theta)(x_2 - p_{xi}) + (v - L/2\cos\theta)y_2}{\sqrt{(x_2 - p_{xi})^2 + y_2^2}} \qquad i = 3,4$$

Therefore the damping force exerted by each leg is given by

$$f_{di} = \xi v_{li} \qquad i = 1,.., 4$$

where ξ is the damping coefficient.

The total force acting on the body is given by

$$f_x = \sum_{i=1}^{2}\left\{(f_{si} - f_{di})\frac{(x_1 - p_{xi})}{\sqrt{(x_1 - p_{xi})^2 + y_1^2}}\right\} + \sum_{i=3}^{4}\left\{(f_{si} - f_{di})\frac{(x_2 - p_{xi})}{\sqrt{(x_2 - p_{xi})^2 + y_2^2}}\right\}$$

$$f_y = \sum_{i=1}^{2}\left\{(f_{si} - f_{di})\frac{y_1}{\sqrt{(x_1 - p_{xi})^2 + y_1^2}}\right\} + \sum_{i=3}^{4}\left\{(f_{si} - f_{di})\frac{y_2}{\sqrt{(x_2 - p_{xi})^2 + y_2^2}}\right\}$$

The total moment τ acting on the body is given by

$$\tau = \sum_{i=1}^{2}\left\{(f_{si} - f_{di})\frac{(x_1 - p_{xi})(-L/2\sin\theta)}{\sqrt{(x_1 - p_{xi})^2 + y_1^2}}\right\} + \sum_{i=3}^{4}\left\{(f_{si} - f_{di})\frac{(x_2 - p_{xi})(L/2\sin\theta)}{\sqrt{(x_2 - p_{xi})^2 + y_2^2}}\right\}$$
$$+ \sum_{i=1}^{2}\left\{(f_{si} - f_{di})\frac{y_1(L/2\cos\theta)}{\sqrt{(x_1 - p_{xi})^2 + y_1^2}}\right\} + \sum_{i=3}^{4}\left\{(f_{si} - f_{di})\frac{y_2(-L/2\cos\theta)}{\sqrt{(x_2 - p_{xi})^2 + y_2^2}}\right\}$$

The equations of motion are given by

$$M\dot{u} = f_x$$

$$M\dot{v} = f_y$$

$$I\ddot{\theta} = \tau$$

where

M = mass of the body

I = moment of Inertia

4. Overview of the control scheme

These equations are highly nonlinear. Further, these equations change depending on whether none of the legs or a single leg or multiple legs are in contact with the ground. The controller for this system should generate a stable gait. A "stable" gait is difficult to define in the traditional sense. Since we expect the gait to repeat itself, the control scheme should generate limit cycles in the phase planes. However, this requirement need not be strict. If the cycles in the phase plane lie within a narrow band, the gait will be stable. Therefore a non-traditional approach is used to solve this problem.

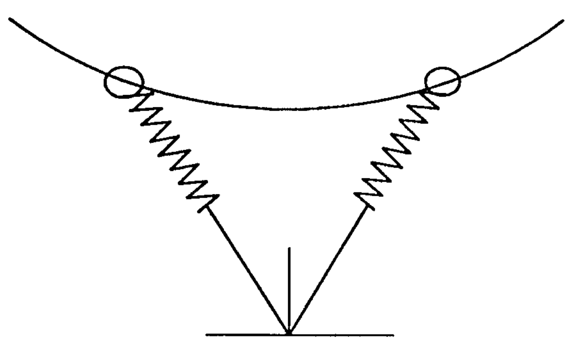

Figure 3.2. Constant speed trajectory.

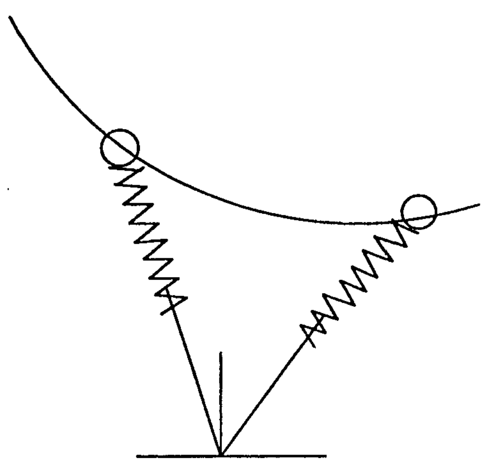

Figure 3.3. The speed increases with trajectory

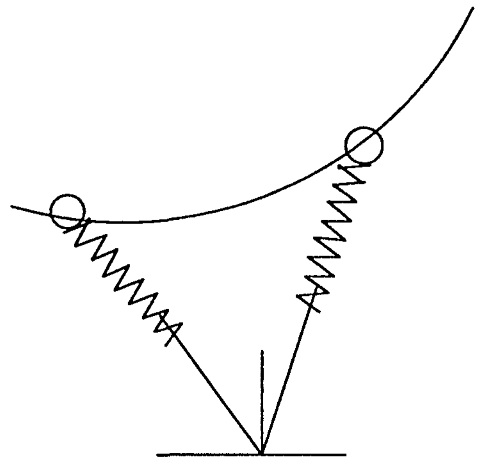

Figure 3.4. The speed decreases with this this trajectory

Consider a simple mass and spring system as shown in Figure 2.1. A stable gait for this system is shown in Figure 3.2. In this case, the speed at the beginning of the stance phase is the same as that at the end of the stance phase. Let the leg angle at the beginning of the stance phase be γ_{eq}. Figures 3.3 and 3.4 show unstable cycles. In Figure 3.3, the speed at the end of the stance phase is greater than the speed at the beginning of the stance phase. In this case the leg angle, γ, at the beginning of the stance phase is less than γ_{eq}. Similarly if the leg angle at the beginning of the stance phase is greater than γ_{eq}, the speed decreases. This case is shown in Figure 3.4. These results suggest a convenient method to control the speed. If the speed has to be reduced the leg angle for the next stance phase is increased and vice versa. We can make another important observation from these results. If the leg angle for the next stance phase is set to be the same as the leg angle at the end of the previous stance phase, then from symmetry, the speed at the end of the next stance phase should be close to the speed at the beginning of the previous stance phase. Therefore, this will enable us to keep the average speed approximately constant. The similarity between the previous trajectory and the next trajectory also ensures stability. If the previous step was stable, then the next step will also be stable. This set of observations forms the backbone of the control scheme.

The above arguments hold for a quadruped gallop also. The gallop introduces a pitching motion of the body. Again from the symmetry arguments, it is hoped that the pitching motion will not require additional control. This will be confirmed from simulations.

5. Control scheme

The above scheme essentially allows us to learn from the previous step and predicts the outcome of the next step without solving the highly nonlinear equations. The above scheme is shown in terms of a block diagram in Figure 3.5. During the aerial phase two important control variables are computed. The first one is the leg angle, γ, at landing. This angle is set equal to the leg angle at the end of the previous stance phase. The other variable is the amount of actuator force, F, required to compensate for the losses in the energy. During the next stance phase, this constant actuator force will be generated by the leg in addition to the spring force. The equations for this scheme are:

$\gamma_{n+1} = \gamma_n$

$F_{n+1} = K_{PF} (E_d - E_n)$

where

γ_{n+1} = leg angle for the next step

γ_n = leg angle for the present step

F_{n+1} = extra actuator force for the next step

K_{PF} = constant

E_d = desired energy level

E_n = Energy level for the present step

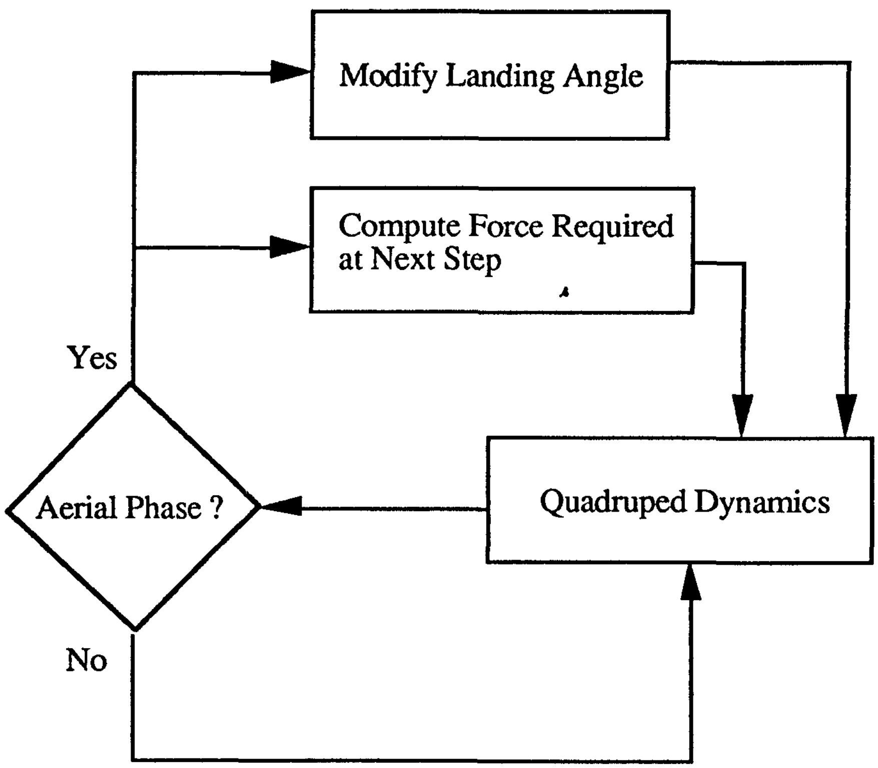

Figure 3.5. Block diagram for the control scheme

The above strategy was used to control a quadruped with the parameters

$M = 680$ kg, $L = 1.5$ m, $K_{sp} = 62260.8$ N/m, $\xi = 0.05$.

The control gains were set to be

$K_{PF} = 15$

The results of this strategy is shown in Figures 3.6. This figure shows the speed of the quadruped, the leg actuator force necessary to overcome the viscous losses, the leg angle at the beginning of every stance phase and the desired energy level and the actual energy level. These plots indicate that the energy controller is stable, but there is a steady state error. The speed controller is performing as expected. The speed is the same for every other step. There is a tendency for the speeds at consecutive steps to diverge. This will ultimately lead to instability. This is not unexpected as there is no direct speed feedback in the system.

To remedy this, a speed feedback was added to the system. The leg angle at the beginning of the next stance phase is set equal to the leg angle at the end of the previous stance phase plus an error value. This error value is equal to a constant multiplied by the difference in the desired speed and the speed during the previous aerial phase. Note that it is not the current speed but the speed during the previous aerial phase which is used for feedback. Since the leg angle is set so that the speed during the next aerial phase will be approximately the same as that during the previous aerial phase, we have to feed back the speed during the previous aerial phase in order to modify the speed. Speed feedback of the current aerial phase leads to an unstable control scheme.

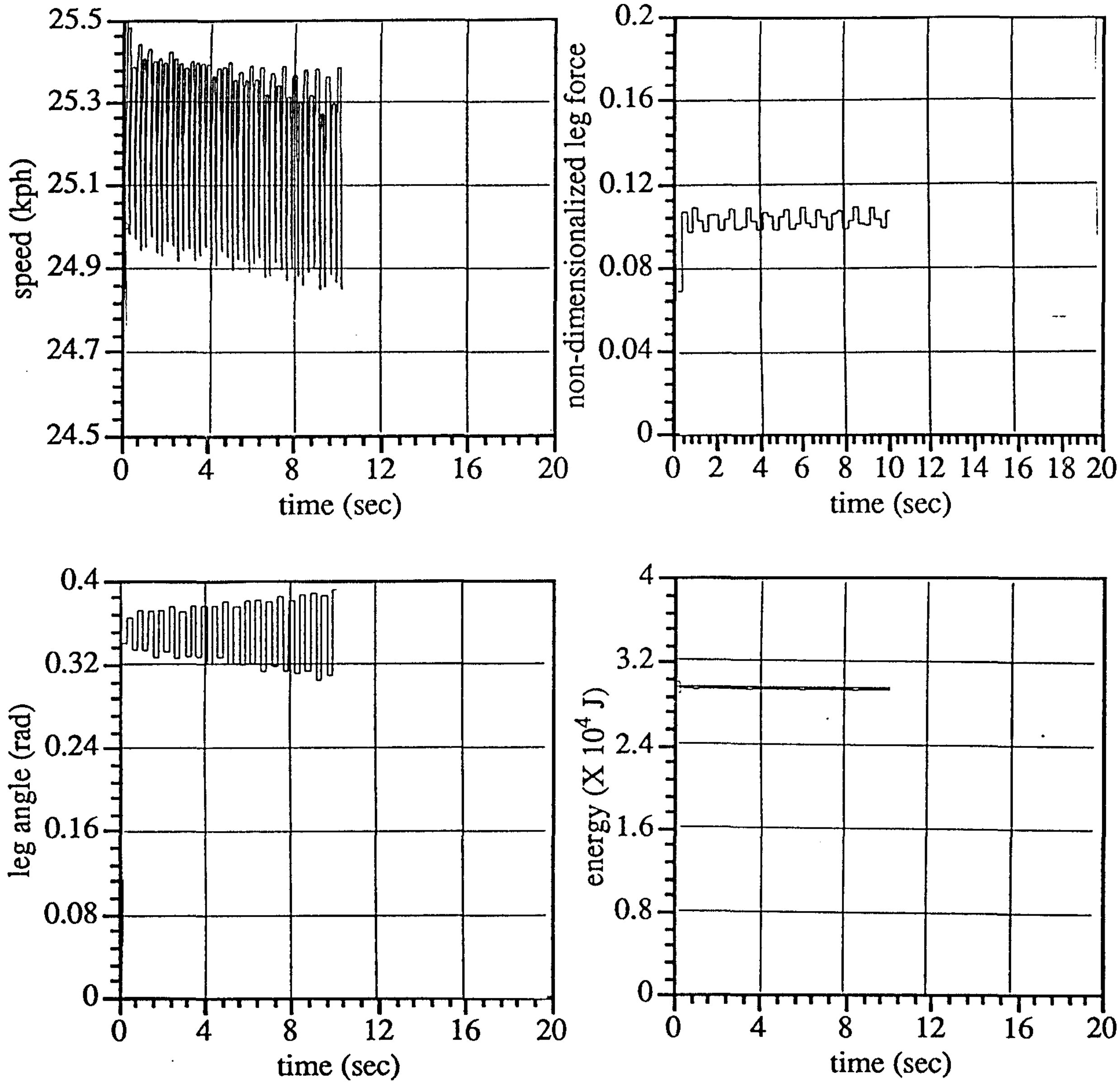

Figure 3.6. Response of the system with a proportional energy controller and without speed feedback.

The energy controller is modified to remove the steady state error. This is achieved by adding an integral control. The actuator force is set equal to a constant multiplied by the difference between the current energy level and the desired energy level, plus the actuator force used in the previous stance phase. This leads to an accumulation of the error term and removes the steady state error. The above equations are now modified to:

$$\gamma_{n+1} = \gamma_n - K_\gamma (u_d - u_{n-1})$$
$$F_{n+1} = K_{PF} (E_d - E_n) + K_{IF} \sum_{i=1}^{n} (E_d - E_i)$$

where

u_d = desired speed

u_{n-1} = horizontal velocity during the aerial phase of the previous step

K_{IF}, K_γ = constants

The control constants were set to be

$K_\gamma = 0.2$, $K_{IF} = 0.2$

The results from these modifications are shown in Figures 3.7. The speed controller is now stable and there is no steady state error in the energy controller. Thus we have been able to construct a controller that seems to generate a stable gait. This controller was successfully tested for different speeds and initial conditions.

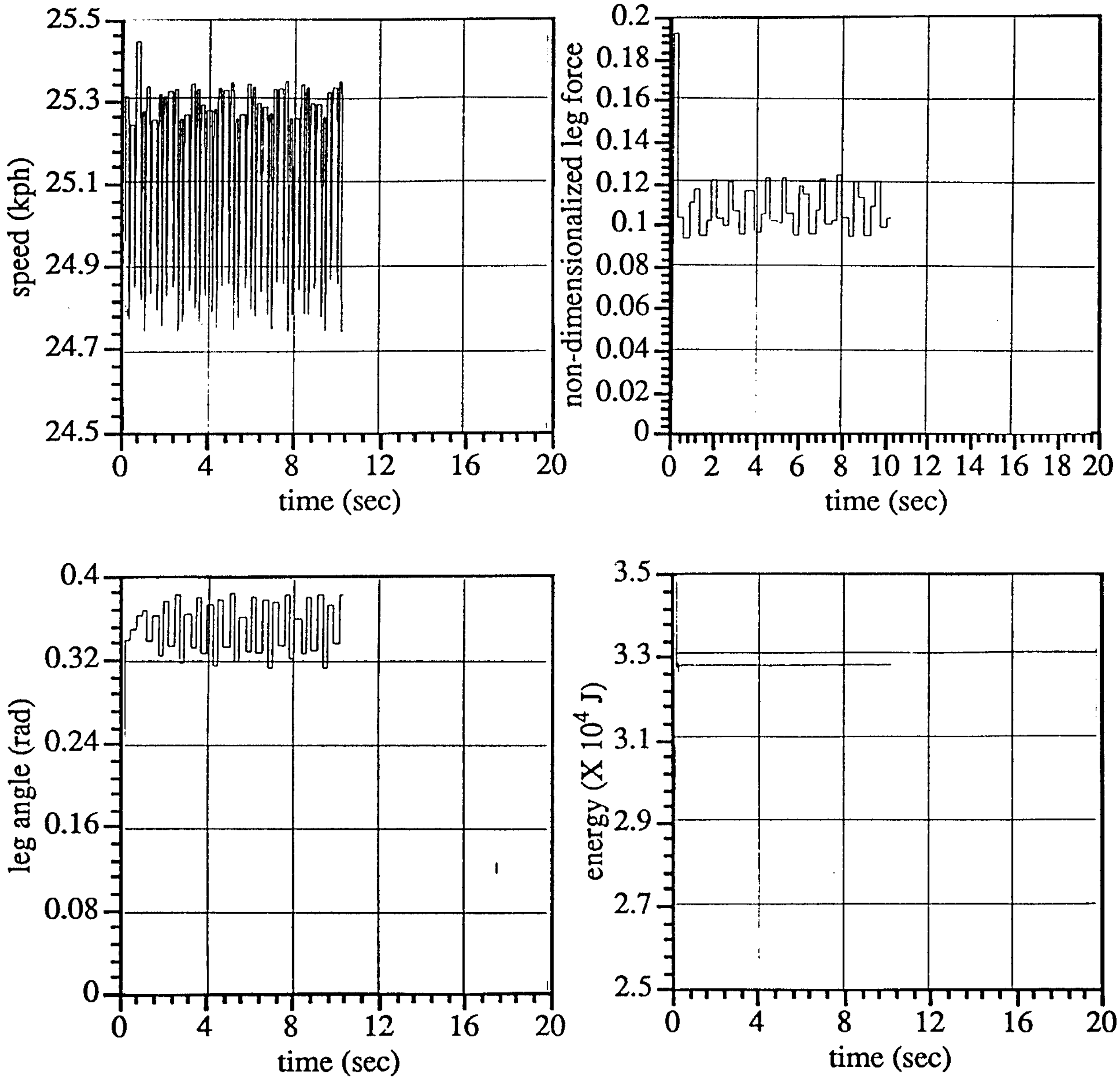

Figure 3.7. Response of the system with speed feedback and proportional-integral energy controller.

6. Stability of the control scheme

Recent investigations in nonlinear dynamics have shown that it is not always possible to predict the behavior of relatively simple dynamical systems, far into the future using computer simulations. These systems have been labelled as chaotic. They should not be confused with random systems. These systems do not have any random inputs and their parameters are deterministic. Nevertheless, they are extremely sensitive to initial conditions. Small differences in initial conditions grow exponentially for these systems and this property makes any long term prediction difficult.

The systems that exhibit chaos typically have the following properties (Moon, 1989).

1) They consist of a nonlinear element like a nonlinear spring, nonlinear damping, nonlinear feedback, etc. A linear system cannot exhibit chaos.

2) They do not have any random inputs.

3) The time history of the signal should not show any pattern or periodicity. This does not ensure that the system is chaotic. The system may have a long period or may be quasiperiodic. A quasiperiodic system consists of two or more incommensurate frequencies, thus the signal may appear to be non-periodic, but it could be broken down into a sum of periodic signals.

4) The phase plane plots of chaotic motions never close or repeat. Thus, the trajectory of the orbits in the phase plane will tend to fill up a section of the phase space. Periodic

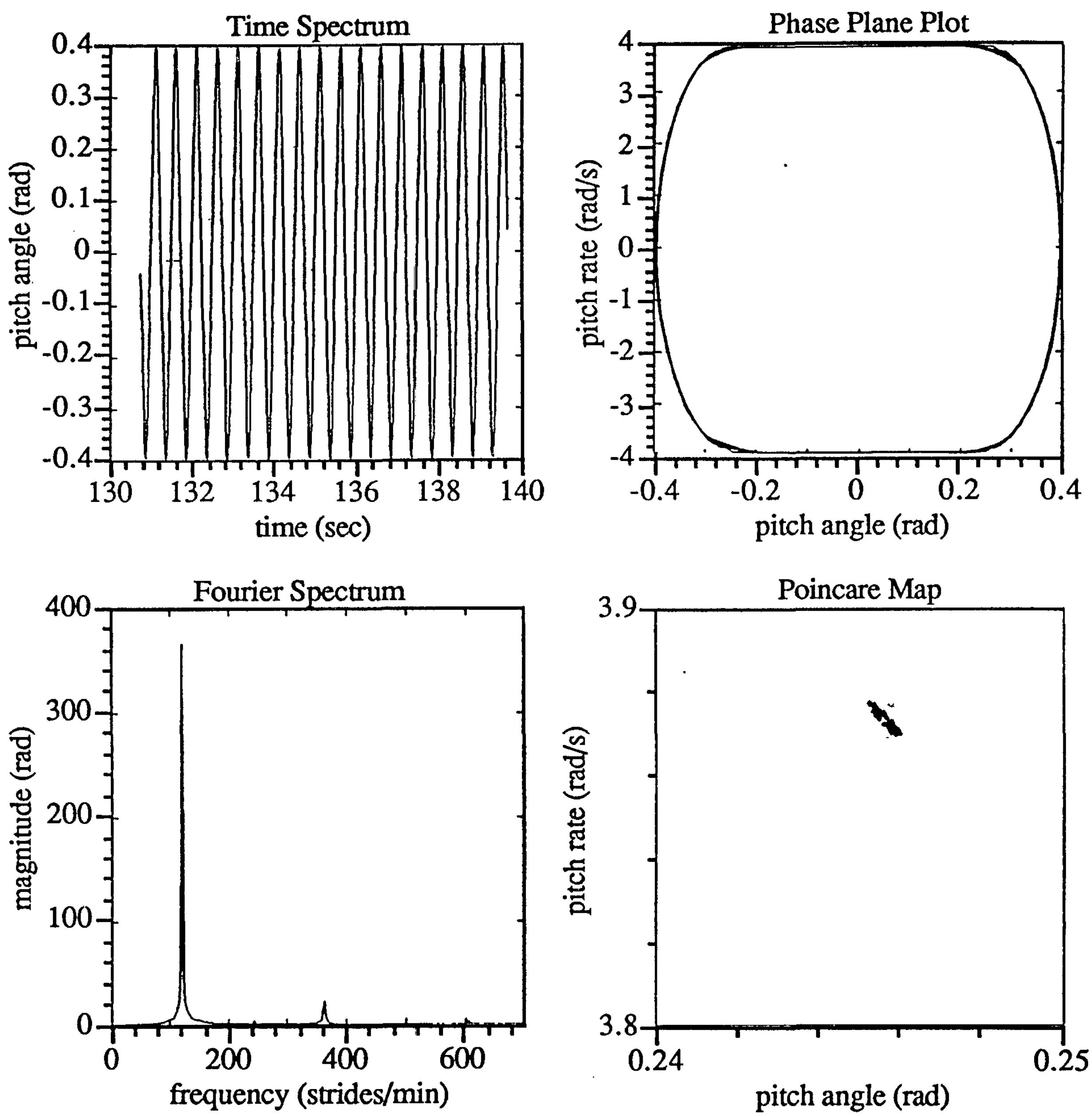

Figure 3.8. Response of a typical periodic quadruped gallop.

signals will exhibit limit cycles. Again, it is not possible to distinguish between quasiperiodic and chaotic signals from the phase plane plots.

5) The Fourier spectrum of the signal should show a broad spectrum of frequencies in the output when the input is a single frequency harmonic motion, or a constant. Often, if there is a dominant frequency component ω_0, a precursor to chaos is the appearance of subharmonics ω_0/n in the frequency spectrum.

6) A useful tool in the study of nonlinear systems is the Poincare map. One of the variables in the system and its derivative is sampled once during every period. A graph is then plotted between the value of the variable and the its derivative. The Poincare map of a periodic system consists of a finite number of points. For a quasiperiodic system, the Poincare map consists of a closed curve. Finally if the system does not consist of either a finite number of points or a closed curve, then the system could be chaotic.

7) The behavior of the system varies with the changes in the initial conditions and the parameters. The system might show periodic or quasiperiodic behavior for some range of input and parameter space. This will ensure that there are no random inputs to the system.

The system under study in this thesis is a nonlinear system with nonlinear feedback. There are no random inputs to the system. It will be shown that the above system shows periodic as well as chaotic behavior. Simulations will be conducted for the two cases and a detailed analysis follows. The two set of initial conditions are:

1) $u_i = 20$ kph, $\theta_i = 0.3$ rad, $y_i = 1.32$ m

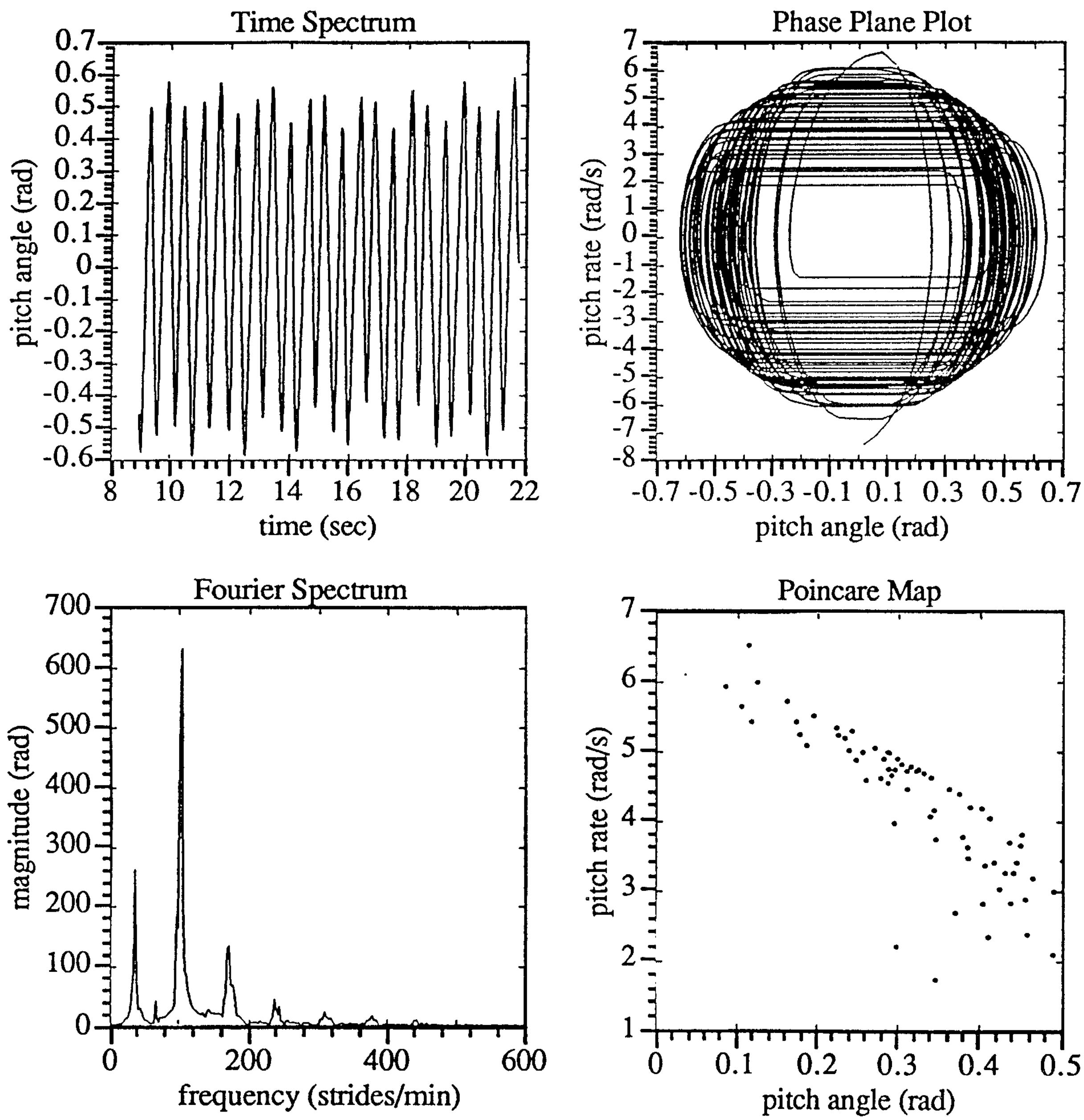

Figure 3.9. Response of a typical chaotic quadruped gallop.

2) u_i = 20 kph, θ_i =0.5 rad, y_i = 1.32 m

The nondimensionalized leg stiffness was assumed to be 14. The pitch of the quadruped is conveniently chosen to study the behavior of the system. The pitch angle for case 1 is shown in Figure 3.8. This can be compared with the response shown for case 2 shown in Figure 3.9. The time history for the first case is shown after the transients have died off. The time history for the first case shows periodic behavior while the second case does not show any periodicity. This is confirmed further from the phase plane plots shown in the figure. These phase plane plots show the pitch rate versus the pitch angle of the quadruped. Case 1 shows a single curve in the phase plane plot while case 2 fills up the a section of the phase plane. The frequency of the periodic system in case 1 can be obtained from the fourier spectrum analysis of the pitch angle. This frequency from Figure 3.8 is 120.0 strides/min which is the stride frequency of the quadruped. The fourier spectrum of the second system again shows a broad spectrum of frequencies. Note that there is still a dominant frequency which corresponds to the stride frequency. The final test for the system is the Poincare map.

To construct the Poincare maps for the above system, the pitch angle is chosen as the Poincare variable. The pitch angle and the pitch rate will be sampled at a specific event once during every period. The specific event is chosen to be the beginning of the stance phase during which the rear legs support the body. These Poincare maps for case 1 and case 2 are shown in Figures 3.8 and 3.9 respectively. From these Poincare maps, it is clear that case 1 is periodic (single point) and case 2 is a chaotic system (the points are spread over the map).

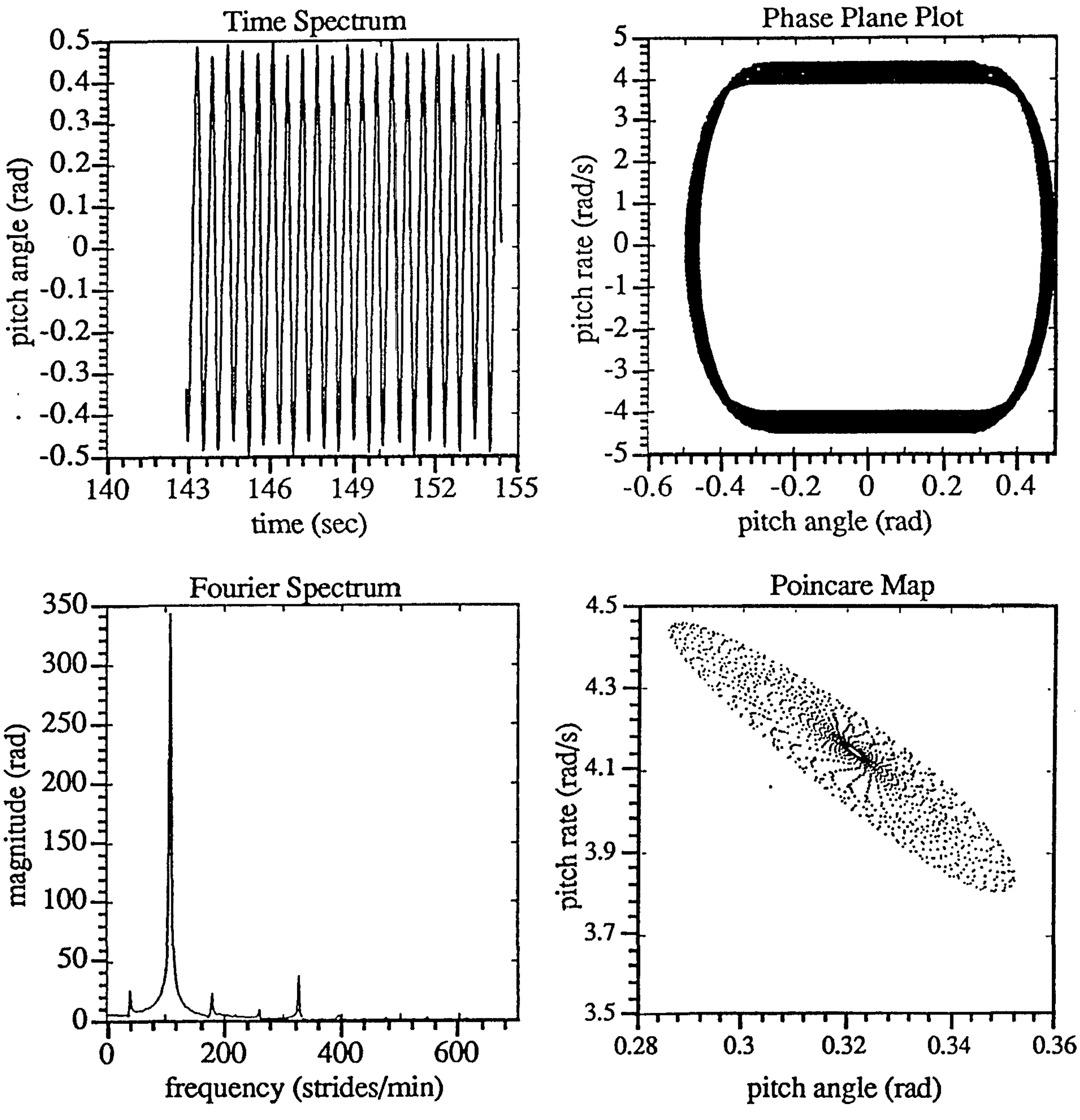

Figure 3.10. Response of a typical quasiperiodic quadruped gallop.

From the above study, an important conclusion can be drawn. The control scheme is stable for some initial conditions and chaotic for the others. The chaotic system is unstable. Thus for the system to be stable, it should not be chaotic. An interesting study would be to examine the route to chaos. This can be examined by means of the response of the system at the marginally stable stage. This will be referred to as case 3 and the initial conditions are shown below.

3) u_i = 20 kph, θ_i =0.42 rad, y_i = 1.32 m

The response of this system is shown in Figure 3.10. The time spectrum is almost periodic. This can be examined further in the phase plane plot. Again the trajectories fill up a band in the phase plane plot. The fourier spectrum of the system shows two dominant frequencies. These are marked out in the plot shown in Figure 3.10. This response is typical of quasiperiodic systems. The Poincare map confirms the quasiperiodic nature of the response. The points fill up a band in the Poincare map. This response results from two incommensurate frequencies in the response.

From the above analysis, it has been shown that the system shows quasiperiodic response before entering chaos. This is a well documented route to chaos (Moon, 1989).

The above analysis was extended further to study the effect of the initial conditions on the system. The control scheme should be robust enough to handle a variety of initial conditions and generate stable gaits.

The first set of simulations were conducted by varying the initial body pitch angle γ. The results are shown in Figure 3.11a and Figure 3.11b. It is clear that the control scheme is stable for a variety of initial pitch angles. At a speed of 20 kph, the system is stable for a range of body pitch angles from 0.2-0.45 rad. The results are shown in Table 3.1.

The simulations were then conducted for the system by varying the initial compression of the spring. This controls the energy level of the system. Again there is a minimum and maximum energy level of the system for which it will generate stable solutions. For the other cases the system is chaotic. These results are shown in Figure 3.12 and Table 3.2.

The simulations were studied by varying the nondimensional leg stiffness, K_{leg}. The nondimensional leg stiffness, K_{leg} was varied from 10 to 70. For this set of simulations, the total energy of the system was set to a constant value to ensure that the energy variations did not induce chaos. This was achieved by varying the initial compression of the leg springs with variation of the leg stiffness. It can again be seen that there is a minimum and maximum value of the leg stiffness (15-50) within which the system is stable. If K_{leg} is outside this range, chaos results. These results are shown in Figure 3.13 and Table 3.3.

The above results are shown for a constant speed of 20 kph. The speed was increased to study the effect of higher speeds on the stability of the system. It was observed that at higher speeds, the system was stable for larger values of K_{leg}. These results are given in Table 3.4. The speed was increased to 35 kph and it was found that stable solutions could not be generated for $K_{leg} < 18$. At a speed of 45 kph, stable solutions were possible only for $K_{leg} > 21$. This indicates the need for a minimum leg stiffness if the quadruped is expected to gallop for a range of speeds.

Table 3.1 Gallop with variation in the initial pitch angle

initial speed, u_i (kph)	initial length of leg spring, y_i (m)	initial body pitch angle, θ_i (rad)	non - dimensional leg stiffness, K_{leg}	stride frequency (strides/min)	nature of system
20	1.32	0.15	14	130	unstable
20	1.32	0.2	14	134	stable
20	1.32	0.25	14	127	stable
20	1.32	0.3	14	121	stable
20	1.32	0.35	14	116	stable
20	1.32	0.4	14	111	stable
20	1.32	0.45	14	106	unstable
20	1.32	0.5	14	102	unstable

7. Summary

In this chapter, a non-linear controller has been developed for a gallop. The controller consists of two sub-controllers; one of them controls the total energy of the system and the other controls the speed of the machine. It has been shown that the controller is stable and that the pitch motion of the body does not have to be explicitly controlled. The stability of the system has been examined using Poincare maps. The system has been shown to be stable for a variety of initial conditions and parameters. The stable system shows either periodic or quasiperiodic behavior. For some initial conditions and parameters, the system is unstable. It has been shown that this instability of the system is due to chaos. Further, it has been shown that there is a range of leg stiffnesses for which the system will always exhibit chaotic and thus unstable behavior. Thus, from a designer point of view, the leg stiffnesses should be kept within a certain range of values for a given range of galloping speeds.

Table 3.2 Gallop with variation in the initial leg spring compression.

initial speed, u_i (kph)	initial length of leg spring, y_i (m)	initial body pitch angle, θ_i (rad)	non - dimensional leg stiffness, K_{leg}	stride frequency (strides/min)	nature of system
25	1.24	0.3	14	89	unstable
25	1.26	0.3	14	87	unstable
25	1.28	0.3	14	105	unstable
25	1.32	0.3	14	120	stable
25	1.34	0.3	14	128	stable
25	1.36	0.3	14	135	stable
25	1.38	0.3	14	141	stable
25	1.4	0.3	14	99	unstable

Table 3.3 Gallop with variation in the leg stiffness.

initial speed, $\frac{u_i}{\sqrt{gL}}$	initial length of leg spring, y_i (m)	initial body pitch angle, θ_i (rad)	non - dimensional leg stiffness, K_{leg}	stride frequency (strides/min)	nature of system
1.4483	1.2637	0.3	10	107	unstable
1.4483	1.2841	0.3	12	113	unstable
1.4483	1.3	0.3	14	114	stable
1.4483	1.3128	0.3	16	114	stable
1.4483	1.3234	0.3	18	114	stable
1.4483	1.3324	0.3	20	115	stable
1.4483	1.3401	0.3	22	115	stable
1.4483	1.3468	0.3	24	115	stable
1.4483	1.3527	0.3	26	115	stable
1.4483	1.358	0.3	28	115	stable
1.4483	1.3628	0.3	30	115	stable
1.4483	1.3671	0.3	32	116	stable
1.4483	1.371	0.3	34	116	stable
1.4483	1.3746	0.3	36	116	stable
1.4483	1.3779	0.3	38	116	stable
1.4483	1.3837	0.3	42	116	stable
1.4483	1.3888	0.3	46	116	stable
1.4483	1.3933	0.3	50	116	stable

Table 3.3 (continued)

initial speed, $\frac{u_i}{\sqrt{gL}}$	initial length of leg spring, y_i (m)	initial body pitch angle, θ_i (rad)	non - dimensional leg stiffness, K_{leg}	stride frequency (strides/min)	nature of system
1.4483	1.3972	0.3	54	112	unstable
1.4483	1.4008	0.3	58	110	unstable
1.4483	1.404	0.3	62	110	unstable
1.4483	1.4069	0.3	66	112	unstable
1.4483	1.4095	0.3	70	122	unstable

Table 3.4 Gallop with variation in the initial speed.

initial speed, $\frac{u_i}{\sqrt{gL}}$	non - dimensional leg stiffness, K_{leg}	nature of system
1.81 (25 kph)	> 14 and < 52	stable
2.5345 (35 kph)	> 18	stable
3.2586 (45 kph)	> 24	stable

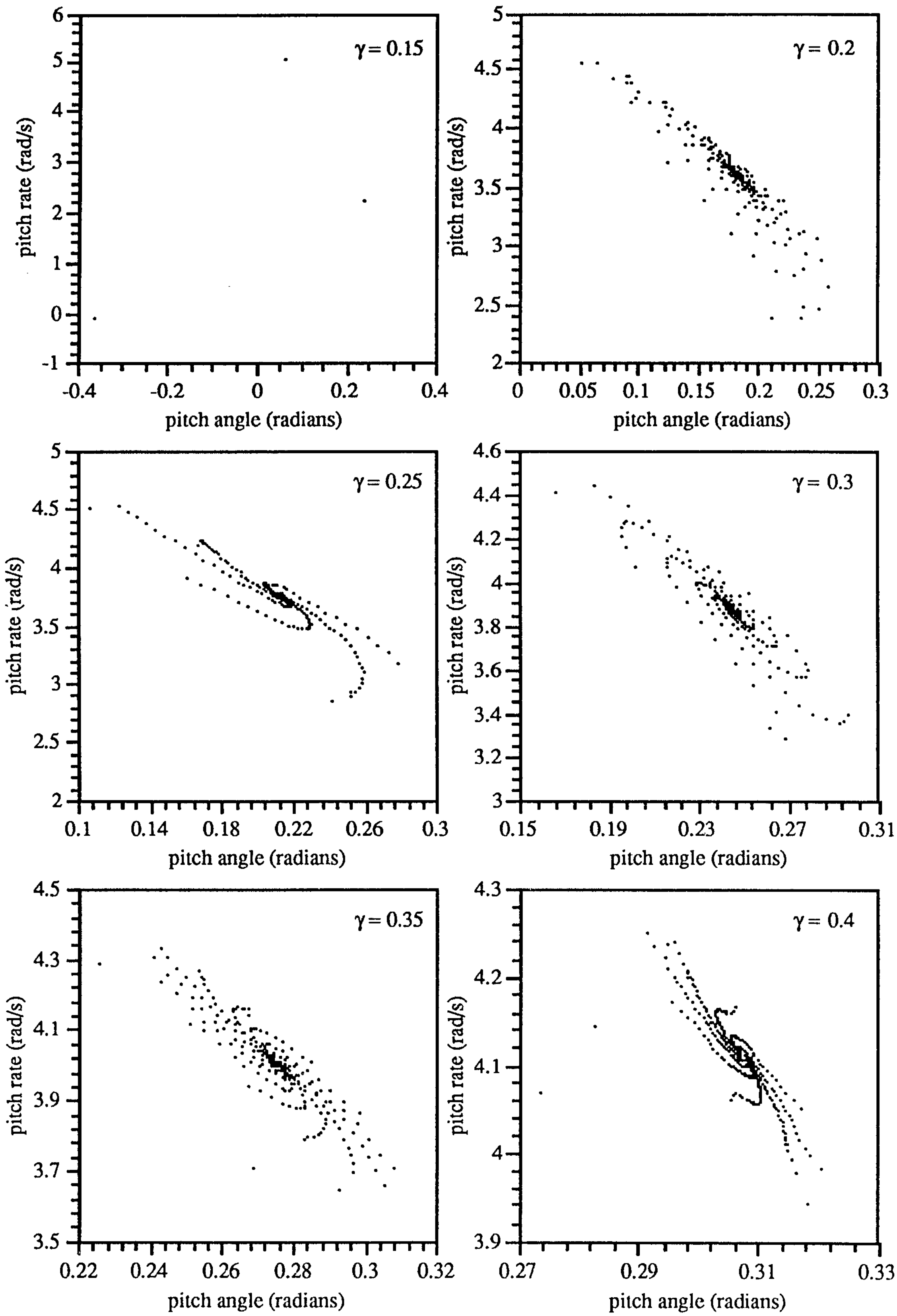

Figure 3.11 Poincare maps with variation of the initial pitch angle.

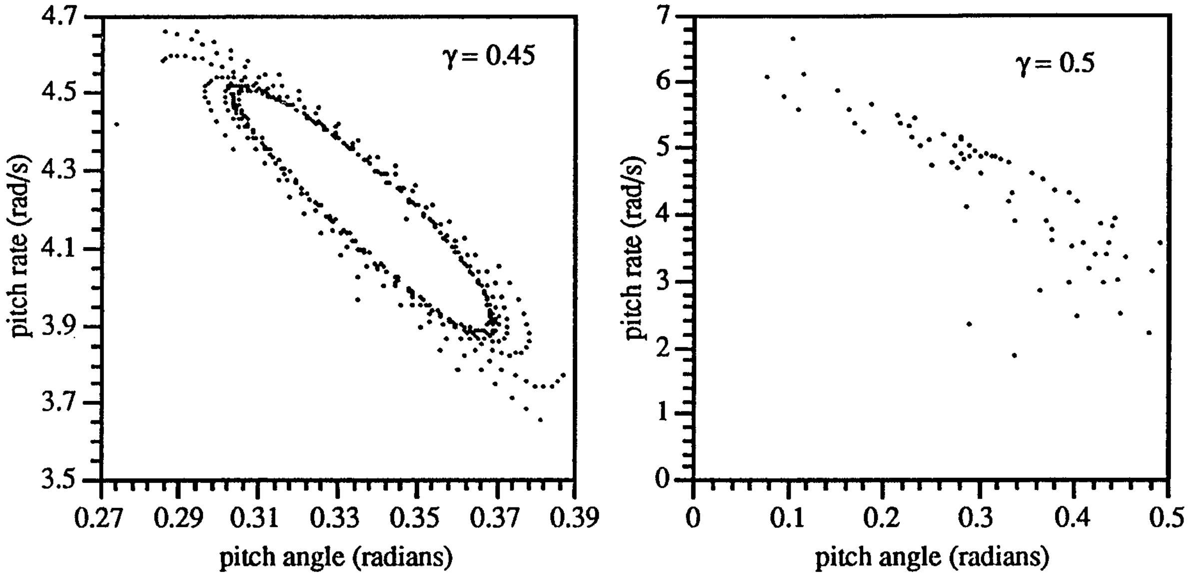

Figure 3.11 (continued)

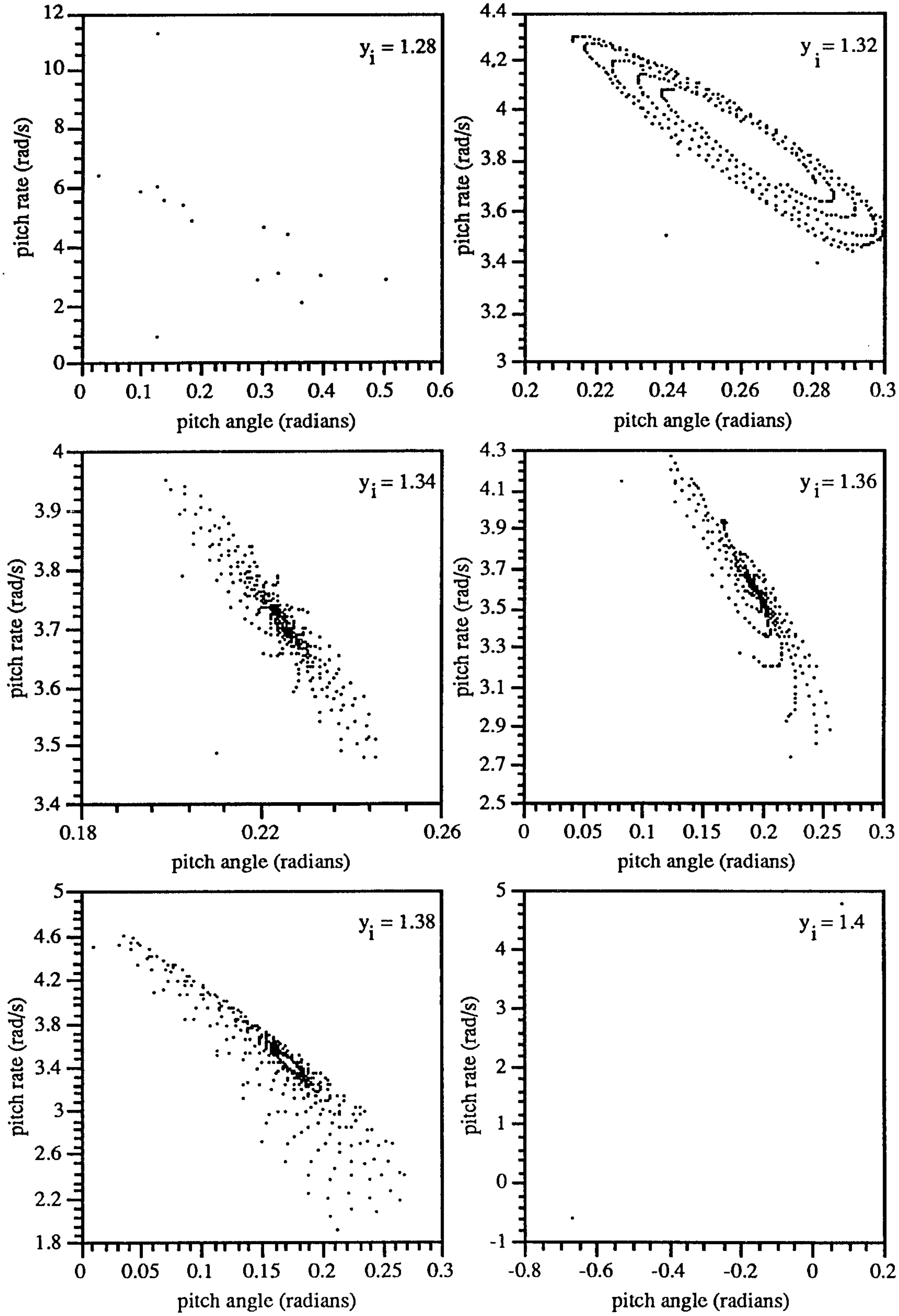

Figure 3.12 Poincare maps for variation in the initial spring compression.

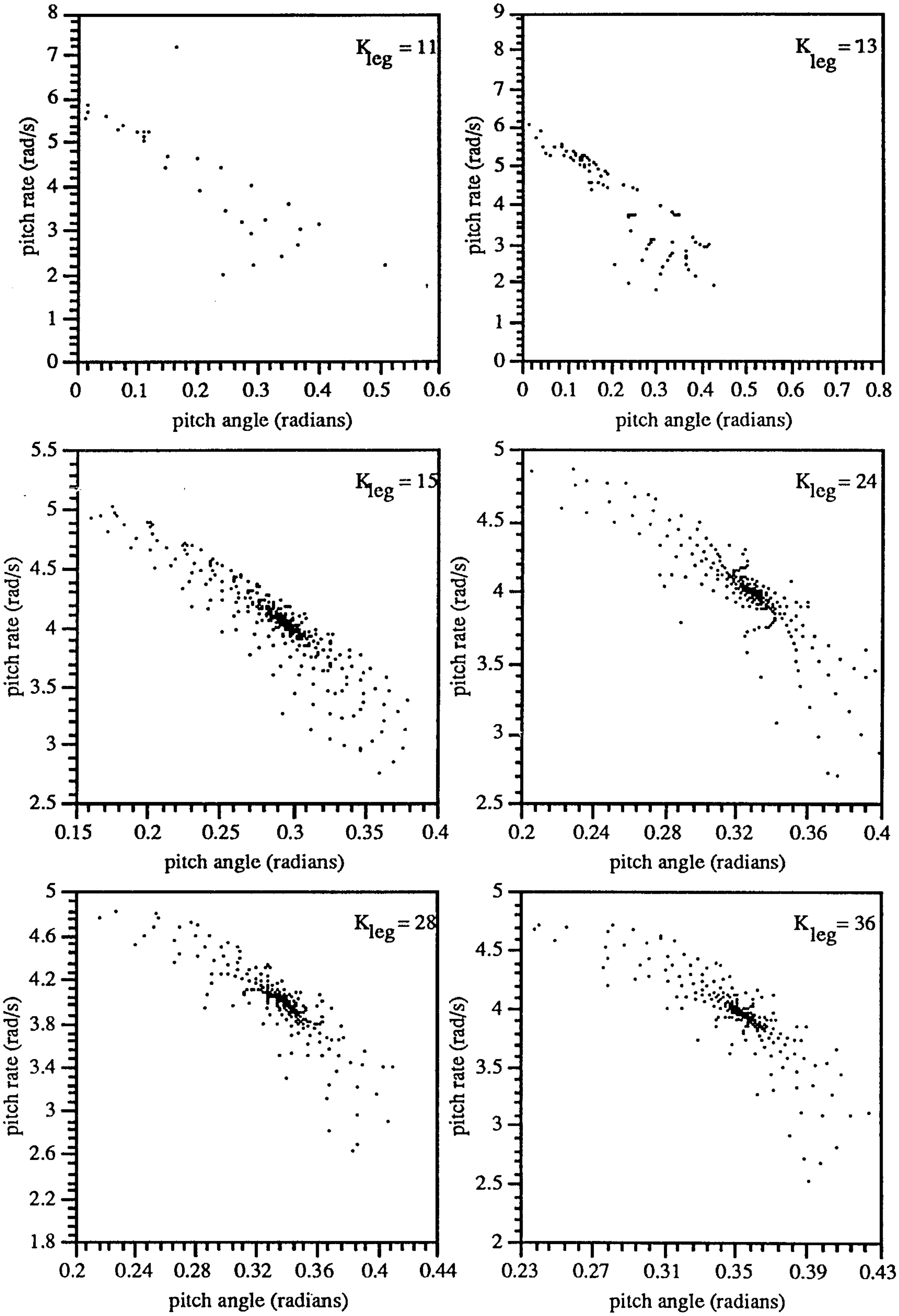

Figure 3.13 Poincare maps with variation in non-dimensional leg stiffness.

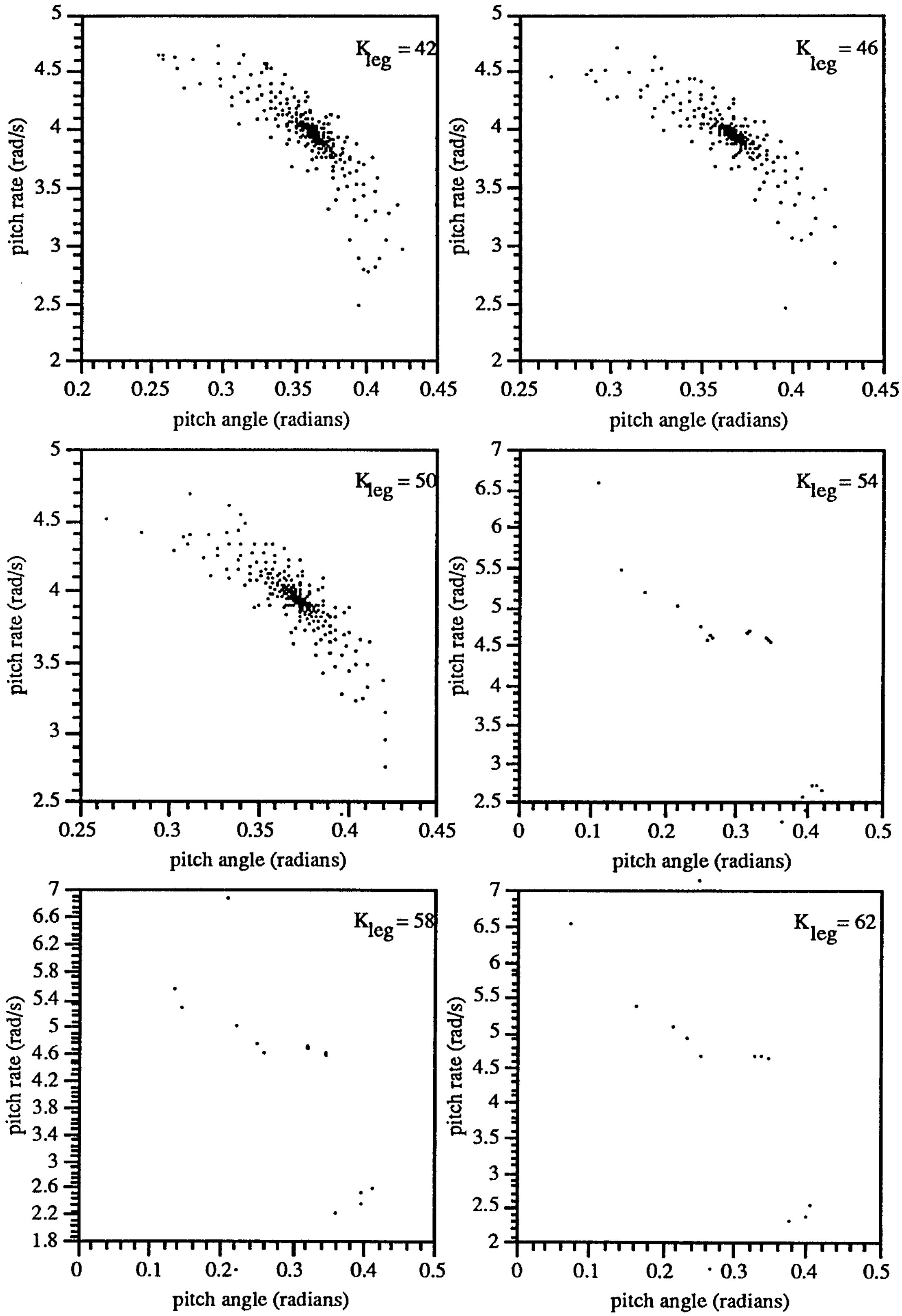

Figure 3.13. (continued).

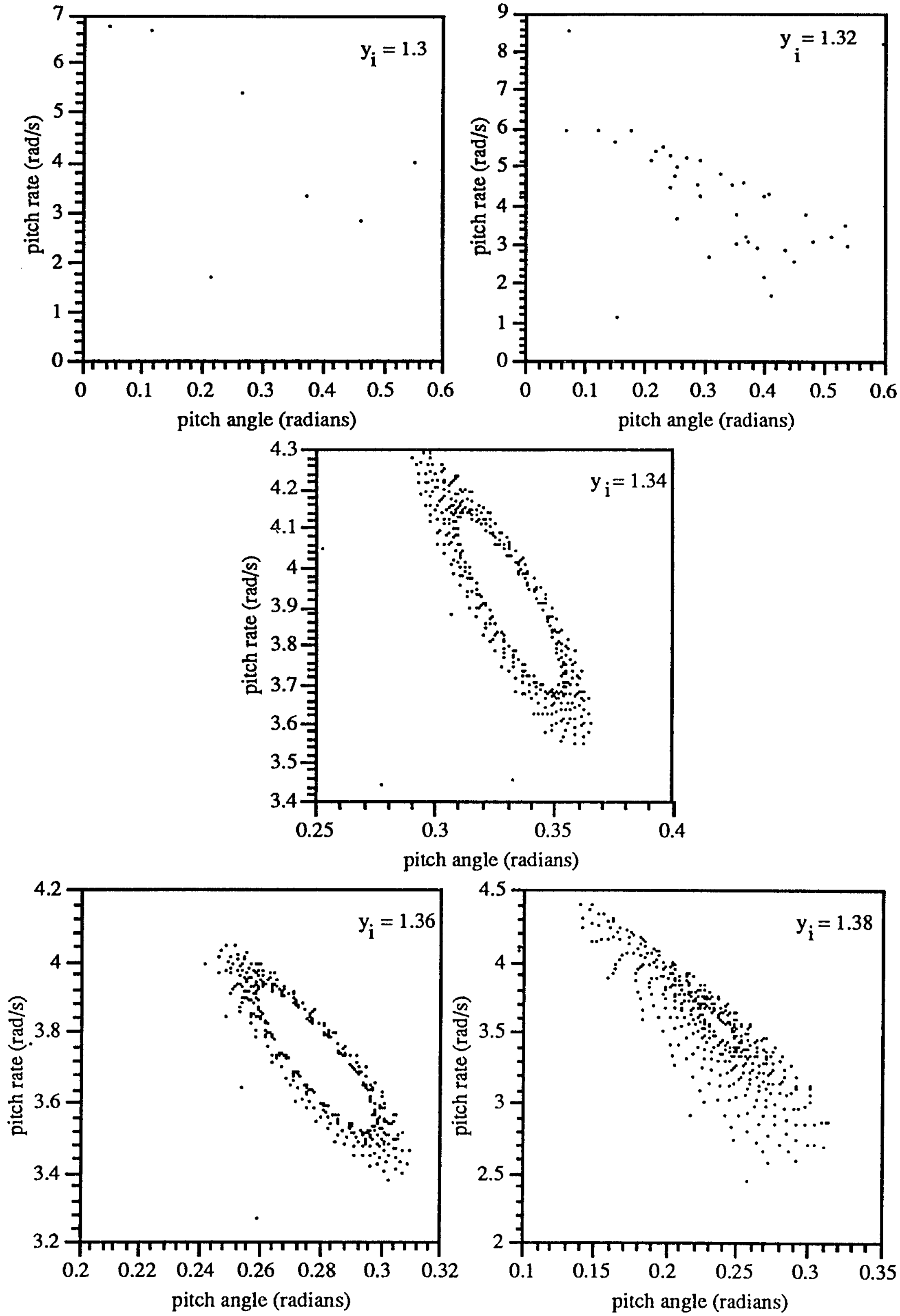

Figure 3.14 Poincare maps with variation of the initial leg compression (speed of 35 kph).

CHAPTER IV

CONTROLLER TO CHANGE SPEED

1. Introduction

This chapter will improve upon the controller developed in the Chapter III. In its present state, the controller generates stable gait at a constant speed set at the beginning of the gait. The modified controller developed in this chapter will enable the quadruped to make a transition from a stable gait to another stable gait at a different speed. The energy controller and the speed controller will be modified to smoothly change the speed. Again the body pitch will not be controlled explicitly. The effect of this controller on the stability of the quadruped will be examined in detail using Poincare maps.

2. Controller to change speed

In the previous chapter a scheme was developed to control a quadruped in gallop and maintain constant speed. A similar scheme is described in this chapter that will allow the quadruped to change its speed. The technique described in this chapter is based on heuristic principles developed from simple observations. The initial part of this section will describe a controller to increase the speed, and in the later part, this controller will be modified to include the decrease in speed.

The controller manipulates the leg angle and the leg actuator force to increase the speed. The leg angle with the vertical at the beginning of the stance phase is decreased by a preset value and held constant during the phase of speed increase. The energy controller is disconnected and a comparatively larger actuator force is applied during the successive steps. This results in a steady increase in speed. When the desired speed has been achieved, the controller for the speed increase is disconnected, the new energy level and speed are sensed, and the constant energy controller is connected again. This generates a stable gait at the new speed and energy level. The mathematical descriptions of the controllers are as follows:

The energy controller is an on-off controller. The magnitude of the actuator force is set equal to a constant gain multiplied by the difference between the desired speed and the present speed. The leg angle is also decreased by an amount equal to a constant multiplied by the difference between the desired speed and the present speed. The equations for the controller are

$$\gamma_{n+1} = \gamma_i - \delta$$
$$F_{n+1} = \begin{cases} K'_F(u_d - u_i) & \text{if} \quad \left|K'_F(u_d - u_i)\right| > F_{max} \\ F_{max} & \text{if} \quad \left|K'_F(u_d - u_i)\right| < F_{max} \end{cases}$$

where

δ = constant

γ_i = leg angle for the initial speed

u_d = desired final speed

F_{max} = constant (maximum allowable force input).

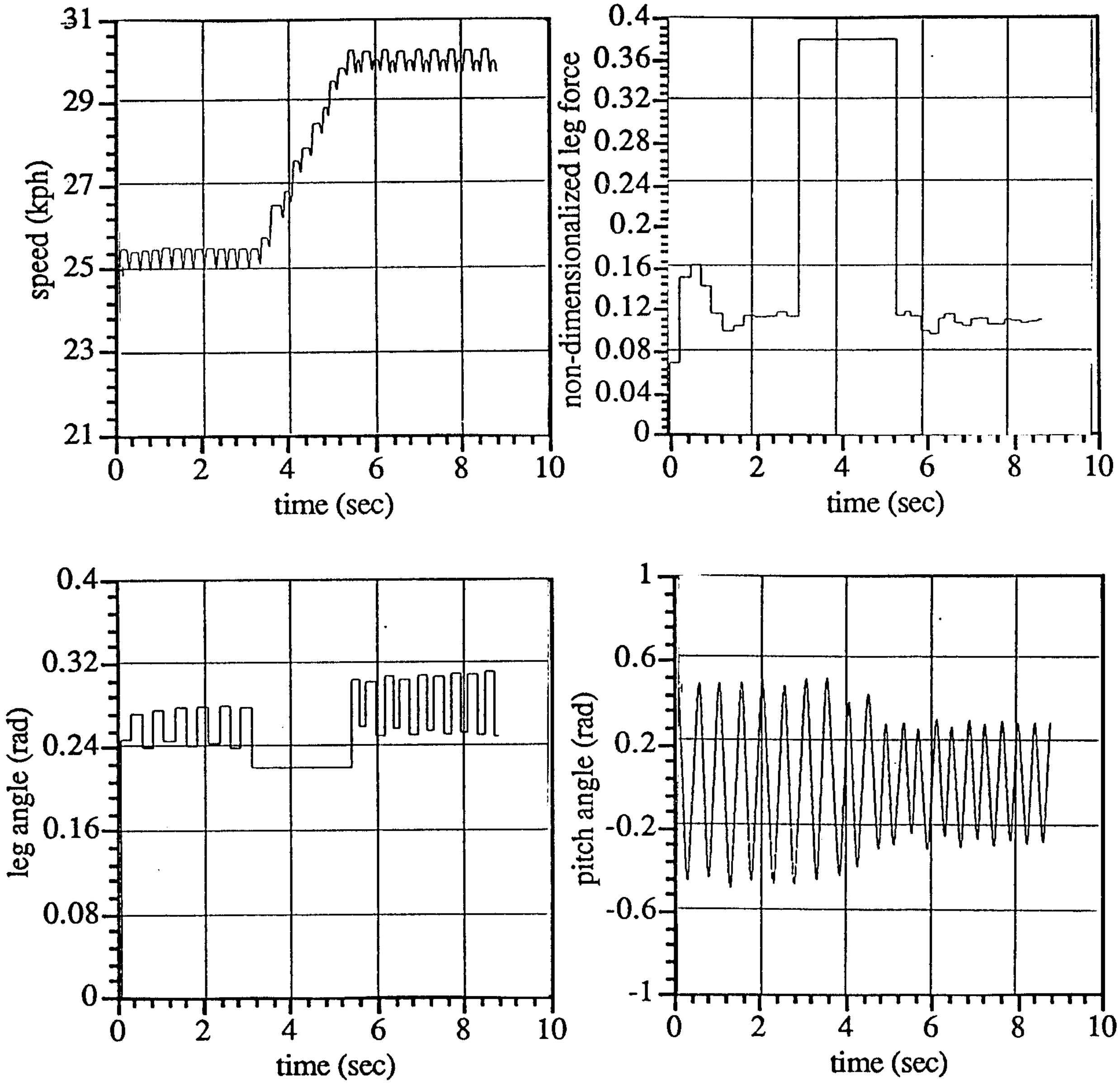

Figure 4.1. Response of the quadruped using a simple controller to increase speed.

K'_F = constant

Note that γ_{n+1} and F_{n+1} are constant till the final, speed has been achieved

The above controller was implemented on the quadruped described in the earlier chapters. The control gains were found by manual iterations. The results from this controller are shown in Figure 4.1. Figure 4.1 shows the speed of the quadruped, the actuator forces applied by the legs, the pitch angle of the quadruped and the leg angle at the beginning of the stance phase. We can observe from this figure, that the amplitude of the body pitch reduces with the increase in speed. If the maximum body pitch drops below a certain critical value, it could lead to instability. One technique to prevent this reduction in the maximum body pitch angle is to manipulate the leg angle further. Figure 4.1 shows that the leg angle increases with the increase in speed. Thus the leg angle, which is reduced at the beginning of the acceleration phase to facilitate the increase of speed, is not held constant for the duration of the acceleration phase. It is increased by a constant amount until the end of the speed increase. The equation for the leg angle now is given by

$\gamma_{i+1} = \gamma_i - \delta$

$\gamma_{n+1} = \gamma_n + \varepsilon$ for n = i+1, ...

where

ε = constant

The new results are shown in Figure 4.2. This figure displays the increase in speed, the actuator forces, the leg angle during the beginning of the stance phase and the magnitude of the maximum body pitch angle. Now the body pitch angle does not reduce by a

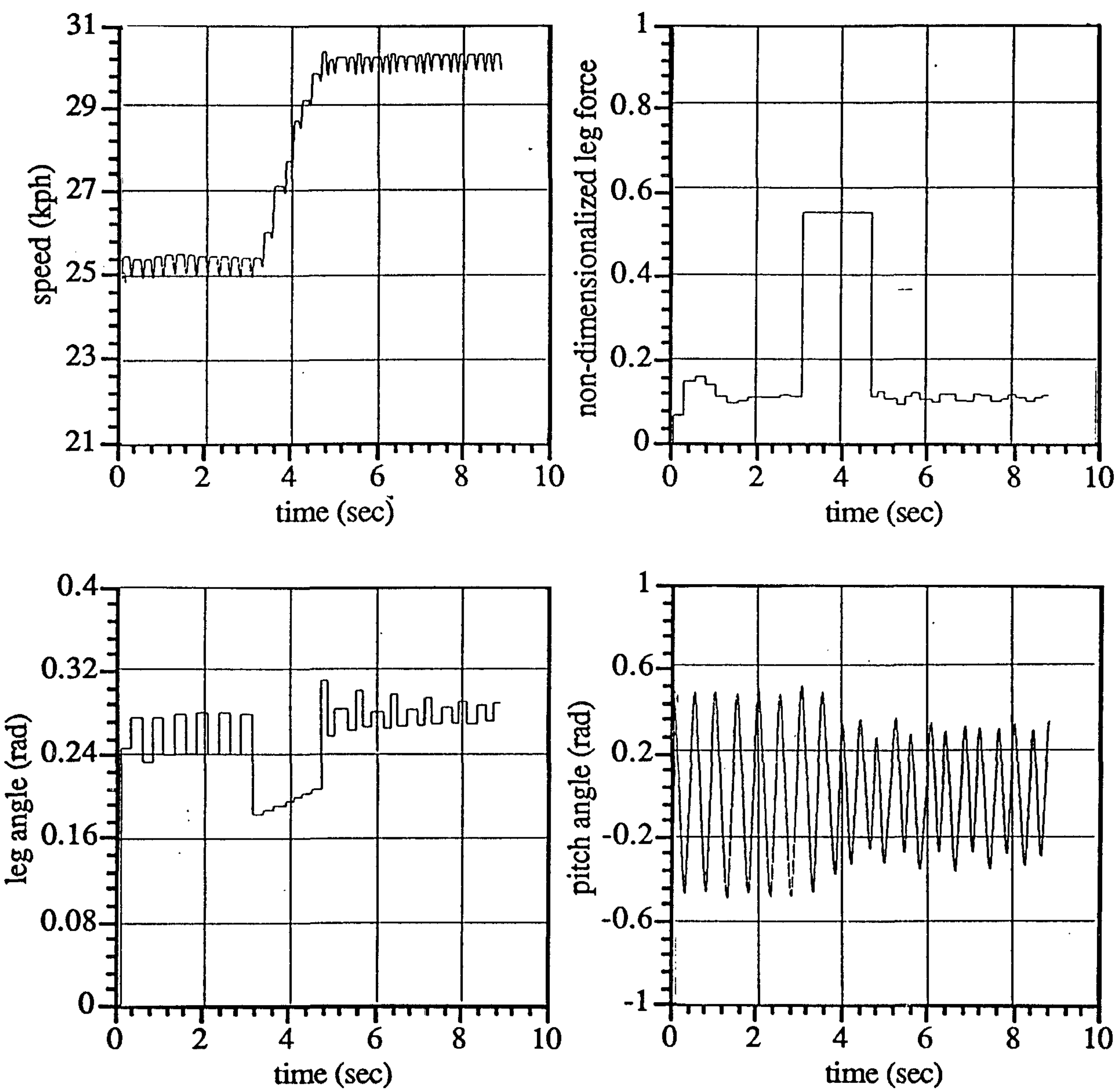

Figure 4.2. Response of the quadruped using a modified speed controller.

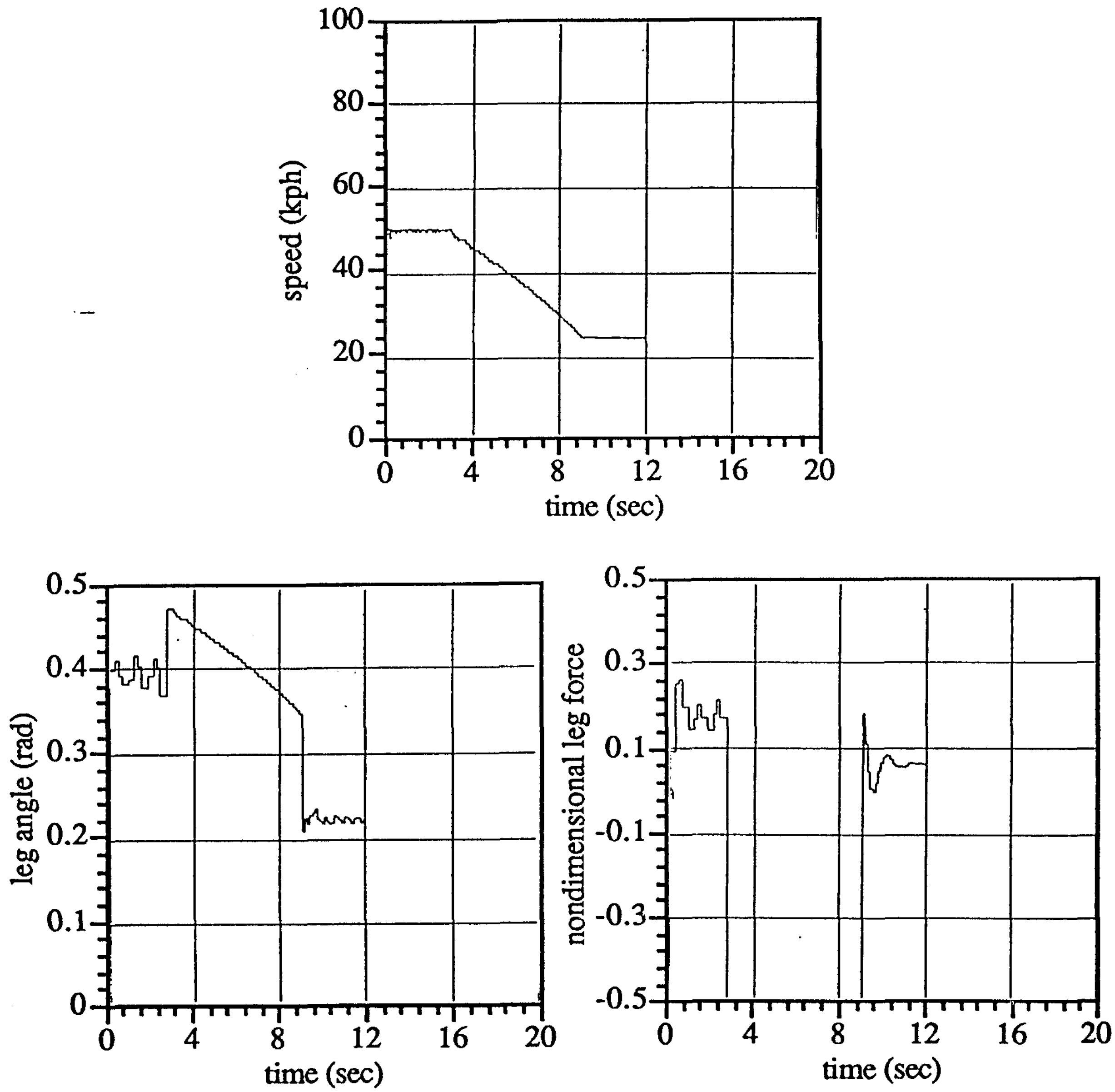

Figure 4.3. Response of the quadruped for a decrease in speed.

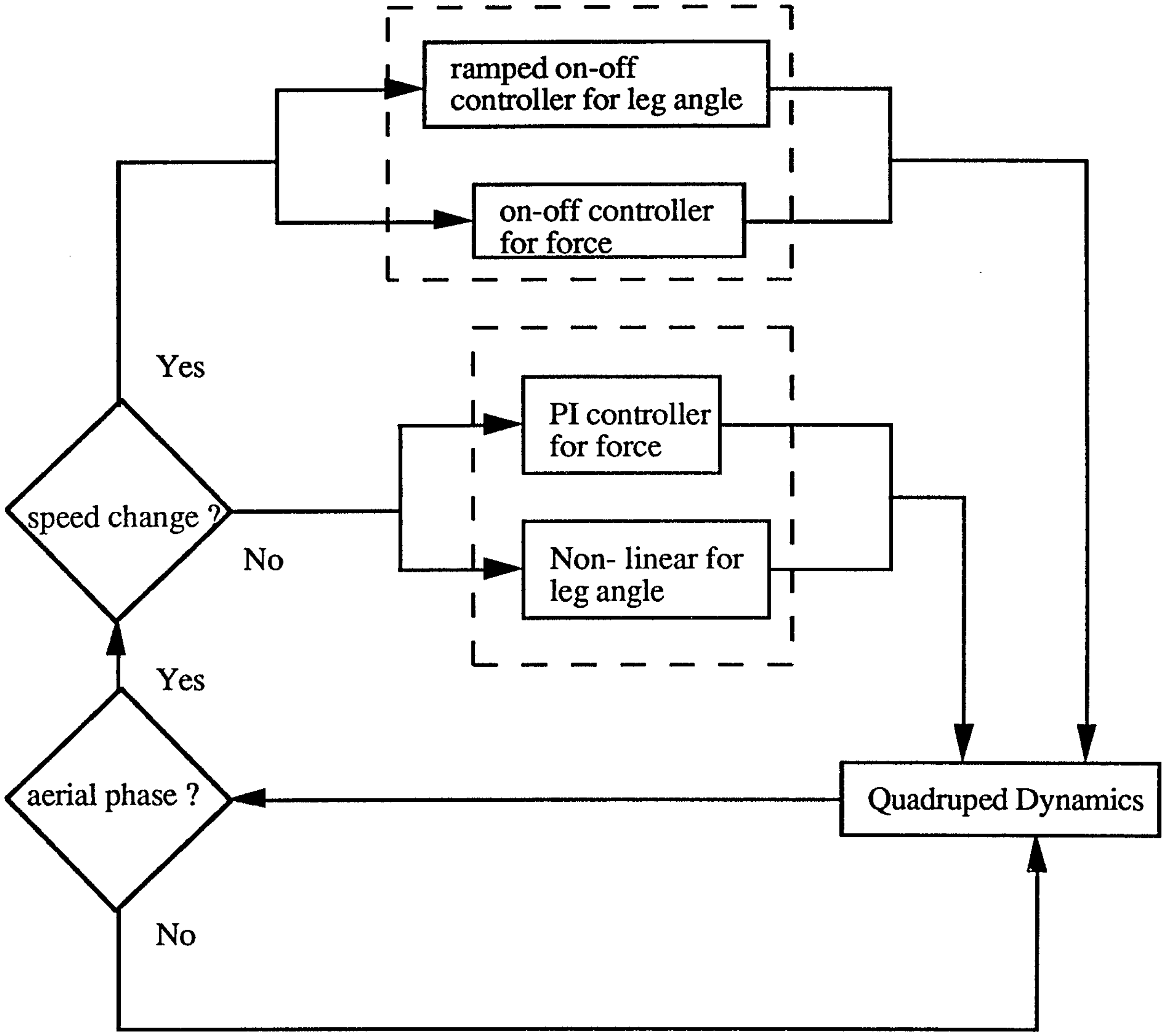

Figure 4.4. Complete controller for the quadruped gallop.

significant amount. Thus the transition to the new speed is smoother. All the gains for the controllers were set by manual iteration. The new controller can be represented by the block diagram shown in Figure 4.4.

A similar controller can be used to reduce the speed of the quadruped. The gains for the speed reduction are slightly different than those for the increase in speed. But the same controller works for both the cases. The results for a typical case are shown in Figures 4.3. This figure displays the decrease in speed, the leg angle and the actuator forces. The final equations for the controller are summarized below.

Controller for constant speed:

$$F_{n+1} = K_{PF}\,(E_d - E_n) + K_{IF} \sum_{i=1}^{n} (E_d - E_i)$$

$$\gamma_{n+1} = \gamma_n - K_\gamma\,(u_d - u_{n-1}).$$

Controller during the transition period:

$$F_{n+1} = \begin{cases} K'_F(u_d - u_i) & \text{if } \left|K'_F(u_d - u_i)\right| > F_{max} \\ F_{max} & \text{if } \left|K'_F(u_d - u_i)\right| < F_{max} \end{cases}$$

$$\gamma_{i+1} = \gamma_i - \delta\,\mathrm{sign}(u_d - u_i)$$

$$\gamma_{n+1} = \gamma_n + \varepsilon\,\mathrm{sign}(u_d - u_i) \qquad \text{for } n = i+1, \ldots\ldots .$$

Figure 4.4 shows the block diagram for the complete controller. The above controller was tested for a variety of speed changes. Figure 4.5 shows the results for different ranges of speed.

3. Stability of the system

As discussed earlier, the change in speed should not disturb the stability of the system. The controller should generate a stable gait at the new speed. This will be possible if the controller does not move the system too far from the stable gait at the new speed. This can be examined in detail using the Poincare maps. The Poincare maps for different ranges of speed changes are shown in Figure 4.6. These maps show that the system does stabilize at the new speed. These maps are for a leg stiffness, K_{leg} of 26. A lower value of leg stiffness would still enable the quadruped to make the transition to the new speed, but then it will enter chaos and destabilize. This was shown earlier in Chapter III.

4. Summary

In this chapter, a controller has been developed that enables the quadruped to change its speed while galloping. The controller is simple to implement. It accomplishes the change in speed by exerting appropriate forces at the legs and manipulating the leg angle at the beginning of the stance phase. The pitching motion of the body is not explicitly controlled. Using Poincare maps, it has been shown that the changes in speed do not affect the stability of the system. This also shows that the controller for a gallop at constant speed is a robust controller.

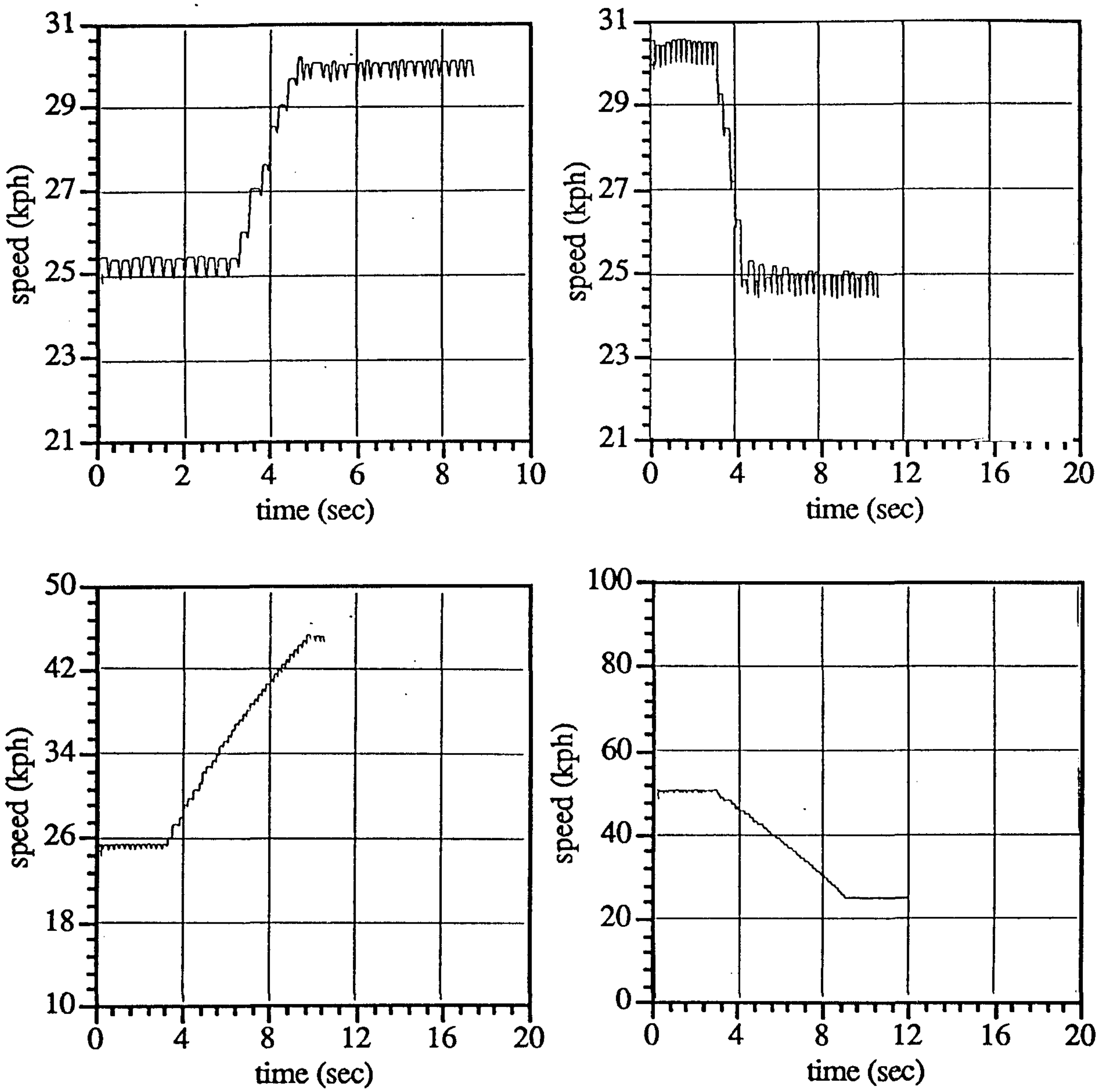

Figure 4.5. Response of the quadruped to a variety of speed changes.

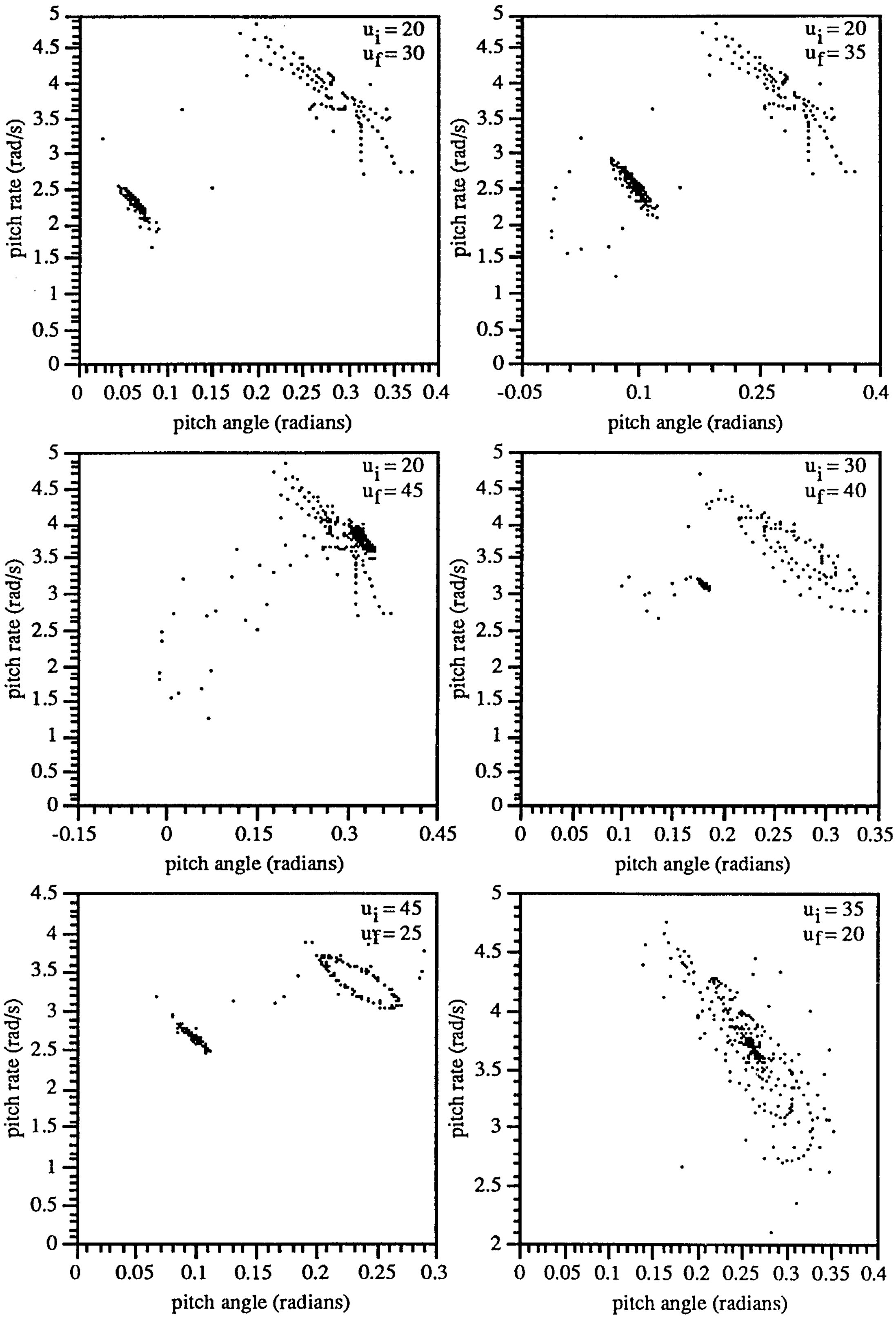

Figure 4.6. Poincare maps for a range of speed changes.

CHAPTER V

CONTROLLER FOR THREE DIMENSIONAL MODEL

1. Introduction

In this chapter, the two dimensional model of the quadruped will be extended to model a three dimensional quadruped. The dynamic equations for the three dimensional model will be developed in the beginning of this chapter. The controller will be adapted to control the three dimensional model of the quadruped. The additional variables to be controlled now are the sideways speed, roll and yaw. It must be ensured that the controllers for these extra variables do not affect the functionality of the controllers for the forward speed and the pitch. In the later part of the chapter additional controllers will be developed to enable the quadruped to turn.

2. Dynamic model for the three dimensional quadruped

The three dimensional model of the quadruped is shown in Figure 5.1. The coordinate system (x, y, z) is fixed to an inertial frame. The coordinate system (l, m, n) is fixed to the body of the quadruped with the origin of the coordinate system at the center of mass and the axes aligned with the principal axes. At any instant of time, the coordinate system (x', y', z') is coincident with the coordinate system (l, m, n) but fixed with respect to (x, y, z). The velocity of the quadruped is denoted by (u, v, w) where u is the speed in the x-direction, v is the speed in the y-direction and w is the speed in the z-direction. The orientation of the body is given by the Euler angles (α, β, γ) where α, β and γ are the roll, yaw and pitch respectively. The angular rates of the body are given by $\dot{\theta}_1$, $\dot{\theta}_2$ and $\dot{\theta}_3$ in the x', y' and z' directions respectively. The rotation matrix R corresponding to the above Euler angles is given by

$$R = \begin{bmatrix} \text{Cos}\beta\text{Cos}\gamma + \text{Sin}\alpha\text{Sin}\beta\text{Sin}\gamma & -\text{Cos}\beta\text{Sin}\gamma + \text{Sin}\alpha\text{Sin}\beta\text{Cos}\gamma & \text{Cos}\alpha\text{Sin}\beta \\ \text{Cos}\alpha\text{Sin}\gamma & \text{Cos}\alpha\text{Cos}\gamma & -\text{Sin}\alpha \\ -\text{Sin}\beta\text{Cos}\gamma + \text{Sin}\alpha\text{Cos}\beta\text{Sin}\gamma & \text{Sin}\beta\text{Sin}\gamma + \text{Sin}\alpha\text{Cos}\beta\text{Cos}\gamma & \text{Cos}\alpha\text{Cos}\beta \end{bmatrix}$$

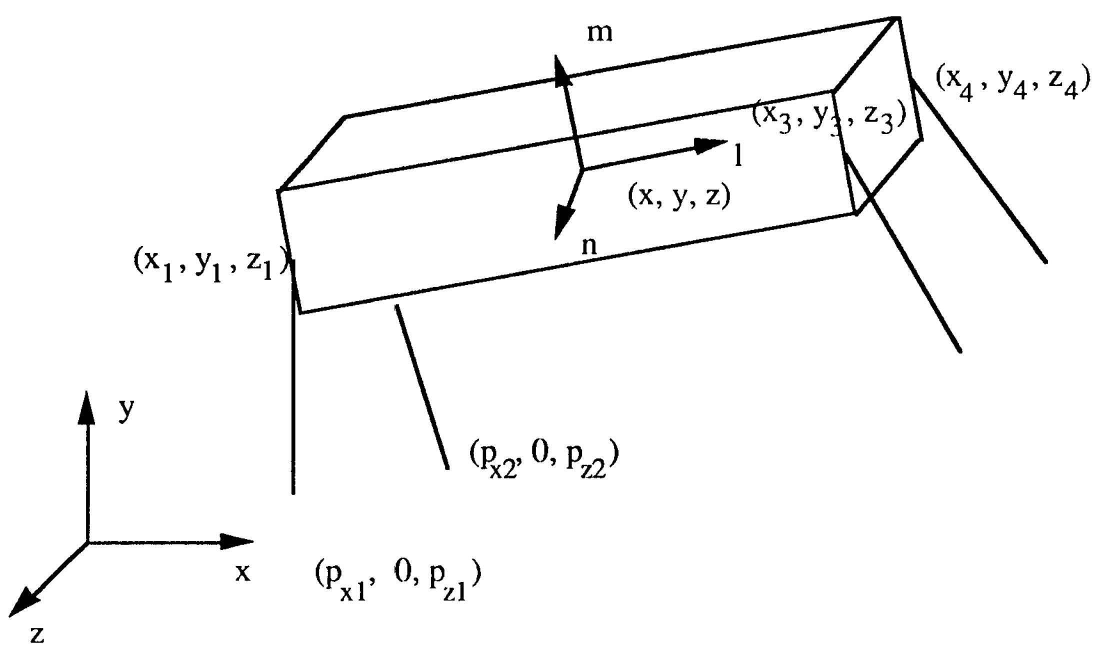

Figure 5.1. Three dimensional model of the quadruped

The equations of motion for the quadruped are given by

$$M\dot{u} = f_x$$
$$M\dot{v} = f_y - Mg$$
$$M\dot{w} = f_z$$
$$I_l\ddot{\theta}_1 = \tau_1' + (I_m - I_n)\dot{\theta}_2\dot{\theta}_3$$
$$I_m\ddot{\theta}_2 = \tau_2' + (I_n - I_l)\dot{\theta}_3\dot{\theta}_1$$
$$I_n\ddot{\theta}_3 = \tau_3' + (I_l - I_m)\dot{\theta}_1\dot{\theta}_2$$

where

M = mass of the body.

g = acceleration due to gravity.

I_l = moment of inertia about the l axis.

I_m = moment of inertia about the m axis.

I_n = moment of inertia about the n axis.

f_x, f_y and f_z are the forces exerted on the main body by the legs in the x, y and z direction respectively. τ'_1, τ'_2 and τ'_3 are the torques exerted on the main body by the legs about the x', y' and z' axes respectively.

The quadruped consists of four legs which are each connected to the body at the hips whose coordinates are (x_1, y_1, z_1), (x_2, y_2, z_2), (x_3, y_3, z_3) and (x_4, y_4, z_4) respectively. Each leg of the quadruped consists of a constant stiffness spring with a damper and a force actuator in parallel. Let the coordinates of the feet when they are placed on the ground be $(p_{xi}, 0, p_{zi})$. The force exerted on the body by the spring in the ith leg given by

$$f_{si} = K_{sp}\left(L - \sqrt{(x_i - p_{xi})^2 + y_i^2 + (z_i - p_{zi})^2}\right)$$

where

L = free length of the spring

The force applied by the damper in the ith leg is given by

$$f_{di} = \xi \, v_{li}$$

where ξ is the damping coefficient and v_{li} is the component of the velocity of the leg end relative to the body along the leg axis. v_{li} is given by the expression

$$v_{li} = \frac{v_{xi}(x_i - p_{xi}) + v_{yi} y_i + v_{zi}(z_i - p_{zi})}{\sqrt{(x_i - p_{xi})^2 + y_i^2 + (z_i - p_{zi})^2}}$$

where v_{xi}, v_{yi}, v_{zi} are the x, y and z components of this velocity.

Thus the force components exerted by each leg on the body in the x, y and z directions are given by

$$f_{xi} = \{f_{si} - f_{di}\}\left(\frac{(x_i - p_{xi})}{\sqrt{(x_i - p_{xi})^2 + y_i^2 + (z_i - p_{zi})^2}}\right)$$
$$f_{yi} = \{f_{si} - f_{di}\}\left(\frac{y_i}{\sqrt{(x_i - p_{xi})^2 + y_i^2 + (z_i - p_{zi})^2}}\right)$$
$$f_{zi} = \{f_{si} - f_{di}\}\left(\frac{(z_i - p_{zi})}{\sqrt{(x_i - p_{xi})^2 + y_i^2 + (z_i - p_{zi})^2}}\right)$$

The total force acting on the body is given by

$$f_x = \sum_{i=1}^{4} n_i f_{xi}$$
$$f_y = \sum_{i=1}^{4} n_i f_{yi}$$
$$f_z = \sum_{i=1}^{4} n_i f_{zi}$$

where $n_i = \begin{cases} 0 & \text{if the leg is in the air} \\ 1 & \text{if the leg is on the ground} \end{cases}$

The torques about the center of mass exerted by each leg on the body is given by

$$\underline{\tau}_i = n_i(\underline{r}_i \times \underline{f}_i)$$

where $\underline{r}_i$ is the difference between the position vectors of the hip on the ith leg and the center of mass

The above equation gives the torque in the fixed coordinate system (x, y, z) and is converted to the torques in the coordinate system (x', y', z') by the following equations

$$\underline{\tau}'_i = R^T \tau_i$$

This completes the development of the equations of motion.

3. Control Scheme

The control scheme used to control the two dimensional model is implemented for this three dimensional model. This will enable us to control the forward speed and the pitching motion. The extra degrees of freedom that have to be controlled in the three dimensional model besides the one present in the two dimensional model are

1) sideways velocity: should be set to zero
2) roll : should be set to zero
3) yaw: should be set to zero

Unlike the two dimensional model where the leg placement could be fixed by a single coordinate, the leg placement for the nth step is now fixed by two coordinates ($(p_{xi})_n$, 0, $(p_{zi})_n$). Similarly to the two dimensional case, $(p_{xi})_n$ will be used to control the forward speed of the quadruped. The other coordinate $(p_{zi})_n$ will be used to control the sideways velocity.

When any of the legs is lifted off the ground, the following quantities are measured: The location of the hip can be calculated knowing the rotation matrix and the position of the center of mass of the main body.

$$(d_{xi})_n = (x_i)_n - (p_{xi})_n$$
$$(d_{zi})_n = (z_i)_n - (p_{zi})_n$$

These displacements are measured in the fixed coordinate system and do not account for the orientation of the body. To overcome this problem, we set up a new coordinate system (x", y", z"). The y"-axis is aligned along the fixed y-axis. The x"-axis is the projection of the x'-axis on to the xz-plane. The third axis z" completes the right handed set.

$$y'' = y$$
$$x'' = \frac{R(1,1)\,\hat{i} - R(3,1)\,\hat{k}}{\sqrt{R(1,1)R(1,1) + R(3,1)R(3,1)}}$$
$$z'' = x'' \times y''$$

where $\hat{i}$, $\hat{j}$ and $\hat{k}$ are unit vectors along the x, y and z-axes respectively.

The displacements can now be computed in the new coordinate system (x", y", z").

$$(d''_{xi})_n = \frac{(d_{xi})_n R(1,1) + (d_{zi})_n R(3,1)}{\sqrt{R(1,1)R(1,1) + R(3,1)R(3,1)}}$$
$$(d''_{zi})_n = \frac{-(d_{xi})_n R(3,1) + (d_{zi})_n R(1,1)}{\sqrt{R(1,1)R(1,1) + R(3,1)R(3,1)}}$$

The two dimensional control scheme can now be implemented to control the forward speed. The above displacements for the (n+1)th step is given by

$$(d''_{xi})_{n+1} = (d''_{xi})_n + K_\theta(u'_d - u'_{n-1})$$

where (u', v', w') is the velocity of the quadruped in the (x', y', z') coordinate system and is given by the equation

$$\begin{bmatrix} u' \\ v' \\ w' \end{bmatrix} = R^T \begin{bmatrix} u \\ v \\ w \end{bmatrix}$$

The other displacement $(d'_{zi})_{n+1}$ can be used to control the sideways speed. A proportional-integral controller is used for this purpose since it is desirable to have zero steady state error.

$$(d''_{zi})_{n+1} = K_s w'_n + K_{is} \sum_{j=0}^{n-1} w'_j$$

where K_s and K_{is} are constants and will be determined by trial and error.

The foot placement can now be completely determined by the following equations

$$(d_{xi})_{n+1} = \frac{(d''_{xi})_{n+1} R(1,1) - (d''_{zi})_{n+1} R(3,1)}{\sqrt{R(1,1)R(1,1) + R(3,1)R(3,1)}}$$
$$(d_{zi})_{n+1} = \frac{(d''_{xi})_{n+1} R(1,1) + (d''_{zi})_{n+1} R(3,1)}{\sqrt{R(1,1)R(1,1) + R(3,1)R(3,1)}}$$

$$(p_{xi})_{n+1} = (x_i)_{n+1} + (d_{xi})_{n+1}$$
$$(p_{zi})_{n+1} = (z_i)_{n+1} + (d_{zi})_{n+1}$$

The above two equations completely determine the foot placement. This controller was tested for the three dimensional model and the result is shown in Figure 5.2. This figure displays the sideways speed of the quadruped and it is clearly small and decaying.

Roll and yaw are controlled by moments applied at the hip joints by the appropriate legs during the stance phase. This controller is a simple proportional-differential (PD) controller with a feedforward term. This controller is expressed by

$$M_{x'} = -M'_{x'} - \left(K_{p\alpha}\alpha + K_{d\alpha}\dot{\alpha}\right)$$
$$M_{y'} = -M'_{y'} - \left(K_{p\beta}\beta + K_{d\beta}\dot{\beta}\right)$$

where

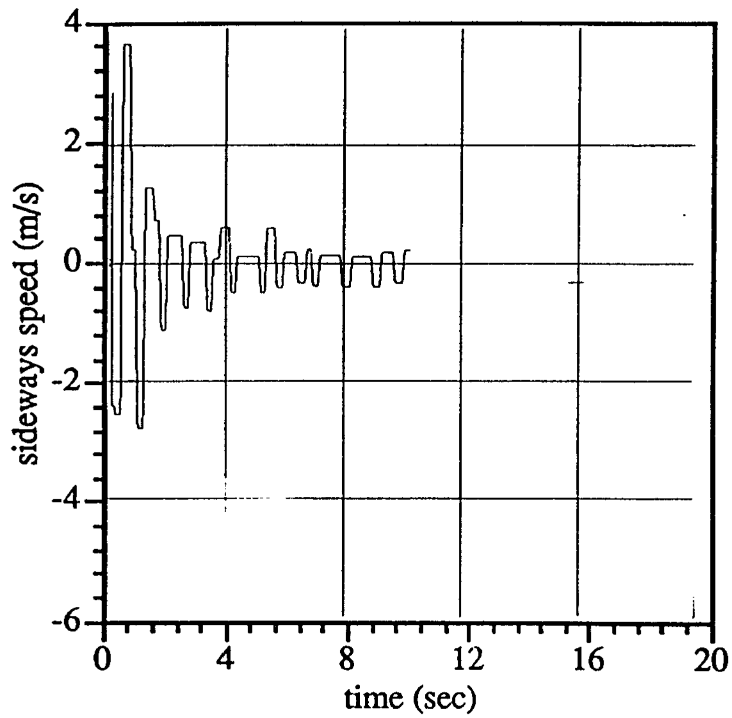

Figure 5.2. Sideways speed of the quadruped.

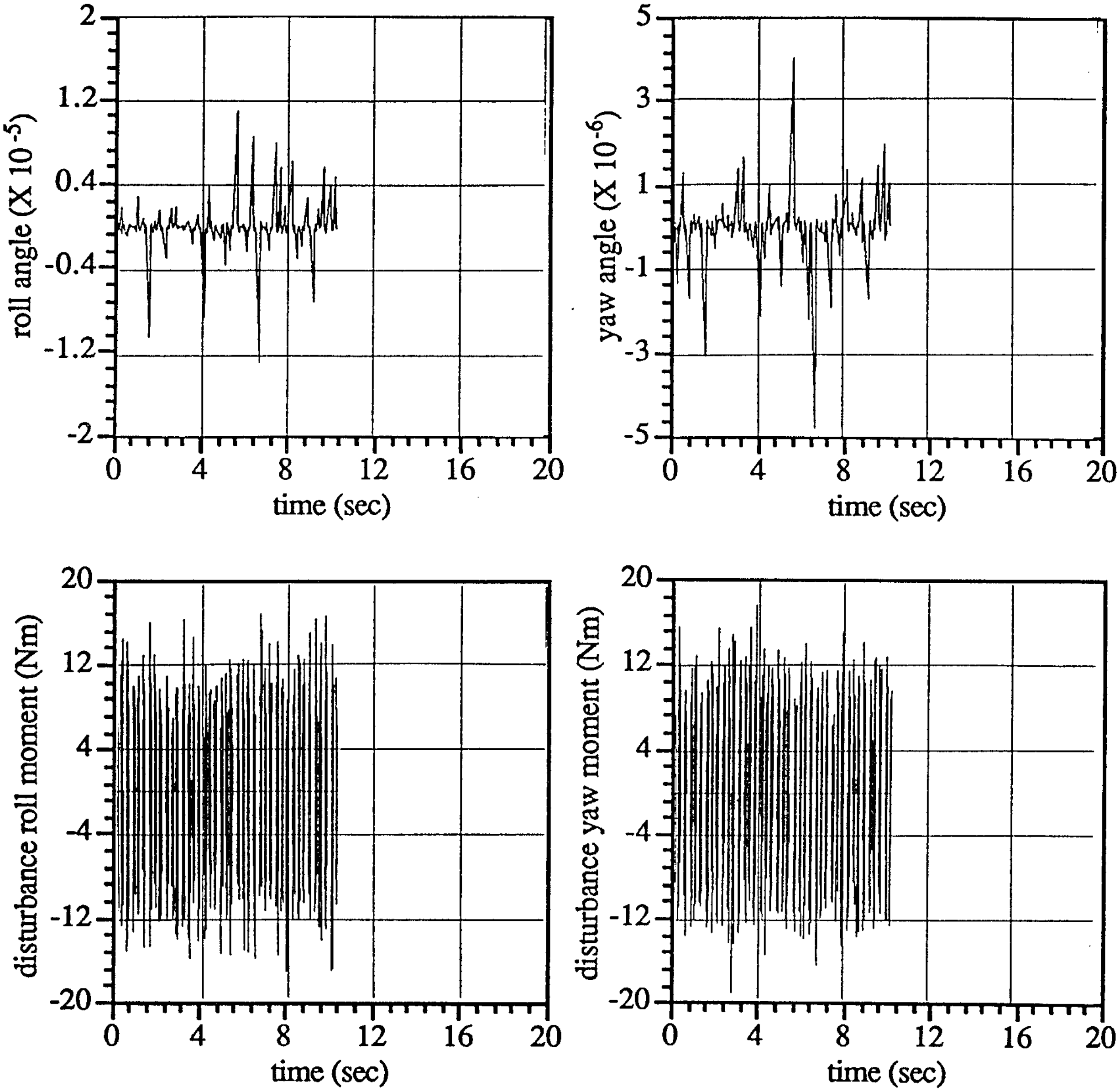

Figure 5.3. . Response of the quadruped to roll and yaw disturbance moments.

$M_{x'}$, $M_{y'}$ are moments applied to the main body in the (x', y', z') coordinate system, $M'_{x'}$, $M'_{y'}$ are estimates of disturbance moments in the (x', y', z') coordinate system, and $K_{p\alpha}$, $K_{d\alpha}$, $K_{p\beta}$, $K_{d\beta}$ are constants.

$\dot{\alpha}$ and $\dot{\beta}$ can be calculated from the following equation:

$$\begin{bmatrix}\dot{\alpha}\\ \dot{\beta}\\ \dot{\gamma}\end{bmatrix}=\begin{bmatrix}\cos\beta & 0 & -\mathrm{Sin}\beta\\ \mathrm{Tan}\alpha\mathrm{Sin}\beta & 1 & \mathrm{Tan}\alpha\mathrm{Cos}\beta\\ \mathrm{Sec}\alpha\mathrm{Sin}\beta & 0 & \mathrm{Sec}\alpha\mathrm{Cos}\beta\end{bmatrix} R \begin{bmatrix}\dot{\theta}_1\\ \dot{\theta}_2\\ \dot{\theta}_3\end{bmatrix}$$

The feedforward terms ensure that the moments applied to the main body do not get too large. A linear PD controller can then be used to control the body attitude for small angles. The above controller also ensures that the moments about the z' axis are not disturbed. This enables the controller developed for the two dimensional case to be used for this three dimensional model. The algorithms developed for the two dimensional case were successfully tested for the above three dimensional model. The results are shown in Figure 5.3. In these cases, small random disturbance moments were applied to the quadruped in the roll and yaw directions. The moments and their effects on the roll and yaw angle are shown in Figure 5.3.

4. Control Scheme for turning maneuver

The objective of this section is to develop a controller that will permit the above three dimensional model to perform turning maneuvers at approximately constant speed. This can be achieved by manipulating the foot placement appropriately. In the above controller, the sideways velocity component is minimized by appropriately changing $(d''_z)_n$. Turning can then be achieved by permitting a sideways velocity component.

For the duration of the turn

$$(d''_z)_{n+1} = \delta_z \,\mathrm{sign}(w')_n$$

where δ_z is a constant.

If δ_z is small, the forward speed controller will not be greatly disturbed and the forward speed will be constant. As the quadruped turns, its orientation has to be changed. This can be achieved by the controller described in the previous section. The controller is modified to

$$M_{x'} = -M'_{x'} - \left(K_{p\alpha}\alpha + K_{d\alpha}\dot{\alpha}\right)$$
$$M_{y'} = -M'_{y'} - \left(K_{p\beta}(\beta - \beta_d) + K_{d\beta}\dot{\beta}\right)$$

We want the orientation of the quadruped to be in the direction of travel. To ensure this, β_d is computed at every stance phase by the equation

$$\beta_d = -\tan^{-1}\left(\frac{w'}{u'}\right)$$

This controller permits the quadruped to turn with a large radius of curvature. The large radius of curvature ensures that the forward speed is almost constant and the quadruped gait is stable. The rate of turn depends on the δ_z.

The results of a typical turn are shown in Figure 5.4. These results are for a turn through about 45 degrees at a constant speed of 25 kph. Figure 5.4 shows the speed in the fixed coordinate system, the forward speed of the quadruped, the sideways speed of the quadruped and the desired and actual yaw angle of the quadruped. The forward speed stays constant and the sideways speed is negligible. The yaw angle closely follows the desired yaw angle.

5. Summary

In this chapter, the controller developed in the earlier chapters for a two-dimensional machine has been extended to control a three-dimensional quadruped machine. Additional controllers have been developed to control the roll motion, yaw motion and the sideways speed of the machine. These controllers have been designed in such a manner so that they do not disturb the controllers for the speed and energy control. Further, these additional controllers have been modified to permit the quadruped to change its direction of motion. This controller permits the quadruped to turn by about 45° in 4 seconds while galloping at approximately 25 kph.

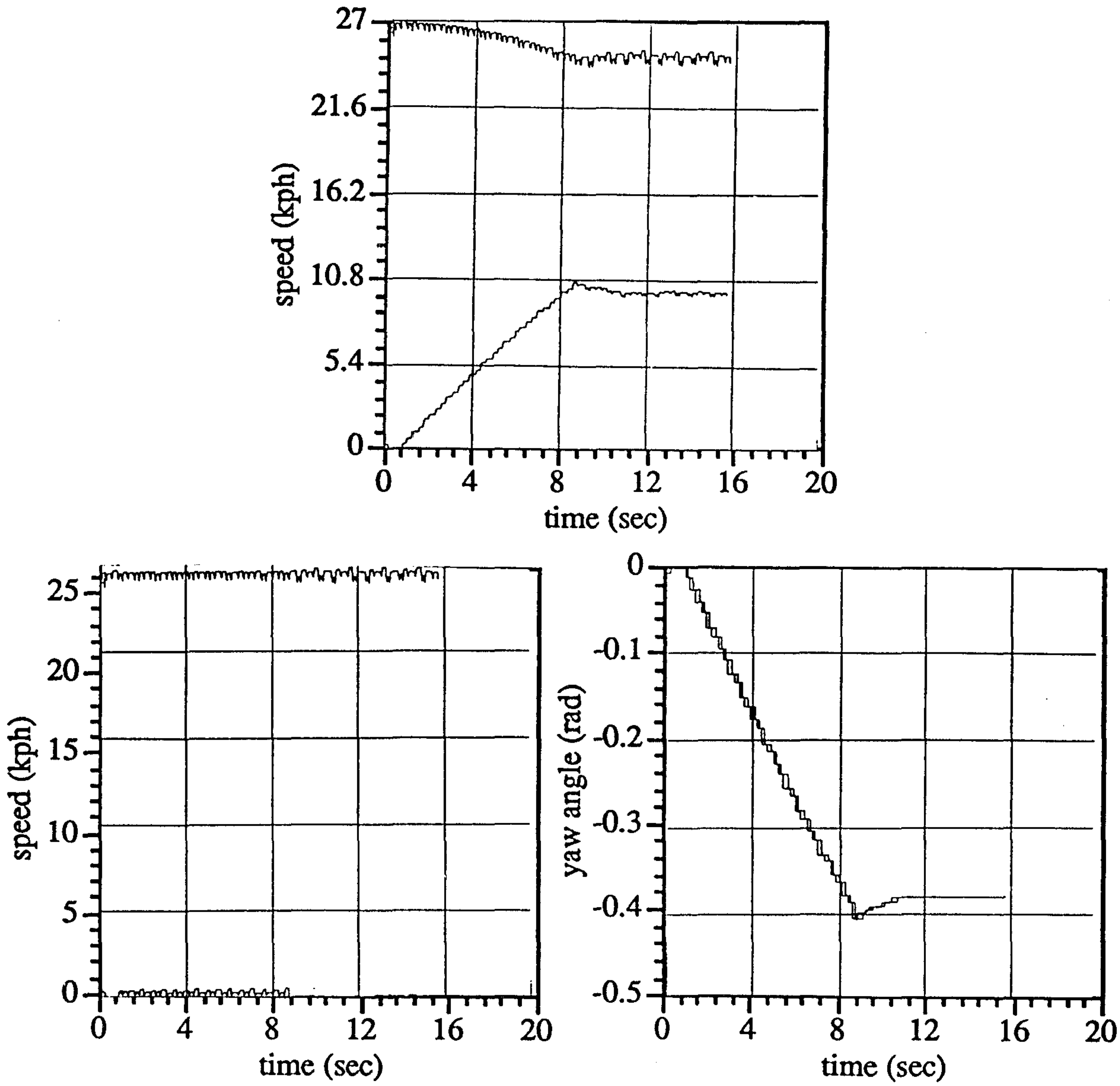

Figure 5.4. Turning maneuver for the quadruped.

CHAPTER VI

CONCLUSIONS

1. Conclusions

In this thesis, the dynamics of the quadruped gaits have been examined. The quadruped has been modelled as a rigid body with constant stiffness springs as legs. In the first chapter, a method was described to generate stable solutions for trot, bound and gallop gaits. The various issues involved in these gaits were discussed in detail. It was shown that a trot is more energy efficient at lower speeds, and a gallop is more energy efficient at higher speeds. These results were compared with actual observations made in the field. An attempt was made to model the flexion of the body using a torsional spring. Various strategies to obtain the stable solution for gallop met with limited success. Further, it was shown that a passive torsional spring does not accurately model the flexion of the body while galloping.

In the next two chapters, a controller was designed to control the speed of a two-dimensional quadruped while galloping. Symmetry principles were used to develop a non-linear controller for a gallop. It was shown that the pitch of the body need not be explicitly controlled. The stability of the controller was examined using Poincare maps. It was shown to be stable for different initial conditions and parameters. The stable system shows either periodic or quasiperiodic behavior. The system was shown to be stable only for a range of leg stiffnesses. Outside this range, the system is unstable. It has been shown that this instability of the system is due to chaos. This has important implications while designing a controller for a range of speeds. If the leg stiffness is below a certain critical value, the system will become unstable at higher speeds and changes in control gains will not restore stability.

The two-dimensional model was extended to a three-dimensional model. Additional controllers were designed to control the sideways speed, roll and yaw. The sideways speed was controlled by foot placement and roll and yaw were controlled by appropriately applying moments at the hip during the stance phase. The control scheme was extended to enable the quadruped to turn.

2. Recommendations

An extension of the work done in Chapter I would be modelling of the energy losses to reposition the leg for the next stance phase and the impact losses. One could then theoretically predict the stride frequency and compare it with the results for various animals. Another area that could be explored further is the modelling of the flexion of the back. An effort was made in this thesis to model the flexion but our attempt was not successful. This could have been due to the chaotic nature of the system and needs to be investigated further. It would be interesting to see if the flexion of the back lowered the energy level of the gallop further. This would result in additional energy savings.

Another area that should be explored further would be the location of the center of mass of the body. In this thesis, the body is assumed to be a uniform bar. Thus the center of mass is in the center of the body. In animals, the center of mass is close to the front legs due to the additional mass of the head. The methods described in this thesis can be easily modified to compute the stable solutions for different locations of the center of mass. Thus an extension of this work would be to quantify the effect of the location of the center of mass on various gaits.

In this thesis, the legs have been modelled as constant stiffness massless springs. The effect of legs with masses could be explored further. Pandy et. al. (1989) have shown, using goat studies, that the inertial effect of the legs is negligible compared to the inertial effects of the body. This could be confirmed in this simulation by adding masses to the legs. The control scheme in this thesis does not require constant stiffness springs in the legs. Nevertheless, there are symmetry requirements that the spring stiffnesses must satisfy. One of the obvious requirements is that the stiffness during the extension of the spring should be the same as that during the compression of the spring. This should be explored further. The type of non-linearities in the spring that can be tolerated by the controller should be investigated. This would be extremely helpful while selecting actuators for a four-legged running machine. The non-linearities of the leg spring will probably modify the chaotic nature of the system, and it would be interesting to observe its effect on chaos.

Another interesting area, that can be explored further is the effect of the center of mass on the controller. Since the controller relies on the symmetry of the model, a change in the location of the center of mass will affect the controller. In the present controller, the leg angle during the takeoff stage of the previous stance phase is used to set the leg angle for touchdown phase of the next stance phase. Thus, the takeoff angle for the front legs is used to set the touchdown angle for the rear legs and vice versa. If the center of mass is offset from the center of the body, then in order to satisfy the symmetry requirements, the leg angle during touchdown of the front legs will have to be set using the leg angle during takeoff from the front legs. Similarly,the leg angle during touchdown of the rear legs will have to be set using the leg angle during takeoff from the rear legs. This would involve storing the leg angles for the next aerial and stance phase, and then using them to set the leg angles for the next stance phase.

The most important recommendation for future work on this thesis would be an experimental validation of the control scheme developed in this thesis. Control schemes designed by other researchers using similar principles have been successful in the past. This should provide sufficient incentive to proceed with an experimental validation of this work.

REFERENCES

Alexander, R. McN., "The Mechanics of Jumping by a Dog (Canis familiaris)", Journal of Zoology (London), vol. 173, pp. 549-573, 1974.

Alexander, R. McN., "Elastic Mechanisms in Animal Movement", Cambridge: Cambridge University Press, 1988.

Alexander, R. McN., "Three Uses for Springs in Legged Locomotion", The International Journal of Robotics Research, vol. 9, pp. 53-61, April 1990.

Alexander, R. McN., Dimery, N. J. and Ker, R. F., "Elastic Structures in The Back And Their Role in Galloping of Some Mammals", Journal of Zoology, A, 207, 467-82, 1985.

Alexander, R. McN. and Vernon, A., "The Mechanics of Hopping by Kangaroos (Macropodidas)", Journal of Zoology (London), vol. 177, pp. 265-303, 1975.

Cavagna, G. A., Heglund, N. C., and Taylor, C. R., "Mechanical Work in Terrestrial Locomotion: Two Basic Mechanisms for Minimizing Energy Expenditure", Am. J. Physiol., 233(5):R243-R261, 1977.

Freeman, P. S. and Orin, D. E., "Efficient Dynamic Simulation of a Quadruped Using a Decoupled Tree-Structure Approach", The International Journal of Robotics Research, vol. 6, pp. 619-627, December 1991.

Gambaryan, P. P., "How Mammals Run: Anatomical Adaptations", John Wiley & Sons, 1974.

Heglund, N., Taylor, C. R., and McMahon, T. A., "Scaling Stride Frequency And Gait to Animal Size: Mice to Horses", Science 186, pp. 1112-1113, 1974.

Hirose, S., "A Study of Design and Control of a Quadruped Walking Vehicle", International Journal of Robotics Research, vol. 3, pp. 113-133, Summer 1984.

Hirose, S., Masui, T., Kikuchi, H., Fukuda, Y., and Umetani, Y., "Titan III: A Quadruped Walking Vehicle", Second International Symposium on Robotics Research, pp. 325-331, MIT Press, 1985.

Hodgins, J., "Legged Robots on Rough Terrain: Experiments in Adjusting Step Length", IEEE International Conference on Robotics and Automation, pp. 824-826,1988.

Hodgins, J. K. and Raibert, M. H., "Biped Gymnastics", The International Journal of Robotics Research, vol. 9, pp. 115-132, April 1990.

Hoyt, D. F. and Taylor, C. R., "Gait and the Energetics of Locomotion in Horses", Nature, 292, 239-40, 1981.

Manter, J. T., "The Dynamics of Quadrupedal Walking", Journal of Experimental Biology, vol. 15, pp. 522-539, 1938.

Moon, F. C., “Chaotic Vibrations”, John Wiley & Sons, 1987.

McGhee, R. B., "Control of Legged Locomotion Systems", Proceedings 18th Automatic Control Conference, pp.205-215, June 1977.

McMahon, T. A., "Using Body Size to Understand The Structural Design of Animals: Quadrupedal Locomotion", J. Appl. Physiol., vol.39, pp. 619-627, 1975.

McMahon, T. A., "Muscles, Reflexes, and Locomotion", Princeton University Press, 1984.

Miura, H. and Shimoyama, I., "Dynamic Walk of a Biped", International Journal of Robotics Research, vol. 3, pp.60-74, Summer 1984.

Mochon, S. and McMahon, T. A., "Ballistic Walking: An Improved Model", Math. BioSci., 52:241-260, 1981.

Murphy, K. N. and Raibert, M. H., "Trotting and Bounding in a Planar Two-Legged Model", Fifth Symposium on Theory and Practice of Robots and Manipulators, pp. 411-420, MIT Press, 1985.

Muybridge, E., "Animals in Motion", New York, Dover Publications, 1957.

Pandy, M. G., Kumar, V., Berme, N. and Waldron, K. J., “The Dynamics of Quadrupedal Locomotion”, ASME Journal of Biomechanical Engineering, vol. 110, pp. 230-237, August 1988.

Pennycuick, C. J., “On the Running of Gnu and Other Animals”, J. Exp. Biol., 63:775-799, 1975.

Raibert, M. H., "Dynamic Stability and Resonance in a One-Legged Hopping Machine", Fourth Symposium on Theory and Practice of Robots and Manipulators, Warsaw, pp. 352-367, Polish Scientific Publishers, 1981.

Raibert, M. H., "Hopping in Legged Systems-Modeling and Simulation for the 2D One-Legged Case", IEEE Transcations on System, Man, and Cybernetics, vol. SMC-14, pp. 451-463, June 1984.

Raibert, M. H., "Running With Symmetry", The International Journal of Robotics Research, vol. 5, pp.3-19, Winter 1986.

Raibert, M. H., "Legged Robots That Balance", Cambridge, Mass: MIT Press, 1986.

Raibert, M. H. and Brown, H. B., "Experiments in Balance with a 2D One-Legged Hopping Machine", Journal of Dynamic Systems, Measurements, and Control, vol. 106, pp. 75-81, March 1984.

Raibert, M. H., Brown, H. B. and Chepponis, M., "Experiments in Balance with a 3-D One-Legged Hopping Machine", The International Journal of Robotics Research, vol. 3, pp.75-92, Summer 1984.

Raibert, M. H., Brown, H. B.and Murthy, S. S., "3-D Balance Using 2-D Algorithms?", First International Symposium on Robotics Research, pp. 297-301, MIT Press, 1984.

Raibert, M. H., Chepponis, M. and Brown, H. B., "Running on Four Legs As Though They Were One", IEEE Journal of Robotics and Automation, vol. RA-2, pp.70-82, June 1986.

Song, S. M. and Waldron, K. J., "Machines That Walk: The Adaptive Suspension Vehicle", Cambridge, Mass: MIT Press, 1989.

Sutherland, I. E. and Ullner, M. K., "Footprints in the Asphalt", International Journal of Robotics Research, vol. 3, pp. 29-36, 1984.

Tabor, M., “Chaos and Integrability in Nonlinear Dynamics”, John Wiley & Sons, 1989.

Wong, H. C., “Control of a Quadruped Standing Jump and Running Jump Over Irregular Terrain Obstacles”, Doctoral dissertation, The Ohio State University, 1992.